Journal of
Science &
Technology
in the Tropics Volume 10 Number 1 June 2014

CONTENTS

INSTRUCTIONS TO CONTRIBUTORS

JOSTT is a multi-disciplinary journal. It publishes original research articles and reviews on all aspects of science and technology relating to the tropics. All manuscripts are reviewed by at least two referees, and the editorial decision is based on their evaluations.

Manuscripts are considered on the understanding that their contents have not been previously published, and they are not being considered for publication elsewhere. The authors are presumed to have obtained approval from the responsible authorities, and agreement from all parties involved, for the work to be published.

Submission of a manuscript to JOSTT carries with it the assignment of rights to publish the work. Upon publication, the Publishers (COSTAM and ASM) retain the copyright of the paper.

Manuscript preparation

Manuscripts must be in English, normally not exceeding 3500 words. Type double spaced, using MS Word, on one side only of A4 size with at least 2.5 cm margins all round. Number the pages consecutively and arrange the items in the following order: title page, abstract, key words, text, acknowledgements, references, tables, figure legends.

Title page

Include (i) title, (ii) names, affiliations and addresses of all authors, (iii) running title not exceeding five words, and (iv) email of corresponding author.

Abstract and key words

The abstract, not more than 250 words, should be concise and informative of the contents and conclusions of the work. A list of not more than five key words must immediately follow the abstract.

Text

Original research articles should be organized as follows: Introduction, Materials and Methods, Results, Discussion, Acknowledgement, References. The International System of Units (SI) should be used. Scientific names and mathematical parameters should be in italics.

References

References should be cited in the text as numbers enclosed with square [ ] brackets. The use of names in the text is discouraged. In the reference section, the following examples should be followed:

1. Yong H.S., Dhaliwal S.S. and Teh K.L. (1989) A female Norway rat, *Rattus norvegicus,* with XO sex chromosome constitution. *Naturwissenschaften* **76**: 387-388.
2. Beveridge W.I.B. (1961) *The Art of Scientific Investigation*. Mercury Book, London.
3. Berryman A.A. (1987) The theory and classification of outbreaks. In Barbosa P. and Schultz J.C. (eds.) *Insect outbreaks* pp. 3-30. Academic Press, San Diego.

Tables

Tables should be typed on separate sheets with short, informative captions, double spacing, numbered consecutively with Arabic numerals, and do not contain any vertical lines. A table should be set up to fit into the text area of at most the entire page of the Journal.

Illustrations

Black-and-white figures (line drawings, graphs and photographs) must be suitable for high-quality reproduction. They must be no bigger than the printed page, kept to a minimum, and numbered consecutively with Arabic numerals. Legends to figures must be typed on a separate sheet. Colour illustrations can only be included at the author's expense.

Proofs and reprints

Authors will receive proofs of their papers before publication. Order for reprints must be made when returning the proofs.

Submission

Manuscripts (including all figures but not original artwork), should be submitted to:

The Editorial Office
Journal of Science and Technology in the Tropics
Academy of Sciences Malaysia
902-4 Jalan Tun Ismail
50480 Kuala Lumpur, Malaysia

E-mail: jostt@akademisains.gov.my

JOSTT is listed in Scopus

EDITORIAL

Water Woes

It is truly a paradox! A friend of mine from Dubai, a dry desert country, emailed me to express his surprise to hear that Malaysia, a country with over 2500 mm of rainfall, is suffereing from water shortage, whereas Dubai and the Arab Emirates which are desert countries that have not seen rain for many years (there was a surprise short downpour recently, I believe) have never experienced water shortages. He asked why? I was not able to give him a credible answer although I tried.

So what are the reasons. Prof Dato' Azizan Abu Samah, a respected Geographer from University Malaysa, was on Television recently where he expressed surprise at the shortage of water as he said "the rivers are flowing with water which are our main source of water and not the dams".

Whatever the cause and reasons are, we cannot dispute that water is a critical and strategic resource. Our industries cannot function without water, our agriculture cannot either and we as common citizens cannot survive without water.

2013 was the United Nations International Year on Water Cooporation. World Water Day takes place every year on 22 March, also will be dedicated to water cooperation. The objective of this International Year is to raise awareness, both on the potential for increased cooperation, and on the challenges facing water management in light of the increase in demand for water access, allocation and services. The Year will highlight the history of successful water cooperation initiatives, as well as identify burning issues on water education, water diplomacy, transboundary water management, financing cooperation, national/international legal frameworks, and the linkages with the Millennium Development Goals. It also will provide an opportunity to capitalize on the momentum created at the United Nations Conference on Sustainable Development (Rio+20), and to support the formulation of new objectives that will contribute towards developing water resources that are truly sustainable.

While that international initiative is lauded, what is critically important to us as Malaysian citizens, is the assurance that we shall continue to enjoy supply of good clean water for all our needs. This requires good management of our water resources. Government had privatised water under the premise that privatisation will result in greater efficiency. Has this been true? Is there a need to review this policy? Are the private water concessionaires being truly responsible? Are they being closely monitored by the relevant Government agencies?

The ultimate source of all our water supply is the forests. They form the watershed for all our rivers. Sustainable forest management must ensure that the function of forests as watersheds and a source of water, is not threatened or diminished. The Forest Research Institute of Malaysia (FRIM) had undertaken research on integrated watershed management. Their findings should be put into practice.

The issue of non revenue water needs to be addressed seriously. This is water that is illegally tapped by unscrupulous individuals through illegal means. Some say that this can amount to as high as 30% of the water consumption.

Finally there is the issue of water conservation. Malaysians take water for granted. Engineers, architects and housing developers should build buildings and houses that collect rain water for use for non drinking purposes. The housing regulations should be amended to make this compulsory and this be strictly enforced. Government should also consider giving incentives for present house owners to install such systems similar to the renewable energy incentives. We can do without electricity for a day or two but we cannot do without water. Thus proper water management must be instituted to ensure that this important and strategic resource is truly sustainable.

Dr Salleh Mohd. Nor
Co-Chairman, JOSTT

Journal of Science and Technology in the Tropics (2014) 10: 5-14

Enterobacter ludwigii, a candidate probiont from the intestine of Asian seabass

F. T. Wendy[1], M. K. Abu Hena[1*], S. K. Wong[1], M. H. Idris[1], S. M. Sharifuzzaman[2] and M. Y. Ina-Salwany[3]

[1]Department of Animal Science and Fishery, University Putra Malaysia Campus Bintulu, 97008 Bintulu, Sarawak, Malaysia

[2]Institute of Marine Sciences and Fisheries, University of Chittagong, Chittagong 4331, Bangladesh

[3]Department of Aquaculture, Faculty of Aquaculture, University Putra Malaysia, 43400 Serdang, Selangor, Malaysia

(*Email: abuhena@upm.edu.my)

Received 15.01.2014, accepted 20.02.2014

Abstract The intestinal tract of healthy animals is assumed to be the natural place of 'good' micro-organisms. The present study investigated different parts of intestine of Asian seabass (*Lates calcarifer* Bloch) to isolate and indentify strains potentially useful as fish probiotics. The total culturable aerobic gut bacteria of both live and dead seabass samples ranged from 1.17–84.00 × 10^6 cfu/g, with counts being higher in posterior intestine (1.97–84.00 × 10^6 cfu/g) compared to the number of cells occurring in anterior (0.21–7.87 × 10^6 cfu/g) and middle (1.17–3.50 × 10^6 cfu/g) parts, although significantly higher numbers were associated with live fish. Thirty-three strains were purified of which only one isolate MS32 inhibited the growth of fish pathogens *Vibrio parahaemolyticus* and *Aeromonas hydrophilla* in a disc diffusion assay. The isolate MS32 produced gamma-hemolysin, indicating no breakdown of red blood cells and thus potentially non-infectious to the host. It was identified by standard biochemical tests and 16S rDNA sequences as *Enterobacter ludwigii*. Based on our findings, *E. ludwigii* could be a potential probiotic for use in seabass aquaculture; however, it should be further studied in disease challenge experiments in fish to validate an *in vivo* effect, i.e. to protect the host against pathogen(s).

Keywords probiotics – *Enterobacter ludwigii* – seabass – gastrointestinal tract – gamma-haemolysis

INTRODUCTION

Studies have suggested several important roles of probiotics in aquaculture related to the productivity and nutrition of cultured animals, modification of host-associated/ambient microbial community, prevention of diseases and/or improvement of water quality [1-3]. Probiotics can inhibit pathogens by competition for nutrients, production of antimicrobial substances or by immune regulation, the later one, in particular, can prevent potential damage of the host by pathogens [4, 5]. Therefore, the application of probiotics or beneficial bacteria is being increasingly viewed as one of the major means (including

vaccines and immunostimulants) to control bacterial diseases in aquaculture and at the same time to improve food safety and the quality of the aquatic environment [6].

Generally, the candidate fish probionts have been obtained from a wide range of sources, including healthy adult fish [7, 8], rearing water [9], fish larvae [10, 11], human probiotics *Lactobacillus rhamnosus* [12] and *L. plantarum* [13] or the gut of chickens [14], all of which led to improved health of farmed fish species. However, it is argued that isolation of putative probiotics from the indigenous microbiota of fish or the rearing environment, assumed to be the natural location of 'good' micro-organisms [15], may have the desirable probiotic effect [1]. Additionally, the mode of action of all probiotics is not similar, but shows variation in their efficacy suggesting one probiotic could not be used commonly for all fish species to control single or multiple diseases [16]. In this study we investigated the gastrointestinal tract of the Asian seabass (*Lates calcarifer* Bloch) in order to select, identify and characterize the potential bacterial isolates to be considered as probiotics for seabass aquaculture.

MATERIALS AND METHODS

Fish sample

Five dead seabass were collected from the local fish market at Bintulu, Sarawak and another five live seabass were collected from Sibuti, Miri, Sarawak. The fish weighed 1–1.5 kg with length 35–40 cm. The fish were brought to the laboratory without any delay prior to dissection of the stomach.

Total viable count in the gut and the putative probionts

Live fish were sacrificed by an overdose of anesthetic (MS-222; Sigma-Aldrich). The surface of the fish was sterilised using 70% alcohol and the peritoneal cavity was opened aseptically with a sterile scalpel. Then, the gastrointestinal tract was removed and divided into anterior (esophagus), middle (stomach) and posterior (intestine) parts. Each part (1 g) was separately minced and homogenized in 9 mL of 1.5% (w/v) sterile saline. Ten-fold dilutions were prepared up to 10^{-6} in fresh saline, and 0.1 mL of each dilution was spread onto triplicate plates of marine agar (MA plates) (Difco, USA). All the plates were incubated aerobically at ambient temperature (~30°C) up to 3 days, and colony forming unit per gram of sample (cfu/g) counted [17]. Afterwards, dissimilar colonies were picked randomly, purified by streaking and re-streaking onto fresh marine agar plates, and the selected isolates, i.e. putative probionts, labelled as 'MS' for dead seabass obtained from market and as 'LS' for live seabass, were tested for their antimicrobial properties following disc diffusion assay.

Disc diffusion assay

In order to screen the potentially beneficial cultures, a disc diffusion assay [5], adapted from Kirby-Bauer disc diffusion method, was used for testing the antagonistic activities of putative probionts against bacterial fish pathogens, *Aeromonas hydrophila* ATCC7966, *Vibrio alginolyticus* ATCC33839 and *V. parahaemolyticus* ATCC43996. Briefly, the pathogens and isolates were cultured in marine broth (MB broth) (Difco, USA) for 24 hours, then the inoculum density of both pathogens and isolates adjusted to the 0.5 McFarland standard (2×10^8 cfu/mL). Subsequently, 10 µL aliquot of the potential strain was pipetted onto sterile paper disc, which was then placed evenly onto MA plates previously inoculated with pathogen. Sterile paper disc dipped with sterile MB broth served as negative control. The diameter of inhibition zone (mm) was measured after 24 hours of incubation.

Haemolytic test

The potential probionts were tested for haemolytic activity. Briefly, selected strains were grown on MA plates for 72 hours at room temperature. Then each strain was inoculated onto Columbia agar supplemented with 5% sheep blood (Bio-Rad). Haemolytic activity was then observed, after incubating the plates for 24 hours, either by a beta, alpha or gamma-haemolytic reaction.

Identification of putative probiont

Both biochemical and molecular tests were carried out to identify the useful isolates. Briefly, the characteristics and cell shape of the isolates were observed as they developed on marine agar. Tests such as Gram staining (Gram staining kit; Fluka, Switzerland), endospore test [18], catalase test (3% H_2O_2), motility test (Biolife, Italy), indole reaction (Becton Dickinson and Company, MD USA), and nitrate reduction test (Fluka, Switzerland) were also carried out for the selected isolates. The alkaline-lysis omitting NaOH method and 16S rDNA gene sequencing was done using standard procedure [19]. The amplification of the 16S rDNA sequencing was done with the forward primer 5' AAG AGT TTG ATC ATG GCT CA 3' and the reverse primer 5' TAA GGA GGT GAT CCA ACC GCA GGT TC 3'.

Statistical analysis

Data (mean of experiment(s) performed in replicates) were statistically analysed by one-way analysis of variance (ANOVA) and Duncan's comparison of means when necessary. All statistical tests were conducted using the computerized software Statistical Package for Social Sciences (SPSS; Release 14.0, SPSS, Chicago, IL, USA). Differences were considered statistically significant when P

< 0.05. The data were plotted using the program Microsoft Excel (Microsoft, Seattle WA, USA).

RESULTS AND DISCUSSION

The gastrointestinal content of seabass, both live and dead specimens, was used as a source of potential probiotics, with the recovery of total bacteria of 1.17–84.00 $\times$ 10^6 cfu/g on MA plates. In particular, higher bacterial counts, i.e. 1.97–84.00 $\times$ 10^6 cfu/g were noted in posterior intestine compared to cell number occurring in middle (1.17–3.50 $\times$ 10^6 cfu/g) and anterior (0.21–7.87 $\times$ 10^6 cfu/g) parts, despite significantly ($P < 0.05$) high number of bacteria were associated with live fish (Table 1). This result agrees with previous results on microbial counts in hindgut of rainbow trout, ~4.8 $\times$ 10^6 cfu/g [20] and with the report of

Table 1. Total aerobic bacterial count from the gastrointestinal tract of seabass. Means in the same column without a common letter differ significantly ($P < 0.05$). Significant difference ($P < 0.05$) from dead seabass specimen is indicated by an asterisk.

Gastrointestinal tract	Total bacterial count ($\times 10^6$ cfu/g)	
	Dead seabass	Live seabass
Anterior: Esophagus	0.21 ± 0.04^{b}	$7.87 \pm 0.04^{*b}$
Middle: Stomach	1.17 ± 0.56^{ab}	$3.50 \pm 0.06^{*c}$
Posterior: Intestine	1.97 ± 0.96^{a}	$84.00 \pm 0.96^{*a}$

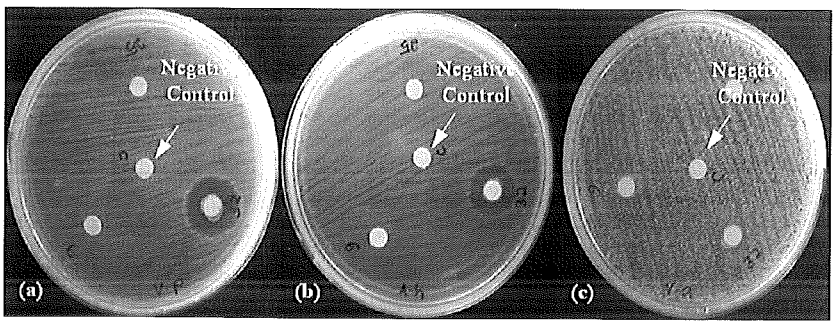

Figure 1. Antimicrobial activity, as indicated by a zone of inhibition on the lawn, by the isolate MS32 against fish pathogens, (a) *V. parahaemolyticus* – zone of inhibition 5.8 mm, (b) *A. hydrophila* – zone of inhibition 5.3 mm, and (c) *V. alginolyticus* – zone of inhibition 0 mm.

a decline of total bacterial cell numbers in the gut of hybrid tilapia, *Oreochromis niloticus* and *O. aureus*, frozen for one month compared to fresh fish sample [21]. Certainly, total viable count of intestinal microflora of fish tends to decrease slowly during frozen storage than that of fresh or live condition [22]. Our results corroborate this statement well by recording higher bacterial counts in live seabass than dead one kept frozen for couple of days.

Of the 33 representatives of the various colony types examined for *in vitro* antagonism, only one isolate MS32 demonstrated inhibitory properties, i.e. interrupted the growth of reference pathogens with inhibition zone of 5.3–5.8 mm (Fig. 1), excluding *V. alginolyticus*. Similarly by using the cross-streaking method of determining antagonism, Capkin and Altinok [23] reported two (*Enterobacter cloacae* and *Bacillus mojavensis*) among 14 isolates recovered from the digestive tract of rainbow trout, were inhibitory against virulent *Yersinia ruckeri*. This emphasizes that a small ratio of resident microbiota of fish or the rearing environment can produce various antagonistic compounds/ substances (i.e. antibiotics or antimicrobial peptides, organic acids or hydrogen peroxide) and inhibit the growth of pathogens [24-26]. In numerous cases, it is these antagonistic bacteria that have been demonstrated to be effective probiotics for use in aquaculture [4, 23].

The putative probiont MS32, when assessed for possible infectious effects on seabass, was non-haemolytic, as suggested by the production of gamma-haemolysin, i.e. no breakdown of red blood cells, and thus potentially non-pathogenic. Although, hemocytolytic test is very much useful for distinction of suspected pathogens, evidence on the correlation between haemolysis and pathogenic bacterium is not conclusive [27-28]. Therefore, disease-producing ability of MS32 to target host should be further studied either by injection or by bath (liquid suspension of putative probiotic) challenge. Moreover, the probiotic potential of MS32 should be further studied in disease challenge experiments in seabass to validate an *in vivo* effect, i.e. protecting the host against single or multiple diseases [1, 29].

The identification of candidate probiont MS32 remains essential since it can provide useful information about the culture requirements and possible virulence gene expression of the bacterium [30]. Using classical microbiological methods, MS32 was tentatively classified as a member of the genus *Enterobacter* (Table 2). This was verified by the partial sequences of the 16S rDNA gene as *E. ludwigii*. The bacterium was characterized as Gram-negative, aerobic, straight rod shaped, motile, catalase-positive, lactose-fermenting, nonendospore-forming and starch-utilizing organism, lacking the capacity to produce hydrogen sulphide and reduce nitrate (NO^3) to nitrite (NO^{2-}). Some *Enterobacter* spp. were recorded as opportunistic pathogen to humans and other organisms [31], for instance *E. cloacae* and *E. ludwigii* cause mortalities in mullet, *Mugil cephalus* [32] and

Table 2. Morphological and biochemical characteristics of isolate MS32. +, Positive; -, Negative; NA, Not available; *after Holt *et al.* [42] and Hoffmann *et al.* [43].

Test	Characteristics	
	MS32	*Genus Enterobacter
Gram staining	–	–
Morphology	Rod	Rod
Endospore	–	NA
Catalase	+	+
Motility	+	+
Indole	–	–
Nitrate reduction	–	+
Starch utilization	+	NA
Lactose	+	+
H_2S	–	–

fairy shrimp, *Branchinella thailandensis* [33], respectively. Moreover, representatives of this genus were reported to include probiotic strains such as *Enterobacter* sp. and *E. amnigenus*, which were successful in controlling *Flavobacterium psychrophilum* infections in rainbow trout [34]. Ghosh *et al.* [35] identified *E. hormaechei* BAC 1010, which was isolated from the gut of flathead grey mullet, as potential probiotic bacteria due to its ability to inhibit the growth of fish, shrimp and human pathogens *in vitro*. Additionally some pathogen species were recognised as potential probiotics for many fish, for example, *Vibrio alginolyticus* (a causative agent of 'vibriosis' in *Epinephelus fuscoguttatus*) [36], was beneficial to turbot, *Scophthalmus maximus* aquaculture due to improved survival of culture stocks [36]. This suggests that pathogens are host specific. Therefore, *E. ludwigii* may not be infectious to sea bass.

Desirable *in vitro* characteristics, such as antagonism (as observed in this study), growth characteristics [38], or the ability to adhere to mucus layer [1, 39], are not necessarily the only suitable characteristics for pre-selection of probiont candidates for use *in vivo* [40]. Gram *et al.* [41] demonstrated that results of *in vitro* pathogen inhibition assays could not be used to completely predict an *in vivo* effect since probiotic *Pseudomonas fluorescens* with a strong antagonism against *A. salmonicida* did not protect Atlantic salmon from furunculosis. Nevertheless, *in vitro* criteria remain necessary for selection of putative

probiotics [1, 40] as the approach has the potential to reduce a large collection of isolates to a smaller number, thereby saving expenditure and time.

In summary, the strain MS32 isolated from the gut of Asian seabass was identified as *E. ludwigii* EN119, and might be a potential probiotic because of its ability to inhibit bacterial fish pathogens *in-vitro*.

Acknowledgements – The authors acknowledge the Research Management Centre (RMC), Universiti Putra Malaysia for providing funds (RUGS/01/02-12-228RU) to M. K. Abu Hena to conduct this research.

REFERENCES

1. Verschuere L., Rombaut G., Sorgeloos P. and Verstraete W. (2000) Probiotic bacteria as biological control agents in aquaculture. *Microbiology and Molecular Biology Reviews* **64**: 655–671.
2. Wang Y.B., Tian Z.Q., Yao J.T. and Li W.F. (2008) Effect of probiotics, *Enteroccus faecium*, on tilapia (*Oreochromis niloticus*) growth performance and immune response. *Aquaculture* **277**: 203–207.
3. Abu Hena M.K., Wong S.K., Idris M.H. and Aftab Uddin S. (2011) Pond health management of black tiger shrimp *Penaeus monodon* Fabricius using bacterial products. *Research Journal of Fishery and Hydrobiology* **6**(1): 17-21.
4. Sharifuzzaman S.M. and Austin B. (2009) Influence of probiotic feeding duration on disease resistance and immune parameters in rainbow trout. *Fish and Shellfish Immunology* **27**: 440–445.
5. Lim H.J., Kapareiko D., Schott E J., Hanif A. and Wikfors G.H. (2011) Isolation and evaluation of new probiotic bacteria for use in shellfish hatcheries: I. Isolation and screening for bioactivity. *Journal of Shellfish Research* **3**: 609–615.
6. Subasinghe R. (1997) Fish health and quarantine. In *Review of the State of the World Aquaculture*, FAO Fisheries circular no. 886, pp. 45–49. Food and Agriculture Organization of the United Nations, Rome.
7. Gildberg A., Mikkelsen H., Sandaker E. and Ringø E. (1997) Probiotic effect of lactic acid bacteria in the feed on growth and survival of fry of Atlantic cod (*Gadus morhua*). *Hydrobiologia* **352**: 279–285.
8. Gram L., Melchiorsen J., Spanggaard B., Huber I. and Nielsen T.F. (1999) Inhibition of *Vibrio anguillarum* by *Pseudomonas fluorescens* AH2, a possible probiotic treatment of fish. *Applied and Environmental Microbiology* **65**: 969–973.
9. Lauzon H.L., Gudmundsdottir S., Steinarsson A., Oddgeirsson M., Petursdottir S.K., Reynisson E., Bjornsdottir R. and Gudmundsdottir B.K. (2010) Effects of bacterial treatment at early stages of Atlantic cod (*Gadus morhua* L.) on larval survival and development. *Journal of Applied Microbiology* **108**: 624–32.
10. Gatesoupe F.J. (1999) The use of probiotics in aquaculture. *Aquaculture* **180**: 147–165.
11. Ringø E. and Vadstein O. (1998) Colonization of *Vibrio pelagius* and *Aeromonas caviae* in early developing turbot (*Scopthalmus maximus* L.) larvae. *Journal of Applied Microbiology* **84**: 227–233.

12. Nikoskelainen S., Ouwehand A.C., Bylund G., Salminen S. and Lilius E.M. (2003) Immune enhancement in rainbow trout (*Oncorhynchus mykiss*) by potential probiotic bacteria (*Lactobacillus rhamnosus*). *Fish and Shellfish Immunology* **15**: 443–452.
13. Picchietti S., Mazzini M., Taddei A.R., Renna R., Fausto A.M., Mulero V., Carnevali O., Cresci A. and Abelli L. (2007) Effects of administration of probiotic strains on GALT of larval gilthead seabream: immunohistochemical and ultrastructural studies. *Fish and Shellfish Immunology* **22**: 57–67.
14. Pan X., Wu T., Song Z., Tang H. and Zhao Z. (2008) Immune responses and enhanced disease resistance in Chinese drum, *Miichthys miiuy* (Basilewsky), after oral administration of live or dead cells of *Clostridium butyricum* CB2. *Journal of Fish Diseases* **31**: 679–686.
15. Gullian M., Thompson F. and Rodriguez J. (2004) Selection of probiotic bacteria and study of their immunostimulatory effect in *Penaeus vannamei*. *Aquaculture* **233**: 1–14.
16. Sharifuzzaman S. M., Al-Harbi A. H. and Austin B. (2014) Characteristics of growth, digestive system functionality, and stress factors of rainbow trout fed probiotics *Kocuria* SM1 and *Rhodococcus* SM2. *Aquaculture* **418–419**: 55–61.
17. Cappuccino J. G. and Sherman N. 1987. Microbiology A Laboratory Manual. Second Edition. The Benjamin/Cummings Publishing Company, Inc. p 75-80.
18. Schaeffer A.B. and Fulton M. (1993) A simplified method of staining endospores. *Science* 77: 194.
19. Bimboim H.C. and Doly J. (1979) A rapid alkaline extraction procedure for screening recombinant plasmid DNA. *Nucleic Acids Research* 7 (6): 1513-1524.
20. Kim D.H., Brunt J. and Austin B. (2007) Microbial diversity of intestinal contents and mucus in rainbow trout (*Oncorhynchus mykiss*). *Journal of Applied Microbiology* **102**: 1654–1664.
21. Al–Harbi A.H. and Uddin M.N. (2005) Microbiological quality changes in the intestine of hybrid tilapia (*Oreochromis niloticus* x *Oreochromis aureus*) in fresh and frozen storage condition. *Letters in Applied Microbiology* **40**: 486–490.
22. Al–Harbi A.H. and Uddin M.N. (2012) Bacterial content in the intestine of frozen common carp Cyprinus carpio. *African Journal of Biotechnology* **11** (30): 7751–7755.
23. Capkin E. and Altinok I. (2009). Effects of dietary probiotic supplementations on prevention/treatment of yersiniosis disease. *Journal of Applied Microbiology* **106**: 1147–1153.
24. Robertson P.A. W., Odowd C., Burrells C., Williams P. and Austin B. (2000) Use of *Carnobacterium* sp. as a probiotic for Atlantic salmon (*Salmo salar* L.) and rainbow trout (*Oncorhynchus mykiss*, Walbaum). *Aquaculture* **185**: 235–243.
25. Spanggaard B., Huber I., Nielsen J., Sick E.B., Pipper C.B., Martinussen T., Slierendrecht W.J. and Gram L. (2001) The probiotic potential against vibriosis of the indigenous microflora of rainbow trout. *Environmental Microbiology* **3**: 755–765.
26. Fjellheim A.J., Playfoot K.J., Skjermo J. and Vadstein O. (2007) *Vibrionaceae* dominates the microflora antagonistic towards *Listonella anguillarum* in the

intestine of cultured Atlantic cod (*Gadus morhua* L.) larvae. *Aquaculture* **269**: 98–106.

27. Chang C.I., Liu W.Y., Shyu C.Z. (2000) Use of prawn blood agar hemolysis to screen for bacteria pathogenic to cultured tiger prawns *Penaeus monodon*. Diseases of Aquatic Organisms **43**:153-157.
28. Nayak S.K., Mukherjee S.C. (2011) Screening of gastrointestinal bacteria of Indian major carps for a candidate probiotic species for aquaculture practices. Aquaculture Research **42**:1034-1041.
29. Brunt J., Newaj-Fyzul A. and Austin B. (2007) The development of probiotics for the control of multiple bacterial diseases of rainbow trout, *Oncorhynchus mykiss* (Walbaum). *Journal of Fish Diseases* **30**: 573–579.
30. Vine N.G., Leukes W.D. and Kaiser H. (2006) Probiotics in marine larviculture. *FEMS Microbiology Reviews* **30**: 404–427.
31. Austin B. and Austin D.A. (2012) Bacterial Fish Pathogens: Disease in Farmed and Wild Fish, 5th Edn. Springer, Dordrecht.
32. Sekar V.T., Santiago T.C., Vijayan K.K., Alavandi S.V., Raj V.S., Rajan J.J.S., Sanjuktha M. and Kalaimani N. (2008) Involvement of *Enterobacter cloacae* in the mortality of the fish, *Mugil cephalus*. *Letters in Applied Microbiology* **46**: 667–672.
33. Purivirojkul W. (2013) Application of probiotic bacteria for controlling pathogenic bacteria in fairy shrimp *Branchinella thailandensis* culture. *Turkish Journal of Fisheries and Aquatic Sciences* **13**: 187–196.
34. Burbank D.R., Shah D.H., LaPatra S.E., Fornshell G. and Cain K.D. (2011) Enhanced resistance to coldwater disease following feeding of probiotic bacterial strains to rainbow trout (*Oncorhynchus mykiss*). *Aquaculture* **321**: 185-190.
35. Ghosh S., Ringo E., Deborah G.S.A., Rahiman K.M.M. and Hatha A.A.M. (2011) *Enterobacter hormaechei* Bac 1010 from the gut of flathead grey mullet as probable aquaculture probionat. *Journal of Nature Sceince and Sustainable Technology* **5** (3): 189-199.
36. Ali H.M., Yussoff N.H.N., Om A.D., Musa C.U.C. and Othman M.F. (2008) Status and prospects of grouper aquaculture in Malaysia. In The Aquaculture of Grouper, ed. Liao, I. C. And Leano, E. M. Asian Fisheries Society, World Aquaculture Society, Fish Soc. Taiwan and National Taiwan Ocean University, p 155–175.
37. Gatesoupe F. J. (1997) Sidephore production and probiotics effect of Vibrio sp. associated with turbot larvae, Scophthalmus maximus. *Aquatic Living Resources* **10**: 239–246.
38. Vine N.G., Leukes W.D. and Kaiser H. (2004) *In vitro* growth characteristics of five candidate aquaculture probiotics and two fish pathogens grown in fish intestinal mucus. *FEMS Microbiology Letters* **231**: 145–152.
39. Chabrillón M., Rico R.M., Balebona M.C. and Moriñigo M.A. (2005) Adhesion to sole, *Solea senegalensis* Kaup, mucus of microorganisms isolated from farmed fish, and their interaction with *Photobacterium damselae* subsp. *Piscicida*. *Journal of Fish Diseases* **28**: 229–237.
40. Balcázar J.L., de Blas I., Ruiz-Zarzuela I., Cunningham D.J.L. Vendrell and

Múzquiz D. (2006) The role of probiotics in aquaculture. *Veterinary Microbiology* **114**: 173–186.

41. Gram L., Lovold T., Nielsen J., Melchiorsen J. and Spanggaard B. (2001) *In vitro* antagonism of the probiont *Pseudomonas fluorescens* strain AH2 against *Aeromonas salmonicida* does not confer protection of salmon against furunculosis. *Aquaculture* **199**: 1–11.
42. Holt J.G, Krieg N.R, Sneath P.H.A., Staley J.T. and Williams S.T. (2000) Bergey's Manual of Determinative Bacteriology, Ninth Edition. Lippincott Williams and Wilkins. pp. 178.
43. Hoffman H., Stindl S., Stumpf A., Mehlen A., Monget D., Heesemann J., Schleifer K. H. and Roggenkamp A. (2005) Description of *Enterobacter ludwigii* sp. nov., a novel *Enterobacter* species of clinical relevance. *Systematic and Applied Microbiology* **28**:206-212.

Journal of Science and Technology in the Tropics (2014) 10: 15-25

Tocotrienol and tocopherol contents of annatto seed accessions

S. T. Yong[1]*, H. K. Wong[1], M. Mardhati[1] and S. L. Tan[2]
[1]Strategic Livestock Research Centre, Malaysian Agricultural Research and Development Institute (MARDI), GPO Box 12301, 50774 Kuala Lumpur, Malaysia
[2]Academy of Sciences Malaysia, Menara MATRADE, West Wing, 20th Floor, Jalan Khidmat Usaha, 50480 Kuala Lumpur, Malaysia
(*E-mail: yongsuting@mardi.gov.my)

Received 8-3-2014; accepted 26-03-2014

Abstract The composition of vitamin E in plants is affected by species, variety, maturity, growing conditions like weather, growing season, intensity of sunlight and soil type, as well as time and manner of harvesting. Screening of 15 accessions of annatto (*Bixa orellana* L.) showed that total tocotrienols in the seeds ranged from 369.60 to 4422.93 µg/g. Delta-tocotrienol is the major tocotrienol, followed by gamma-tocotrienol. Alpha-tocotrienol was not detectable in 7 of the accessions. For 11 annatto accessions, the vitamin E content in dry seeds was higher than in the fresh seeds while in other 4 accessions, the vitamin E content was higher in fresh seeds compared with the dry seeds. Almost all the vitamin E in annatto seeds was made up of tocotrienols with a range in composition of 88.28 to 99.94%. Delta-tocotrienol was the highest, ranging from 53.67 to 93.51% of the total vitamin E. By comparison, gamma-tocotrienol made up 1.09 to 37.31%, while alpha-tocotrienol made up 0 to 16.72% of the total vitamin E content in the seeds. The content of vitamin E in annatto fruit skin (29.72 µg/g) was much lower than the vitamin E content in the seed. Annatto contains high levels of tocotrienols that are increasingly being associated with multiple health benefits. Several studies have shown that high levels of alpha-tocopherol depress the bioavailability of tocotrienols and inhibit tocotrienols in their chemo-preventive activity against degenerative diseases. This study shows that the seeds of the annatto plant are a rich source of tocotrienols which are virtually free of tocopherols.

Keywords annatto – seed – tocotrienol – tocopherol – reversed-phase HPLC

INTRODUCTION

Vitamin E is a collective term for eight naturally occurring compounds: four tocopherols, namely, alpha (α), beta (β), gamma (γ) and delta (δ), and four tocotrienols (α, β, γ and δ), that can exhibit the biological activities of α-tocopherol [1]. Both structures are similar except that the tocotrienol structure has double bonds on the isoprenoid units. This group of compounds are potent, lipid-soluble, chain-breaking antioxidants that prevent the propagation of free radical reactions [1]. Tocopherols are synthesized by most plants and are particularly abundant in seeds. Most plant-derived foods, especially fruits and vegetables in

the US diet, contain low to moderate levels of vitamin E while the α- and γ-tocotrienols were at levels usually less than 0.1 mg/100 g [2]. Due to the abundance of plant-derived foods in our diets, these foods can provide a significant and consistent source of vitamin E [3]. The amount of vitamin E in fruits and vegetables is affected by species, variety, maturity, growing conditions (weather, growing season, intensity of sunlight, and soil type) and time and manner of harvesting [4]. Sattler *et al.* [5] have reported that in plants the tocopherols are essential for seed longevity and for preventing lipid peroxidation during germination. Dicotyledoneous plants (e.g., soybean, groundnut) typically contain tocopherols, predominantly as γ-tocopherol, and secondarily as δ-tocopherol and α-tocopherol [6]. Monocotyledoneous plants (e.g., oil palm and rice) typically contain tocotrienols, predominantly as γ-tocotrienol, and secondarily as δ-tocotrienol and α-tocotrienol [6]. β-tocopherol and β-tocotrienol are insignificant in abundance in plants, and have negligible or unknown activity [7]. Dicotyledoneous plants that contain tocopherols may have less (~5%) tocotrienols, and monocotyledoneous plants that contain tocotrienols may have more (~30%) tocopherols.

Tocopherol-free tocotrienols [7] are rare and have been reported in plants like *Bixa orellana* L., commonly known as annatto. Tocotrienols have been associated with multiple health benefits [7-10], and it has been reported that the unsaturated carbon 'tail' provides tocotrienols with greater anti-oxidative activity as well as unique functions in lowering cholesterol, providing neuro-protection and anti-tumorigenesis (anti-cancer) activity, and are thus considered functionally superior to tocopherols. In human nutrition, vitamin E requirements increase when intakes of polyunsaturated fatty acids are increased [11]. Several methods to perform tocopherol and tocotrienol analysis using different detectors have been reviewed and published [12]. Normal-phase high performance liquid chromatography (HPLC) methods with a silica column as well as reversed-phase HPLC methods with a C18 column are commonly used. This paper describes the screening of annatto accessions and some vegetable oils for tocopherols and tocotrienols composition using HPLC with a reverse phase C18 silica column.

MATERIALS AND METHODS

Standards of pure tocotrienol isomers (α), (β), (γ) and (δ) from Davos Life Science Pte. Ltd. (Singapore) were weighed and dissolved with methanol to provide a 0.04 g/ml stock solution. Standards of tocopherol isomers (α), (β), (γ) and (δ) were purchased from Sigma Aldrich (St. Louis, MO) and stock solutions (0.04 g/mL) were made as described above. Working standard

solutions with concentration of 10 ug/ml were prepared by diluting the stock solutions with methanol. Standards were filtered with a 0.20 μM PVDF syringe filter prior to injection into the HPLC. The HPLC consisted of a binary pump, a photodiode array detector, a reverse phase C18 silica column and an auto injector. Column temperature was set at 40°C. Different ratios of methanol: water (v/v) as the mobile phase were studied in order to determine the ratio which gave the best separation of the different component peaks of tocopherols and tocotrienols. The mobile phases that were evaluated to separate the vitamin E isomers were the following methanol:water ratios – 99:1, 98:2, 97:3, 96:4 and 95:5. The wavelength was set at 290 nm absorption and the column was equilibrated with the mobile phase at a flow rate of 1.0 mL/min until the baseline was stable for analysis to commence.

Sample preparation

Seeds of dry and fresh fruits from 15 accessions of annatto were collected for determination of vitamin E profile. In this paper, dry fruit refer to fruit naturally dried on the plant and dehisced, while fresh fruit refer to those which have fully developed colour but not dehisced. Vegetable oils (palm, soybean, olive, corn, ricebran and sunflower) were purchased from retail outlets in Petaling Jaya for determination of their vitamin E profile.

Extraction of vitamin E

The samples were ground in a dry mill kitchen blender to fine particles before vitamin E extraction. Tocopherols and tocotrienols are fat-soluble and readily dissolve in organic solvents. For vegetable oils, the vitamin E was extracted using the cold extraction method [13] with slight modifications. A chloroform:methanol (1:1) mixture (50 mL) was added to an accurately weighed test sample (approximately 1.0 g for vegetable oils) in a 100-mL beaker, covered and left overnight. The chloroform:methanol containing lipid was then filtered into a round flask and evaporated to dryness using a Buchi Rotavapor R-205 set at 40°C. Twenty-five millilitres of methanol were then added to dissolve the extracted vitamin E, and the samples were filtered with a 0.2-μM PVDF syringe filter prior to injection into the HPLC. For the annatto seeds, an accurately weighed test sample (approximately 1.0 g) was extracted by the method of Xu [14] which includes a saponification and heating step to weaken sample matrices to allow the solvent to fully access all tocopherols and tocotrienols in the sample. Each sample was analyzed in duplicate and if the results were different by more than 10%, the analysis was repeated. The final results were expressed in μg/g.

RESULTS AND DISCUSSION

Quantification of tocopherols and tocotrienols

Evaluation of the different mobile phases showed that the α- and δ-tocopherols and tocotrienols were adequately separated by the methanol:water ratio of 95:5 at a flow rate of 1.0 mL/min. However the reversed-phase HPLC method [15] could not completely separate the isomers of β- and γ-tocopherols and tocotrienols, and these isomers were reported together as a single value. In reversed-phase HPLC on a C18 column, separation is based on the structure of the side chain and the number of methyl substituents. It is thus difficult to completely separate β- and γ-tocotrienols by reversed-phase HPLC, because both have a similar side-chain structure and number of methyl substituents on the chromanol ring [14]. As reported by Tan [7], the contents of β-tocopherol and β-tocotrienol are insignificant in plants, so in this paper the isomers of β- and γ-tocopherols and tocotrienols are reported as γ-tocopherols and tocotrienols.

The tocopherols and tocotrienols were identified according to the retention times of the standard solutions. Quantification of the respective vitamin E isomers was by using linear regression from the calibration curve of the respective isomers.

The vitamin E elution profiles of annatto seeds and vegetable oils are shown in the chromatograms in Figures 1, 2, 3, 4 and 5. The elution time for all the vitamin E isomers was less than 12.0 min. The first isomer to elute was δ-tocotrienol at about 6.77 min while the last isomer to elute was α-tocopherol at 11.96 min.

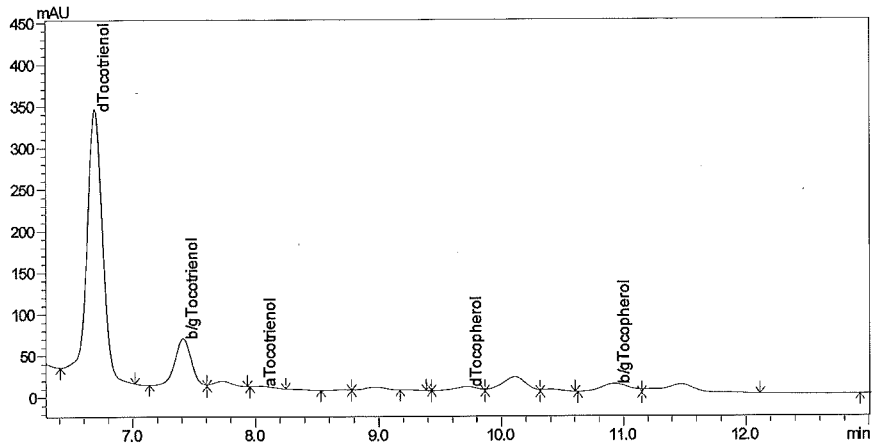

Figure 1. Chromatogram of tocopherol and tocotrienol isomers in annatto seeds. a Tocotrienol = α-tocotrienol; b/g Tocotrienol = β/γ-tocotrienol; d Tocotrienol = δ-tocotrienol; a Tocopherol = α-tocopherol; b/g Tocopherol = β/γ-tocopherol; d Tocopherol = δ-tocopherol.

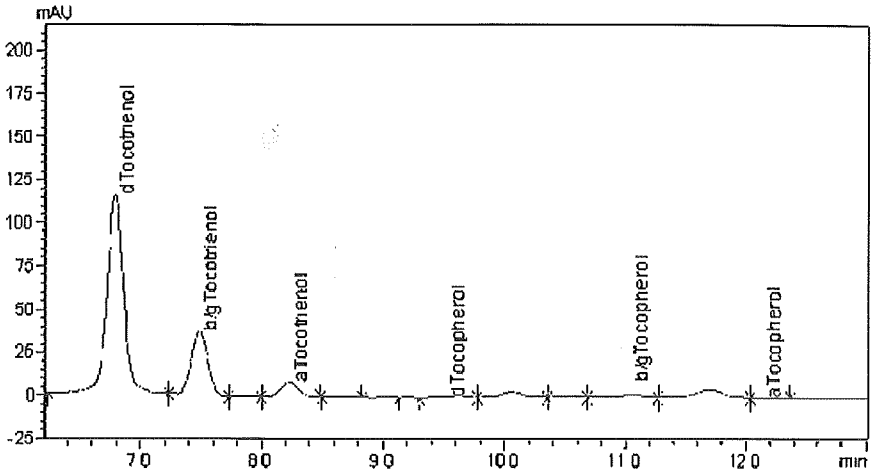

Figure 2. Chromatogram of tocopherol and tocotrienol isomers in an annatto seed accession showing significant levels of α-tocotrienol.

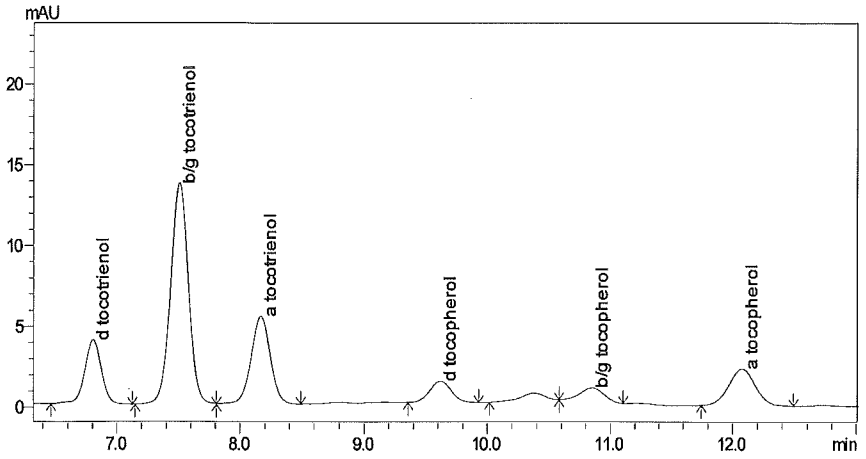

Figure 3. Chromatogram of tocopherol and tocotrienol isomers in palm oil.

Vitamin E content in dry seeds was higher than fresh seeds in 11 of the annatto accessions, while in the remaining 4 accessions, the vitamin E content was higher in the fresh seeds. There is a big variation in total vitamin E content among the accessions ranging from a low 377.87 to a high 4426.47 μg/g (Table 1). Within the vitamin E family, annatto has very high levels of tocotrienols ranging from 143.94 to 4422.93 μg/g. By comparison, Frega *et al.* [16] using GC-MS reported that dry annatto seeds contain 1400-1470 μg/g tocotrienols, almost all it being δ-tocotrienol. In this study, for most of the annatto accessions, δ-tocotrienol was the main tocotrienol followed by

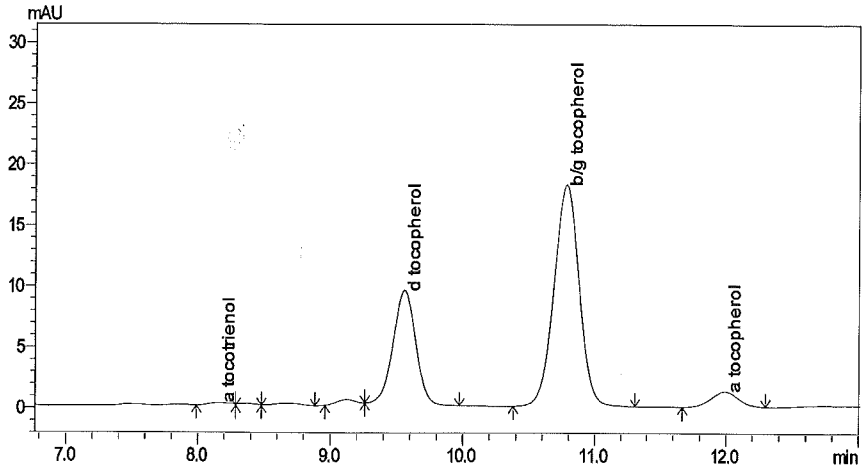

Figure 4. Chromatogram of tocopherol and tocotrienol isomers in soyabean oil.

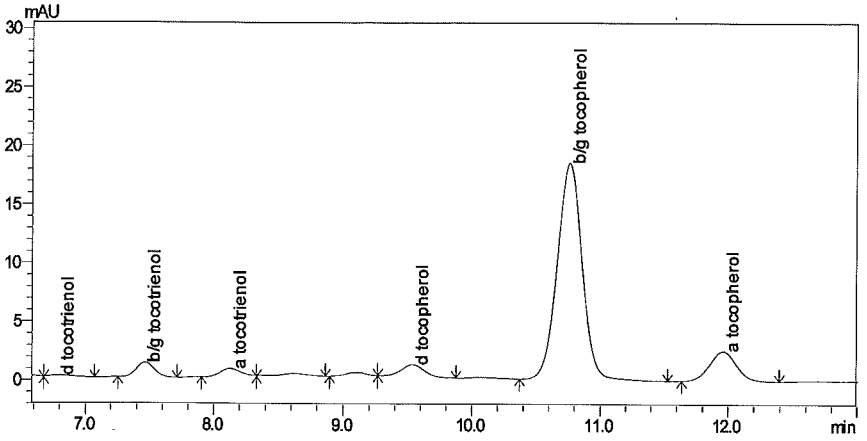

Figure 5. Chromatogram of tocopherol and tocotrienol isomers in corn oil.

γ-tocotrienol, and the presence of these major isomers has been reported by several researchers [7, 16-18].

Almost all the vitamin E in annatto seeds was made up of tocotrienols with a range of 88.28 to 100% (Table 2). Delta-tocotrienol was the highest, ranging from 54.17 to 95.53% of the total vitamin E content. By comparison, γ-tocotrienol made up 1.09 to 37.31% while α-tocotrienol made up 0 to 16.72% of the total vitamin E content (Table 2). The content of vitamin E in annatto fruit skin (29.72 μg/g) was much lower than the vitamin E content in the seed (Table 1), and for the skin, tocotrienols made up 99.23% (Table 2) of the vitamin E. The presence of significant levels α-tocotrienol in this study (Fig. 2) is unique as it has not been reported by other researchers [7, 16-18].

Table 1. Tocotrienols and tocopherols content (μg/g) in the seeds of the top 5 annatto accessions having the highest total tocotrienol content.

Accession	αT	αT3	βγT	βγT3	δT	δT3	T	T3	Total Vit E
Dry seed 1	12.12	14.06	19.25	582.56	2.3	3427.70	33.67	4024.33	4058.01
Dry seed 6	6.51	77.33	15.80	937.36	6.84	3087.32	29.15	4102.01	4160.31
Fresh seed 7	11.77	108.87	44.42	802.37	4.34	2561.41	60.53	3472.65	3533.18
Dry seed 9	ND	58.35	3.54	1005.49	ND	3359.09	3.54	4422.93	4426.47
Dry seed 15	10.41	ND	1.66	1543.80	2.15	2835.56	14.22	4379.36	4393.58
Mean values for 15 seed accessions (fresh and dry) (n=30)	23.22	57.22	17.20	406.57	10.86	1409.24	51.29	1873.03	1928.76
Range for 15 seed accessions (fresh and dry) (n=30)	ND-294.63	ND-157.23	1.45-72.84	7.75-1005.49	ND-101.05	284.37-3427.70	1.45-368.81	369.60-4422.93	377.87-4426.47
Annatto fruit skin (n=3)	ND	ND	ND	12.87	0.23	16.62	0.23	29.49	29.72

T = Tocopherol; T3 = Tocotrienol; ND = non detectable

Table 2. Tocotrienols and tocopherols content as % of total vitamin E in the seeds of the top 5 annatto accessions.

Accession	αT	αT3	βγT	βγT3	δT	δT3	T	T3
Dry seed 1	0.30	0.35	0.47	14.36	0.06	84.47	0.83	99.17
Dry seed 6	0.16	1.86	0.38	22.53	0.16	74.21	0.70	98.60
Fresh seed 7	0.33	3.08	1.26	22.71	0.12	72.50	1.71	98.29
Dry seed 9	ND	1.32	0.08	22.72	ND	75.89	0.08	99.92
Dry seed 15	0.27	ND	0.04	35.14	0.05	64.54	0.32	99.68
Mean data for 15 seed accessions (fresh and dry) (n=30)	0.93	4.30	1.33	19.43	0.74	73.07	3.00	96.79
Range for 15 seed accessions (fresh and dry) (n=30)	ND-9.37	ND-16.72	0.06-7.02	1.09-37.31	ND-7.84	53.67-93.51	0.06-11.72	88.28-99.94
Annatto fruit skin (n=3)	ND	ND	ND	43.31	0.77	55.92	0.77	99.23

T = Tocopherol; T3 = Tocotrienol; ND = non-detectable

Vegetable oils are a major source of vitamin E in the human diet, and the content of vitamin E in vegetable oils is shown in Table 3. Palm oil has the highest content of vitamin E, while olive oil has the lowest content and sunflower oil has the highest tocopherol content. Palm oil also has the highest tocotrienol content followed by rice bran oil (Table 3). Tocotrienol content was non-detectable in olive oil and was very low in sunflower and soybean oils.

Gamma-tocotrienol is the main tocotrienol in palm oil and rice bran oil, followed by α-tocotrienol. The percentage of tocotrienols and tocopherols as proportions of total vitamin E (Table 4) show that tocotrienols were the major vitamin E isomers in palm oil (74.38%) and rice bran oil (64.25%) and were only a very minor portion of the vitamin E in sunflower, soybean and corn oils.

Vitamin E is one of the most important antioxidants in animals and plants. It helps to protect unsaturated lipids in eukaryotic cells against free radicals that damage DNA and cause age-related pigmentation and skin ageing, cataract, neuritic plates in Alzheimer's disease, arteriosclerosis, stroke, heart attack and tumours [7-10]. Reviews in the literature [7, 19, 20] also show that high levels of α-tocopherol depress or attenuate the bioavailability of tocotrienols and interfere with the activity of tocotrienols in chemo-prevention against degenerative diseases. Paradoxically, a meta-analysis of human randomized controlled trials showed that natural but not synthetic α-tocopherol supplementation significantly increases all-cause mortality [19]. The annatto plant has a very high tocotrienol content, and indeed some accessions are virtually tocopherol-free. The reported tocotrienols in the literature contain about 90% δ-tocotrienol and 10% γ-

Table 3. Tocotrienols and tocopherols content (ug/g) in selected vegetable oils.

Sample	αT	αT3	βγT	βγT3	δT	δT3	T	T3	Total Vit E
Palm oil (n=3)	154.21	101.73	3.77	307.36	4.46	62.67	162.44	471.76	634.2
Soya bean oil (n=3)	27.44	3.64	79.62	ND	30.55	ND	137.61	3.64	141.25
Olive oil (n=2)	75.16	ND	2.44	ND	ND	ND	77.60	ND	77.60
Rice bran oil (n=2)	75.31	41.35	30.98	148.46	0.38	1.90	106.69	191.71	298.40
Sunflower oil (n=2)	345.09	ND	5.57	ND	ND	0.61	350.66	0.61	351.27
Corn oil (n=2)	39.08	8.41	57.95	9.56	2.51	ND	99.54	17.97	117.52

T = Tocopherol; T3 = Tocotrienol; ND = non-detectable

Table 4. Tocotrienols and tocopherols content as % of total vitamin E in selected vegetable oils.

Sample	aT	aT3	βγT	βγT3	δT	δT3	T	T3
Palm oil (n=3)	24.32	16.04	0.59	48.46	0.70	9.88	25.61	74.38
Soya bean oil (n=3)	19.43	2.58	56.37	ND	21.63	ND	97.42	2.58
Olive oil (n=2)	96.86	ND	3.14	ND	ND	ND	100	ND
Rice bran oil (n=2)	25.24	13.86	10.39	49.75	0.13	0.64	35.75	64.25
Sunflower oil (n=2)	98.24	ND	1.58	ND	ND	0.17	99.82	0.17
Corn oil (n=2)	33.25	7.16	49.31	8.14	2.13	ND	84.70	15.29

T = Tocopherol; T3 = Tocotrienol; ND = non-detectable

tocotrienol [7, 17, 18]. Researchers have reported that the order of potency among the isomers for cancer inhibition is δ-tocotrienol > γ-tocotrienol > α-tocotrienol where α-tocopherol is inactive and δ-tocopherol is weakly active. Delta-tocotrienol has been shown to inhibit the growth and survival of pancreatic cancer cells *in vitro* and *in vivo* [24, 25], and clinical trials sponsored by the US National Cancer Institute using pure δ-tocotrienol to treat pancreatic cancer patients is in progress at the Moffitt Cancer Center. In November 2011, the Malaysian government [26] announced funding for six clinical trials to be conducted by medical experts in U.S., Singapore and Malaysia to determine whether tocotrienols are able to prevent the recurrence of stroke, breast cancer tumour progression and colorectal cancer, and to prolong the survival of patients with prostate cancer. Two other projects also seek to investigate the effect of tocotrienols on diabetes mellitus, and ADHD (attention deficit hyperactive disorder).

This study detected significant levels of α-tocotrienol in some annatto accessions (up to 157.23 μg/g), a level higher than the content in palm oil. Several researchers [10, 21-23] have reported that α-tocotrienol has unique functions and was shown to protect rodents and canine brain from stroke damage, and they concluded that this isomer of tocotrienol is a natural neuroprotective agent. Besides oil palm, the seeds of the annatto plant are very rich sources of tocotrienols which are virtually tocopherol-free. Tan [7], Gee [19, 20] and Trias and Tan [27] have suggested that α-tocopherol should be eliminated, or at least reduced, in order to enhance the potency and bioavailability of the tocotrienol-rich fraction (TRF) for chemo-prevention. They also proposed that for vitamin E health supplements to be effective, it is desirable to enhance the δ-tocotrienol

and γ-tocotrienol contents in TRF as these forms have higher potencies for chemo-prevention of cancers and cardiovascular diseases.

REFERENCES

1. Brigelius-Flohe R. and Traber M.G. (1999) Vitamin E: function and metabolism. *The FASEB Journal* **13**(10): 1145-1155.
2. Chun J., Lee J., Lin Y., Exler J. and Eitenmiller R.R. (2006) Tocopherol and tocotrienol contents of raw and processed fruits and vegetables in the United States diet. *Journal of Food Composition and Analysis* **19**: 196-204.
3. Eitenmiller R.R. and Lee J. (2004) *Vitamin E: Food Chemistry. Composition and Analysis*. Marcel Dekker, New York.
4. Bauernfeind J. (1980) Tocopherols in foods. In Machlin L.J. (ed.) *Vitamin E: A Comprehensive Treatise* pp. 99-167. Marcel Dekker, New York.
5. Sattler S.E., Gilliland L.U., Magallanes-Lundback M., Pollard M. and DellaPenna D. (2004) Vitamin E is essential for seed longevity and for preventing lipid peroxidation during germination. *Plant Cell* **16**(6): 1419-1432.
6. Sheppard A.J., Pennington J.A.T. and Weihrauch J.L. (1993) Analysis and distribution of vitamin E in vegetable oils and foods. In Packer V.L. and Fuchs J. (eds.) *Vitamin E in Health and Disease* pp. 9-31. Marcel Dekker, New York.
7. Tan B. (2005) Appropriate spectrum vitamin E and new perspectives on desmethyl tocopherols and tocotrienols. *Journal on Nutraceuticals and Nutrition* **8**(1): 35-42.
8. Theriault A, Chao J.T., Wang Q., Gapor A. and Adeli K. (1999) Tocotrienol: a review of its therapeutic potential. *Clinical Biochemistry* **32**: 309-319.
9. Nesaretnam K. (2008) Multitargeted therapy of cancer by tocotrienols. *Cancer Letters* **269**: 388-395.
10. Sen C.K., Rink C. and Khanna S. (2010) Palm oil–derived natural vitamin E α-tocotrienol in brain health and disease. *Journal of the American College of Nutrition* **29**(3 Suppl.): 314S-323S.
11. Horwitt M.K. (1962) Interrelations between vitamin E and polyunsaturated fatty acids in adult men. *Vitamins and Hormones* **20**: 541-58.
12. Panfili G., Fratianni A., and Irano M. (2003) Normal phase high performance liquid chromatography method for the determination of tocopherols and tocotrienols in cereals. *Journal of Agricultural and Food Chemistry* **51**: 3940-3944.
13. Sundram K. and Rosnah M.N. (2002) Analysis of tocotrienols in different sample matrixes by HPLC. *Methods in Molecular Biology* **186**: 221-232.
14. Xu Z.M. (2002) Analysis of tocopherols and tocotrienols. In *Current Protocols in Food Analytical Chemistry* pp. D1.5.1-D1.5.12. John Wiley & Sons, Inc., New York.
15. Mardhati M., Wong H. K., Azim H. and Tan H.Y. (2012) Detection and identification of beta and gamma tocotrienol using reverse phase C18 silica column. In Wong H.K., Farahiyah I.J., Ainu Husna M.S.S., Tan H.Y. and Azim H. (eds.) *Proceedings of the 5th International Conference on Animal Nutrition*, pp.263-264. MARDI, Serdang, Selangor

16. Frega N., Mozzon M. and Bocci F. (1998) Identification and estimation of tocotrienols in the annatto lipid fraction by gas chromatography–mass spectrometry. *Journal of the American Oil Chemists' Society* **75**: 1723–1727.
17. Tan B. and Foley J. (2002) Tocotrienols and geranylgeraniol from *Bixa orellana* byproducts. United States Patent 6,350,453.
18. Tan B. and Llobrera J. (2013) Annatto extract compositions including tocotrienols and tocopherols and methods of use. United States Patent 8,586,109.
19. Gee P.T. (2011) Unleashing the untold and misunderstood observations on vitamin E. *Genes & Nutrition* **6**: 5-16.
20. Gee P.T. (2011) Vitamin E – essential knowledge for supplementation. *Lipid Technology* **23**(4): 79-82.
21. Khanna S., Roy S., Slivka A., Craft T.K., Chaki S., Rink C., Notestine M.A., DeVries A.C., Parinandi N.L. and Sen C.K. (2005) Neuroprotective properties of the natural vitamin E alpha-tocotrienol. *Stroke* **36**(10): 2258-2264.
22. Rink C., Christoforidis G., Abduljalil A., Kontzialis M., Bergdall V., Roy S., Khanna S., Slivka A., Knopp M. and Sen C.K. (2008) Minimally invasive neuroradiologic model of preclinical transient middle cerebral artery occlusion in canines. *Proceedings of the National Academy of Sciences USA* **105**(37):14100-14105.
23. Rink C., Christoforidis G., Khanna S., Peterson L., Patel Y., Khanna S., Abduljalil A., Irfanoglu O., Machiraju R., Bergdall V.K. and Sen C.K. (2011) Tocotrienol vitamin E protects against preclinical canine ischemic stroke by inducing arteriogenesis. *Journal of Cerebral Blood Flow and Metabolism* **31**(11): 2218-2230.
24. Husain K., Francois R.A., Yamauchi T., Perez M., Sebti S.M. and Malafa M.P. (2011) Vitamin E δ-tocotrienol augments the antitumor activity of gemcitabine and suppresses constitutive NF-κB activation in pancreatic cancer. *Molecular Cancer Therapeutics* **10:** 2363-2372.
25. Husain K., Centeno B.A., Chen D.T., Hingorani S.R., Sebti S.M. and Malafa M.P. (2013) Vitamin E δ-tocotrienol prolongs survival in the *LSL-Kras$^{G12D/+}$*; *LSL-Trp53$^{R172H/+}$*; *Pdx-1-Cre* (KPC) transgenic mouse model of pancreatic cancer. *Cancer Prevention Research* **6**:1074-1083.
26. Anon. (2011) (online at http://etp.pemandu.gov.my/Media_Release-@-Malaysia_invests_RM20_million_in_palm_oil_medical_research.aspx accessed on 18 March 2014).
27. Trias A.M. and Tan B. (2012) Alpha tocopherol: A detriment to tocotrienol benefits In Tan B., Watson R.R. and Preedy V.R. (eds.) *Tocotrienols: Vitamin E beyond tocopherols, Second edition* pp. 61-78. CRC Press, Boca Raton.

Journal of Science and Technology in the Tropics (2014) 10: 27-38

Description of a new species of *Topomyia* (*Topomyia*) *aliyusopi* (Diptera: Culicidae) from Kelabit highlands, Sarawak, Malaysia

Ichiro Miyagi[1,2*], Takako Toma[1,2], Takao Okazawa[3], Siew Fui Wong[4], Moi Ung Leh[4] and Hoi Sen Yong[5]

[1]The University Museum (Fujukan), University of the Ryukyus, Senbaru 1, Nishihara, Okinawa, 903-0213, Japan
[2]Laboratory of Mosquito Systematics of Southeast Asia and Pacific, c/o Ocean Health Corporation, 4-21-11, Iso, Urasoe, Okinawa, 901-2132 Japan
[3]Faculty of Medicine, Kanazawa University, Kakuma, Kanazawa, Ishikawa, 920-1192 Japan
[4]Sarawak Museum Department, 93566, Kuching, Sarawak, Malaysia
[5]Institute of Biological Sciences, University of Malaya, 50603 Kuala Lumpur, Malaysia
(*E-mail: topmiyagii@ybb.ne.jp)

Received 15-04-2014; accepted 28-04-2014

Abstract A new species, *Topomyia* (*Topomyia*) *aliyusopi* is described from Sarawak, Malaysia. The adult male, female, pupa and larva are described in detail and illustrations of the male genitalia, pupa and larva are provided. This species occurs in secondary rain forests in the Kelabit highlands, Bario and Ba'Kelalan at elevation from 1,000 to 1,700 m. It breeds mainly in the leaf axils of a wild banana (Musaceae), sometimes in those of taro (*Alocasia* sp.) and Screw pine (*Pandanus* sp.). The new species described in the present paper is attributed to Miyagi and Toma.

Keywords genus *Topomyia* – new species – phytotelmata – Kelabit highlands – Sarawak

INTRODUCTION

Topomyia is the Oriental genus, with most of the species occurring in Southeast Asia [1]. After the pioneer works by Leicester [2] and Edwards [3], extensive surveys for *Topomyia* mosquitoes throughout Peninsular Malaysia, Sarawak and Sabah were carried out by Ramalingam [4—6], Ramalingam *et al.* [7] and Miyagi *et al.* [8—21], and to our knowledge, 27 species of the genus have been described in these regions. The species of this genus generally show a high degree of endemism. Adult females of the genus are non-blood feeding mosquitoes and their immature stages are found exclusively in phytotelmata, cryptic mosquito habitats [22]. Therefore, taxonomic work of the genus still remains to be done.

Since 2005, in connection with the project "Study on taxonomy and bionomics of two winged flies, Diptera in Sarawak", with the coordination and cooperation of the Sarawak Museum in Kuching, extensive mosquito larval collections have been made in the secondary forest. Many collections of the genus *Topomyia* were

made from the Kelabit highlands, Bario in 2006 and Ba'Kelalan in 2007, 2008 and 2013. They included a series of adult males and females, larvae and pupae and associated exuviae.

In the course of investigating the collection, we have found some specimens with interesting male genitalia. As the result of close examination, it was found to be an undescribed species belonging to the subgenus *Topomyia* Leicester [23]. In the present paper, we describe the new species.

The terminology follows mostly Harbach and Knight [24], and Harbach and Peyton [25]. Holotype and some paratypes are deposited in the Smithsonian Institution, Washington D.C., USA, and some paratypes are in the Sarawak Museum, Kuching, Sarawak, Malaysia.

DESCRIPTION AND DISCUSSION

***Topomyia* (*Topomyia*) *aliyusopi* Miyagi and Toma new species** (Figs.1－3)

Description

Male (Fig.1) — Wing, 3.13 mm. Proboscis, 2.0 mm. Forefemur, 2.25 mm. Abdomen about 2.2 mm, long. Samll dark brown with silver markings on head and thorax. Head. Vertex, occiput and side of head covered with broad, flat, dark brown decumbent scales with blue lustre. A large patch of flat silvery scales present on vertex, similar patch on side of head below eye. Erect scales absent. One interocular and 4 or 5 ocular setae present. Clypeus elongate; dark brown integument, bare of scales. Maxillary palpus entirely covered with brown scales; about 0.15 of proboscis. Proboscis elongate, narrow at base and slightly enlarged towards distal end; ventral side of the proboscis has a pale line of scales on basal 1/3. Pedicel of antenna dark with few narrow scales on inner side. Flagellum pillose, approximately 1.8 mm, long. Thorax. Scutum covered with small, narrow, curved, brown scales, with a median line composed of two rows of flat, round, silvery scales; silver line extending all the way to the scutellum and getting slightly broader in the posterior third. Dorsocentral, humeral, supra-alar and prescutellar setae present. Central lobe of the scutellum covered with a patch of silver scales, side lobes with only brown scales dorsally and a row of setae on anterior side. Postpronotum covered with brown scales on upper 2/3 and with silvery scales on lower half; single seta present on posterior border. Four prespiracular setae present. Postspiracular setae absent. Paratergite bare. A large patch of round silvery scales covering the post- and subspiracular areas, mesokaptepimeron and the mesanepimeron. Several setae present in patches on prealar and upper mesepimeron. Leg. Coxae of all three legs with patches of silver scales. All legs covered dorsally with brown scales. A pale

line of scales present on the ventral side of the all legs; this line extending all the way down the femur to tarsi V. Foretarsomere Ta-I_2 slightly shorter than Ta-I_3, apical tarsomeres usually not elbowed. Ungues of all legs small, simple and

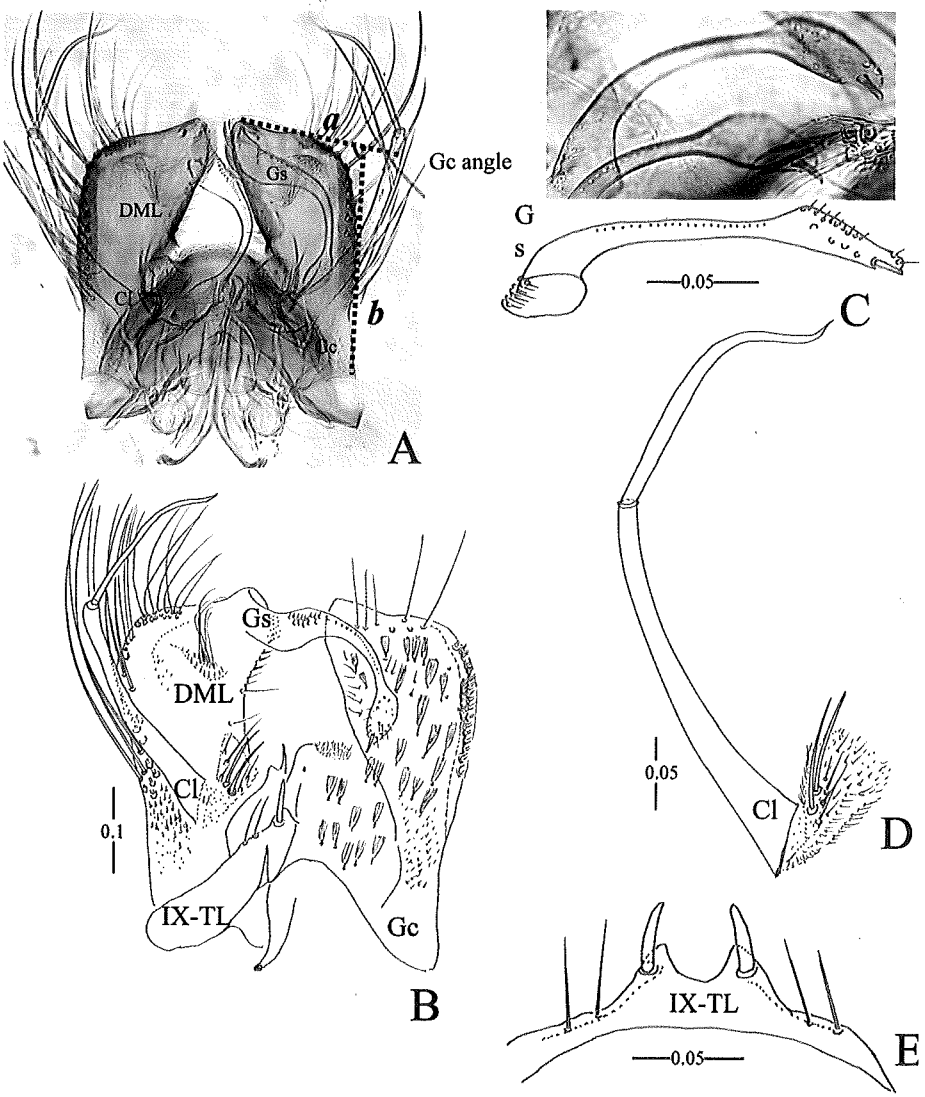

Figure 1. *Topomyia* (*Topomyia*) *aliyusopi,* n. sp. Male (A—E). A, genitalia in dorsal view (paratype: 20080823-2, G-13); B, genitalia (prerotaion sense), in dorsal (left) and ventral (right) views (holotype: 20130611-1, G-43); C, gonostylus (Gs) in lateral view (paratypes: 20060915-1, G-24; 20090902-4, G-66); D, Claspette (Cl) in dorsal view (holotype: G-43); E, Tergum IX (IX-TL). Gc, gonocoxite; DML, dorsomesal lobe; Gc angle, an angle of the point intersect lines ***a*** (horizontal line) with ***b*** (vertical line) of gonocoxite. Scales in mm.

equal in size. Wing. Brown scaled. Squame scales densely covering wing veins; plume scales narrow. Cell R_2 about 4.0 times the length of its stem. Anal vein ending beyond fork of Cu. Alula with several hair-like scales. Upper calypter bare. Haltere. Pedicael with light brown scales, capitellum scales darker. Abdomen. Terga I—VIII densely covered with dark brown scales, with the lateral aspect of each tergum having a strip of yellow-gold scales. Tergum I with several well developed setae dorsally. Sterna II—VIII entirely covered with flat, pale golden scales.

Male genitalia (Fig. 1A—D). As figured. Tergum IX broad, with the two lobes close to each other; each lobe bearing 2 minute lateral setae smaller than a flat, broad and pointed spinulate seta medially inserted. Sternite IX broadly conical and covered with scales and scattered setae; apical area with very fine setae. Gonocoxite narrow at base and broadest at distal end; length about 1.5 (1.4—2.0) its breadth at distal end (Fig. 1A, B); ventral aspect covered with many scales and fine setae uniformly; dorsal aspect with a row of about 20 long curved setae on outer lateral side and with a patch of several curved setae present on the distal end and some very fine setae present on the inner apical side of the gonocoxite (Fig. 1B). Dorsomesal lobe (DML) undeveloped with a row of 3—5 filamentous pale setae and with many fine setae laterally (Fig. 1A, B). Claspette (CL) is composed of a long slightly curved stem and with a narrow, elongate, curved spine with pointed filament; the stem is longer than the spine; ventral lobe bears a patch of setiforms, with 2—3 being more prominent than the others (Fig. 1A, B). Gonostylus (Gs) (Fig. 1C) slightly expanded from base to middle, with minute setae in cluster at base dorsally and with a row of several minute setae on middle dorsally. Apical part of gonostylus swollen remarkably like an oval, with a dark sharp gonostylar claw and several scattered minute setae. Paraproct elongate with pointed apex. Phalosome long and slender.

Female—Wing, 2.90—3.25 mm. Proboscis, 1.72—2.0 mm. Forefemur, 1.8—2.1 mm. Abdomen about 1.9 mm, long. Proboscis without pale ventral line. Leg. A pale ventral line present but not so clear as in the male. Foretarsomere Ta-I_2 slightly shorter than TaI_3, apical tarsomeres usually not elbowed.

Pupa (Fig. 2, Table 1) — Abdomen (I—VIII), mean 2.75 mm. Trumpet, mean 0.32 mm. Paddle, mean 0.53 mm. Integument of cephalothorax and abdomen pale yellow, with yellow brown stripes on dorsal aspect of abdominal segments I—VII. Chaetotaxy as figured. Seta 1-CT long bifid curved on the inside. Seta 1-I fanlike with aciculate dendritic branches. Setae 3-I—III, 5-IV—VI, 4-VIII long and single. *Cephalothorax* (Fig. 2B): Trumpet (T), dark yellow, with distinct sculpturing; index, mean 3.25. *Abdomen* (Fig. 2A, C), microtrichia present on all

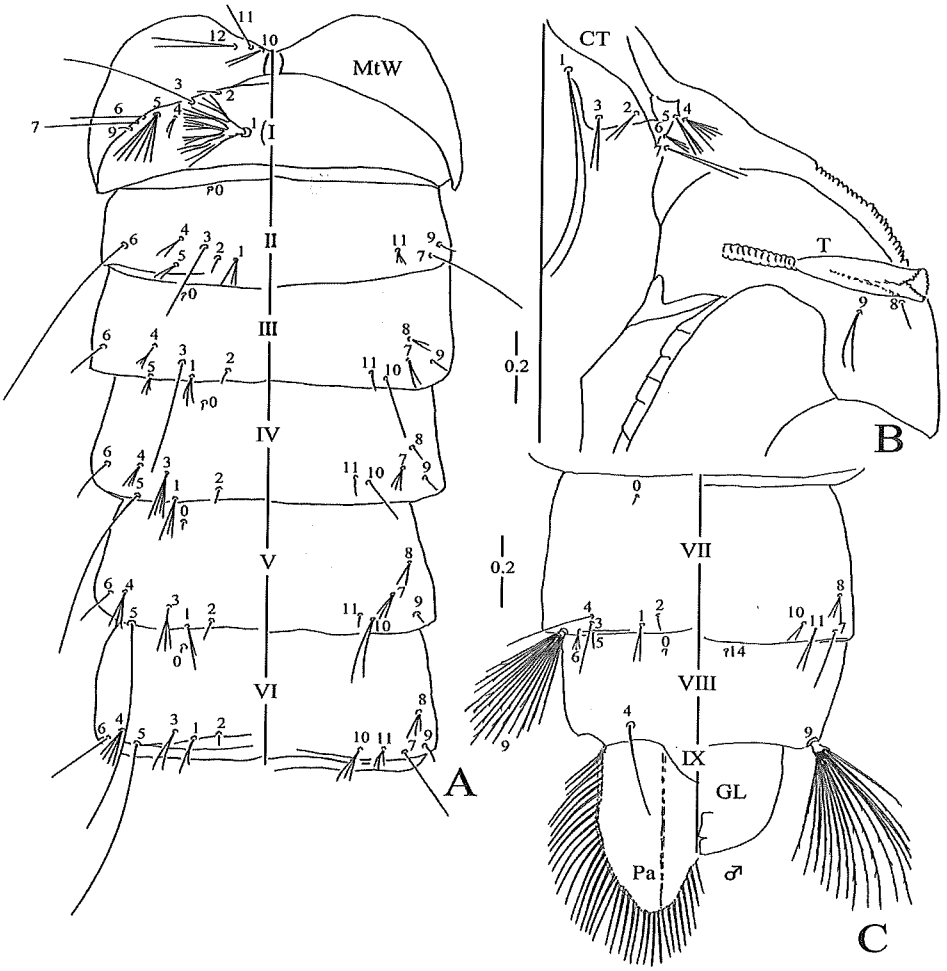

Figure 2. Pupal exuviae (A—C) of paratypes of *Topomyia* (*Topomyia*) *aliyusopi*, n. sp. A, metathoracic wing (MtW) and abdominal segments I—VI; B, cephalothorax (CT); C, abdominal segments VII—IX with male genital lobe (GL) and paddle (Pa); T, Trumpet. Scales in mm.

abdominal segments; setae 9-VII, VIII long many aciculated branched. Paddle with midrib from base to apex and with marginal long fringe of filamentous spicules. Male genital lobe large, extending to 0.64 of paddle, 0.38 in female lobe.

Fourth-instar larva (Fig. 3 A—E) — Head, length slightly shorter than width, 0.64—0.82 (mean, 0.76) of width. Siphon, 0.62—0.76 mm (0.67). Chaetotaxy of head, thorax and abdominal segments as Fig. 3. Setae lightly pigmented. Thorax seta 8-M conspicuous, 7—17 branched with forked-tip. Abdominal seta 8-II well developed, single. *Head*: Integument smooth, pale yellow in color. Maxillar

Table 1. Numbers of branches for pupae of *Topomyia* (*Topomyia*) *aliyusopi* n. sp.

Seta no	Cephalo-thorax	Abdominal segments							
		I	II	III	IV	V	VI	VII	VIII
0	-	-	1	1	1	1	1	1	1
1	2	M	2−5	3−7	2−7	1−6	1−5	1−3	-
2	2, 3	1, 2	1 (1, 2)	1	1	1	1	1	-
3	2, 3	1	1	1	3−5	1−3	1−3	1	-
4	1−5	1−3	2−4	1−4	2, 3	2−7	2−4	1, 2	1
5	2−6	3−7	2, 3	1−3	1	1	1	1	-
6	2−4	1	1	1 (1, 2)	1−3	1, 2	1	1−7	-
7	1−4	1	1 (1, 2)	2−5	1−5	3−5	1	1	-
8	1, 2	-	-	1−4	1−3	1−3	2−4	3−8	-
9	2	1, 2	1	1	1	1	1	22−35*	17−34*
10	1, 2	-	-	1−3	1−3	1, 2	1−4	1−3	-
11	1, 2	-	1-3	1, 2	1, 2	1−3	2−4	1, 2	-
12	1−4	-	-	-	-	-	-	-	-
14	-	-	-	-	-	-	-	-	1

M: dendritic with many branches. *Aciculated.
Obsolete and missing setae are shown with a hyphen (-).
Specimens examined: 5 pupal exuviae from Ba'kelalan, Mt, Murud, Sarawak, East Malaysia.

(Fig. 3, Mx); maxillary horn absent; apical tooth (AT) developed indistinctly. Dorsomentum (Dm) with a prominent middle tooth with 9 to 10 small regular teeth on either side. Seta 1-C single, prominent, about 0.17 mm, thick and slightly curved inwardly, with blunt end; setae 4−7 prominent, single; 14-C prominent, as long as or longer than 11-C, with 3−6 branches. *Antenna*: Long, 0.30−0.41 (0.34) mm; integument smooth, without spicules; seta 1-A single, placed at 0.73 from base. *Abdomen*: Abdominal setae 4-III−V long, usually single. Segment VIII: Comb scales 22−28 (24.3), in irregular row or patch; scale variable in size, pointed, without marginal fringe (Fig. 3, CS). Segment X (Fig. 3E): Saddle incomplete, several spicules present on caudolateral border; anal papilla tapering, longer than setae 4-X. Seta 1-X long, aciculated with 2 branches; 2-X single and simple; 3-X 9−15 branched, longer than seta 4-X which with 8−14 branched. Siphon (Fig. 3E): Pale yellow pigmentation, smooth integument. Seta 1-S paired with 5−8 branches; ventral setae (1a-S) 10−13 in numbers, each 2−7 branched on irregular line; ventral setae (2a-S) 11−17 in number (7 or 8 pairs, often 5, 6 pairs) each with 3−7 branches. Pecten teeth (Fig. 3, PT) variable in number, usually 10−25 extending from base to apical 0.23 but in some paratypes, 48−80 scattered from base to apex of the siphon; siphonal index variable, 4.47−6.63 (5.30).

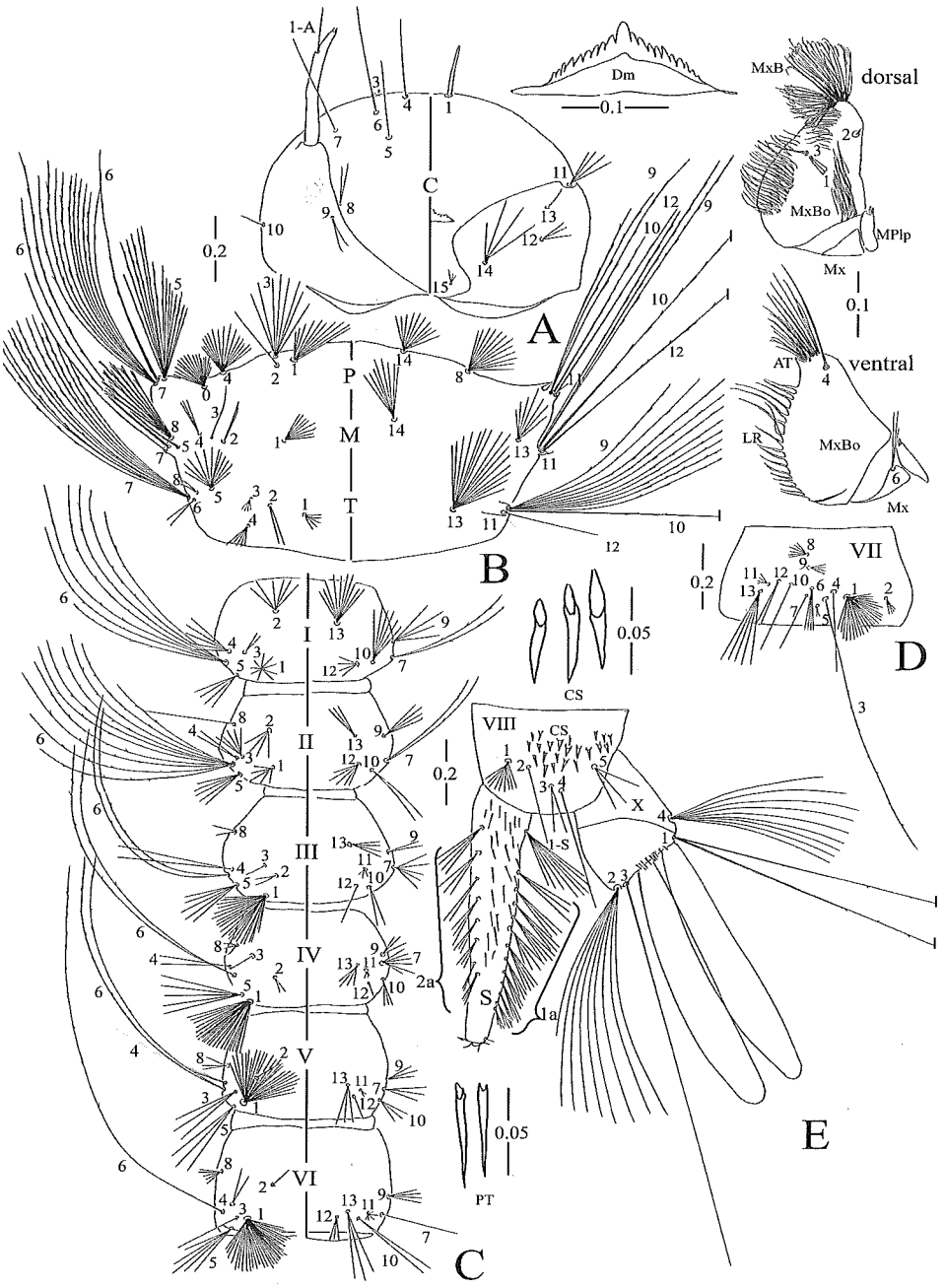

Figure 3. Paratypes of *Topomyia* (*Topomyia*) *aliyusopi,* n. sp. 4th-instar larva (A—E); A, head; B, thorax; C, abdominal segments I—VI; D, abdominal segment VII; E, abdominal segments VIII, X with siphon (S). 1-A, antennal seta 1; Dm, dorsomentum; Mx, maxilla; MPlp, maxillary palpus; MxB, maxillary brush; MxBo, maxillary body; AT, apical teeth; LR, laciniarastrum; CS, comb scale; PT, pecten; 1-S, 1a, ventral (posterior) setae of siphon; 2a, dorsal (anterior) setae of siphon. Scales in mm.

Table 2. Numbers of branches for fourth-instar larvae of *Topomyia* (*Topomyia*) *aliyusopi* n. sp.

Seta no	Heade	Thorax			Abdominal segments							
		P	M	T	I	II	III	IV	V	VI	VII	VIII
0	-	17−35	-	-	-	-	-	-	-	-	-	-
1	1	10−18	7−13	3−8	3−9	2−8	21−25†	20−28†	23−36†	26−34†	23−34†	11−17
2	-	1	1, 2	1, 2	6−14	3−9	1−4	1, 2	2, 3	1−3	1−10	1
3	1	6−9	1	3−8	2, 3	5−9	1	1, 2	2−4	1, 2	1*	2, 3
4	1	13−32	1−4	5−11	5−11	1, 2	1, 2	1−3	1	2−4	1	1
5	1, 2	15−18*	1*	11−27	4−7	5−8	3−6	5−7	2−5	3−7	2, 3	3−5
6	1	1*	1*	1−4	7−10*	9−11*	2*	2*	2*	1*	4−7	-
7	1	10−15*	1	11-18*	2, 3*	2, 3*	5−9	4−9	3−6	1	1, 2	1-X=2*
8	1−3	6−13	7−17**	1−5	-	1	2−4	2−4	3−5	6−13	6−10	
9	3−7	2−4*	2−4*	9−17*	4−9	5−7	3−5	3−7	2−7	3−9	3−7	2-X=9-15
10	1, 2	1*	1*	1*	6−15	1, 2	1−3	1−4	2−5	2	1, 2	
11	3−5	1, 2	1, 2	1, 2	-	-	3−5	2−4	2−4	5−8	4−7	3-X=1
12	2−5	1*	1*	1	2−6	5−10	1	1	1, 2	3−6	2−4	
13	1, 2	-	7−11	15−25	8−18	4−6	3−6	2−5	3−5	2−4	5, 6	4-X=8−14
14	3−6	6−12	8−16	-	-	-	-	-	-	-	-	
15	2−4	-	-	-	-	-	-	-	-	-	-	-

*Aciculated. **Forked-tipped. †Stellate.

Obsolete and missing setae are shown with a hyphen (-).

Specimens examined: 5 fourth-stage larvae from Ba'kelalan, Mt, Murud, Sarawak, Malaysia.

Type specimens

Holotype

♂ (20130611-1) on pin with L (larva) and P (pupa) exuviae mounted on slide 138 and G-43 with following collection data: *Mt. Murud, Sarawak, Malaysia on 11 June, 2013 by I. Miyagi and T. Okazawa.*

Paratypes

The following specimens collected in wild banana leaf axils, Ba'kelalan to Mt. Murud (01°49' 684"N,109°41' 720"E; Elevation, 1,000−1,500m above see level), *Sarawak, Malaysia on 10−14 June, 2013 by I. Miyagi and T. Okazawa*: 8 ♂♂ (20130610-1) with pupal (P) or/and larval (L) exuviae and genitalia (G) mounted on a slide (75), and genitalia (G-31), (82, G-32), (93, G-28), (135, G-41), (137, G-42), (G-1), (1,G-2) and (188); 4♂♂ (20130611-1) with (123, G-39), (78, G-29), (84, G-26), (138, G-43) and (90, G-33); 3 ♂♂ (20130811-1) with P, L on slides 109, 184, 191; 1♂ (20130614-7) with P, L (18, G-8); 11♀♀ (20130611-1) with P, L on 98, 103, 117, 121, 133, 172, 178, 182, 192, 195, 199. 7 whole larvae (20130610-1, 11-1).

Collected in wild banana leaf axils, Ba'kelala (1,000 m), on 23−26 August, 2008 by I. Miyagi and T. Toma: 4♂♂ (2080826-6) with P, L and G on slide (470, G-47), (466, G-45), (269, G-63) and (467, G-44); 1♂ (20080824-20) with (30, G-28); 1♂ (20080824-2) with (51, G-52); 1♂ (20080824-20) with (30, G-28); 1♂ (20080824-25) with (20, G-16); 2♂♂ (20080824-30) with P, L and G on slide (377, G-111), and (G-107); 1♂ (20080824-32) with (19, G-18); 5♂♂ (20080823-2) with P, L and G on slide (337, G-114), (15, G-13), (289, G-70), (315, G-101), (58); 2♂♂ (20080825-4) with (23, G-12), (395, G-108); 2♂♂ (20080826-4) with (31, G-29), (93, G-35).

Collected in wild banana leaf axils, Bario (3°44' 27" N, 115°27" 59" E; Elevation 1,066m), *on August−September, 2007. I. Miyagi and T. Toma*: 1♂ (20070909-16) with P, G (349, G-137), (463, G-146); 1♂ (20070909-2) with P, L and G (330, G-158); 1♂ (20070904-29) with P, L, G(162, G-173); 5♂♂ (20070904-2) with (395, G-140), (329, G-154), (345, G-165), (394, G-143), (133, G-167); 1♂ (20090902-4) with (174, G-66); 1♂ (20060915-1) with (301, G-24).

Etymology

The species name *aliyusopi* is in honour of Haji Ali Bin Yusop, Director of Forest Department of Sarawak for his kind support and granting permission for sampling of two-winged flies in the Pulong Tau National Park.

Taxomic discussion

In general appearance, the adult and immature stages of *Topomyia aliyusopi* are very similar and may be confused with *Topomyia sabahensis* Ramalingam and Ramakrisna, 1988 [7] from Sabah and *Topomyia tenuis* Edwards, 1922 [3] from

Peninsular Malaysia but easily differentiated by the details of male genitalia: 1. Gonocoxite with a patch of several (8—13) curved setae on outer distal corner; 2. Gonostylus is swollen remarkably like oval at apical part; and 3. Dorsomesal lobe of gonocoxite is indistinctly developed with 3 to 5 weak, filamentous pale setae and many fine setae. In order to compare general appearance of male genitalia in dorsal (prerotation sense) aspect, an angle of outer apical corner of gonocoxite (Gc) is employed here as Gc angle. The angle is measured on a point intersect lines ***a*** (vertical line of outer lateral Gc) with ***b*** (horizontal line of apical Gc) as shown in Fig. 1A. The angle is right, 80—100° in *To. aliyusopi*, but 60—70° in description of *To. sabahensis* [7].

The larva of *To. aliyusopi* is very similar to *To. sabahensis*, the only reliable distinction is found in thoracic, abdominal and siphonal setae. In *To. aliyusopi*, the seta 8-M is specialized, 7—17 forked-tipped branched, abdominal seta 4-V very long and single, and 12 (6 pairs) of 1a-S, while in *To. sabahensis*, 8-M is 3—5 simple branched, seta 4-V short 2—6 branched and 1a-S with 8 or 10 (4 or 5 pairs). The larva of *To. aliyusopi* shows variation in the index and number of seta tufts (1a- and 2a-S) and pecten of the siphon. These morphological variations, we suspect, may be owing to some environmental variations in the larval habitat. In the individual larval rearing, the genital characters of the species are uniform in the specimens examined.

Clear distinctions of females and setal branches in the pupal stages could not be found between *To. aliyusopi* and *To. sabahensis*. Female, pupa and larva of *To. tenuis* are not known.

Biological notes

Topomyia aliyusopi is a high mountain species. The immature stages were collected from mountain forest at an elevation of 1,000—1,700 m of Ba'Kelalan and Bario in the leaf axils of wild banana (Musaceae), sometimes in taro and screw pine (*Pandanus* sp.). This species was found to breed in association with *Topomyia* (*Suaymyia*) *auriceps*, *Topomyia* (*Topomyia*) sp. near *Topomyia malaysiensis* and *Malaya genurostris*.

Distribution

Sarawak, Malaysia. So far known only from Bario and Ba'Kelalan, Kelabit highlands.

Acknowledgements — We wish to express our gratitude to the Forest Department of Sarawak for granting permission for sampling of the two-winged flies (Diptera) and for providing facilities in Lepo Bunga, the Pulong Tau National Park.

REFERENCES

1. Walter Reed Biosystematics Unit (2011) *Systematic Catalog of Culicidae.* Water Reed Biosystematics Unit [accessed July 1, 2011]. hittp://www.mosquito catalog. org/
2. Leicester G.F. (1908) The Culicidae of Malaya. *Studies of Medical Research Federated Malay States* **3**: 18—261.
3. Edwards F.W. (1922) A synopsis of adult Oriental Culicidae (including Megarhinine and Sabethine) mosquitoes. Part II. *Indian Journal Medical Research* **10**: 430—475.
4. Ramalingam S. (1975) A new species of *Topomyi*a from Peninsular Malaysia (Diptera: Culicidae). *Mosquito Systematics* **7**: 185—192.
5. Ramalingam S. (1983) *Topomyia haughtoni* Feng, a new record in Malaysia and a redescription of the adult and immature stages. *Mosquito Systematics* **15**: 33—40.
6. Ramalingam S. and Banu Q. (1987) Studies on the genus *Topomyia:* 2. Description of a new species from Sabah, Malaysia (Diptera: Culicidae). *Tropical Biomedicine* **4**: 119—124.
7. Ramalingam S. and Ramakrishna K. (1988) Studies of the genus *Topomyia* 1. A new species from Sabah, Malaysia. *Mosquito Systematics* **20**: 33—40.
8. Miyagi I., Toma T., Ramakrishna K. and Ramalingam S. (1989) Studies on the genus *Topomyia*: 3. Redescription of *spathulirostris* and transfer to the subgneus *Suaymyia. Mosquito Systematic* **21**: 40—49.
9. Miyagi I., Toma T. and Ramalingam S. (1989) *Topomyia (Topomyia) hardini*, a new species from Sarawak Malaysia (Diptera: Culicidae). *Tropical Biomedicine* **6**: 91—98.
10. Miyagi I., Toma T. and Ramalingam S. (1990) *Topomyia (Topomyia) yongi*, a new species of mosquito from Peninsular Malaysia (Diptera: Culicidae). *Mosquito Systematics* **22**: 185—191.
11. Miyagi I. and Toma T. (2005) *Topomyia roslihashimi*, a new species of the subgenus *Suaymyia* (Diptera: Culicidae) from Gombak, Peninsular Malaysia. *Medical Entomology and Zoology* **56**: 275—282.
12. Miyagi I., Toma T. and Okazawa T. (2006) Redescription of *Topomyia argenteoventralis* Leicester, 1908 (Diptera, Culicidae) from Malaysia. *Medical Entomolgy and Zoology* **57**: 347—354.
13. Miyagi I. and Toma T. (2007) A redescription of *Topomyia decorabilis* Leicester, 1908 (Diptera, Culicidae) from Malaysia and Indonesia. *Medical Entomology and Zoology* **58**: 251—259.
14. Miyagi I. and Toma T. (2007) A new mosquito of the genus *Topomyia* (Diptera: Culicidae) from *Nepenthes* pitcher plants in a Bario highland of Sarawak, Malaysia. *Medical Entomology and Zoology* **58**: 164—174.
15. Miyagi I. and Toma T. (2008) Description of a new species *Topomyia (Suaymyia) lehcharlesi* (Diptera: Culicidae) from Sarawak, Malaysia. *Medical Entomology and Zoology* **59**: 163—170.
16. Miyagi I., Okazawa T., Toma T., Higa Y. and Leh M.U. (2009) Culicidae and Corethrellidae (Diptera) collected in Sarawak, Malaysia from 2005 to 2008. *Sarawak Museum Journal* **66**: 313—331.
17. Miyagi I. and Toma T. (2010) Descriptions of *Topomyia auriceps* Brug and

Topomyia pseudoauriceps, n. sp. from Sarawak, Malaysia (Diptera: Culicidae). *Medical Entomology and Zoology* **61**: 27—38.

18. Miyagi I. and Toma T. (2010) *Topomyia (Suaymyia) kelabitensis* (Diptera: Culicidae), a new species from Sarawak, Malaysia. *Medical Entomology and Zoology* **61**: 353—361.
19. Miyagi I., Toma T., Okazawa T. and Leh M.U. (2011) Description of pupa and larva of the Malaysian mosquito *Topomyia (Topomyia) rubithoracis* Leicester (Diptera, Culicidae). *Medical Entomology and Zoology* **62**: 93—99.
20. Miyagi I., Toma T., Okazawa T., Wong S. F., Leh M. U. and Yong H. S. (2012). Three new phytotelma mosquitoes of the genus *Topomyia* (Diptera: Culicidae) from Katibas, Lanjak-Entimau, Sarawak, Malaysia. *Journal of Science and Technology in the Tropics* **8**: 97—117.
21. Miyagi I., Okazawa T. Toma T. Higa Y., Wong S. F., Leh M. U. and Yong H. S. (2013) A redescription of *Topomyia trifida* Edwards (Diptera: Culicidae) from Sarawak, Malaysia. *Journal of Science and Technology in the Tropics* **9**: 103—111.
22. Mogi M. (2000) Phytotelmata: cryptic mosquito habitats. In F.S.P. Ng and H.S. Yong (eds) *Mosquitoes and mosquito-borne diseases* pp. 255—272. Academy of Sciences Malaysia, Kuala Lumpur.
23. Thurman E.B. (1959) *A Contribution to a Revision of the Culicidae of Northern Thailand. Bull. A-100,* 182 pp. University of Maryland Agriculture Experiment Station, Maryland.
24. Harbach R.E. and Knight K.L. (1980) *Taxonomists' glossary of mosquito anatomy*. Plexus Publishing Inc., Marlton.
25. Harbach R.E. and Peyton E.L. (1993) Morphology and evolution of the larval maxilla and its importance in the classification of the Sabethini (Diptera: Culicidae). *Mosquito Systematics* **25**: 1—16.

Journal of Science and Technology in the Tropics (2014) 10: 39-44

Gnetum gnemon (Gnetaceae) : a new host plant of carambola fruit fly *Bactrocera carambolae* (Insecta: Tephritidae)

Hoi Sen Yong[1,*], Phaik Eem Lim[1,2], Ji Tan[1,2] and I. Wayan Suana[3]

[1]Institute of Biological Sciences, University of Malaya, 50603 Kuala Lumpur, Malaysia
[2]Institute of Ocean and Earth Sciences, University of Malaya, 50603 Kuala Lumpur, Malaysia
[3]Faculty of Science and Mathematics, Mataram University, Mataram, Indonesia
(*Email: yong@um.edu.my)

Received 30-04-2014; accepted 12-05-2014

Abstract The carambola fruit fly *Bactrocera carambolae* was reared from the small variety of *Gnetum gnemon* fruit. This is a first record of a gymnosperm serving as host plant for *B. carambolae*. Another Dacine fruit fly *Bactrocera mcgregori* was reared from the large variety of *G. gnemon* fruit. The infestation rate was low. In a sample of 77 big-sized *G. gnemon* fruits from University Malaya campus, 48 larvae successfully pupated, an incidence of 0.62 fly per fruit. Sixteen adult flies emerged from the 48 pupae, indicating a pupal mortality of 66.66%. Three species of braconid wasps – *Fopius arisanus*, *Diachasmimorpha longicaudata* and *Psytallia* cf *makii* – parasitized different developmental stages of these fruit flies.

Keywords new host plant – *Bactrocera mcgregori* – braconid parasitoids – biocontrol agents – Kuala Lumpur – Penang – Malaysia

INTRODUCTION

The carambola fruit fly *Bactrocera carambolae* is a member of the *Bactrocera dorsalis* species complex [1, 2]. It occurs in Malaysia and other parts of Southeast Asia, and had been introduced into Guyana, Suriname, French Guiana and Brazil [3]. It is of especial economic importance, infesting a great variety of fruit and vegetable crops. The damage may be tremendous and limit production and cultivation of affected crops.

In Asia, over 70 species in 28 families have been recorded to be host plants of *B. carambolae* [4–6]. In Peninsular Malaysia, *B. carambolae* is the predominant taxon attacking fruits of Combretaceae, Myrtaceae, Oxalidaceae, Sapindaceae and Sapotaceae [6, 7]. We report here a new host plant *Gnetum gnemon* L. (Gnetaceae) which is also a new host-plant family for *B. carambolae*.

MATERIALS AND METHODS

Two kinds of ripe *Gnetum gnemon* fruit (Fig. 1), small and big varieties from different trees, were collected over the years during fruiting seasons. They were brought back to the laboratory and kept in screened plastic aquaria with suitable substrate for the larvae to develop and pupate [5]. Pupae were collected and placed in small plastic tubes for development. Emerging adult fruit flies were collected and identified. Parasitoids that emerged were also recorded.

RESULTS AND DISCUSSION

The small and big varieties of *G. gnemon* fruit were attacked by different species of *Bactrocera* fruit flies (Table 1). *Bactrocera carambolae* (Fig. 2) was the only

Table 1. *Bactrocera* fruit flies and parasitoids from two varieties of *Gnetum gnemon* fruit.

Fruit variety	Location	Fruit flies	Parasitoids
Small	UM, Kuala Lumpur	*B. carambolae* (10♂♂, 22♀♀)	*Fopius arisanus* (1♂, 2♀♀)
Big	UM, Kuala Lumpur	*B. mcgregori* (8♂♂, 8♀♀)	None
Big	Penang	*B. mcgregori* (1♀)	*F. arisanus* (6♂♂, 5♀♀) *Diachasmimorpha longicaudata* (1♀), *Psytallia* cf *makii* (1♂)

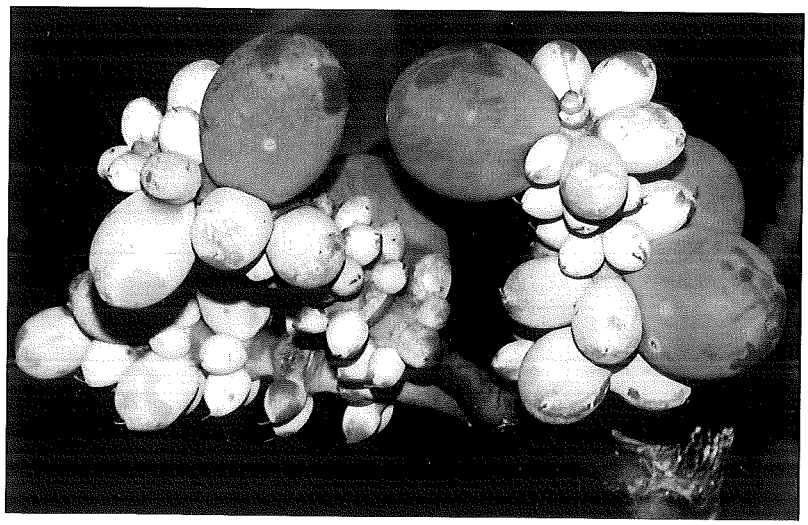

Figure 1. Small variety of *Gnetum gnemon* fruit. (photo: H. S. Yong)

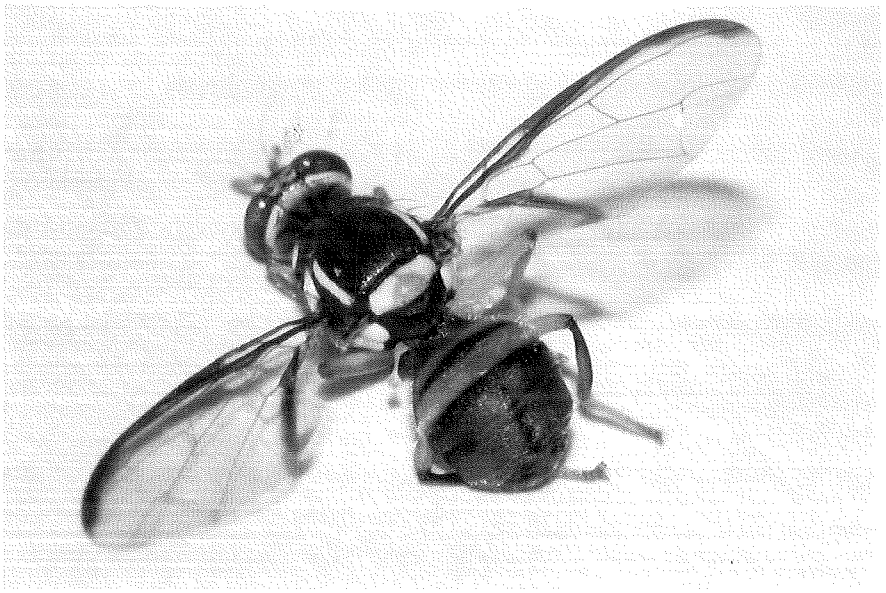

Figure 2. *Bactrocera carambolae*. (photo: H. S. Yong)

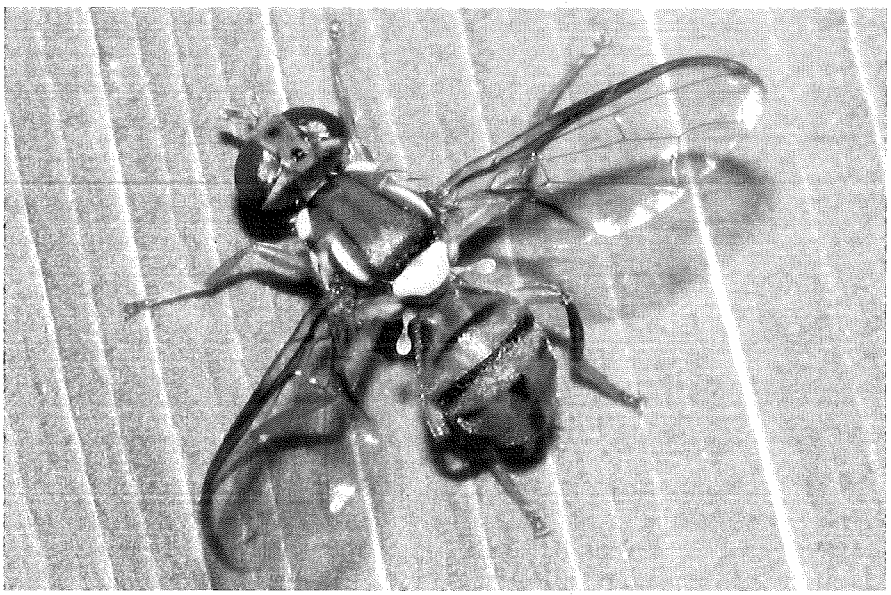

Figure 3. *Bactrocera mcgregori*. (photo: H. S. Yong)

fruit fly species recovered from fruits of the small variety of *G. gnemon* fruit collected in the University of Malaya campus from March 2010 to January 2013 (Table 1). This is a new host species record and also a new plant family record for *B. carambolae*. Interestingly *G. gnemon* is a gymnosperm; hitherto only

angiosperms have been recorded as host plants of *B. carambolae*. Most of the fruits were however not attacked by this fruit fly.

Bactrocera mcgregori (Fig. 3) was recovered from the big variety of *G. gnemon* fruit; *G. gnemon* has been recorded as host of this fruit fly in the Philippines and Singapore [8], Peninsular Malaysia [9] and Car Nicobar Island [10]. However in Fiji, *G. gnemon* is the host of *Bactrocera gnetum* [11]. In Suriname, no fruit flies were recovered from *Gnetum nodiflorum* [12]. The factor(s) influencing the selection of big-sized *G. gnemon* fruit by *B. mcgregori* need to be investigated.

For the big-sized *G. gnemon* fruits collected in University Malaya campus in December 2012, 48 pupae resulted from 77 fruits, i.e. an average of 0.62 fly per fruit. The emergence rate was 33.33% (16/48 pupae), indicating high pupal mortality.

Braconid parasitoids were recovered from the pupae of the fruit flies infesting both the small- and big-sized *G. gnemon* fruits (Table 1). Of these braconid wasps, *Fopius arisanus* (Fig. 4) has short ovipositor and parasitises the egg stage of fruit fly, while *Dichasmimorpha longicaudata* (Fig. 5) has long ovipositor and parasitises the later instar of the fruit fly larvae. *Psytallia* cf *makii* (Fig. 6) and another common species *Fopius vandenboschi* have ovipositor of intermediate length and parasitise the early instars of the fruit fly larvae. These braconid parasitoids together act as effective biocontrol agents of tephritid fruit flies.

In summary, *G. gnemon* constitutes a new host plant as well as a new host plant family for the carambola fruit fly *B. carambolae*. Only small-sized *G. gnemon* fruits appeared to serve as host for *B. carambolae*. The big-sized *G. gnemon* fruits

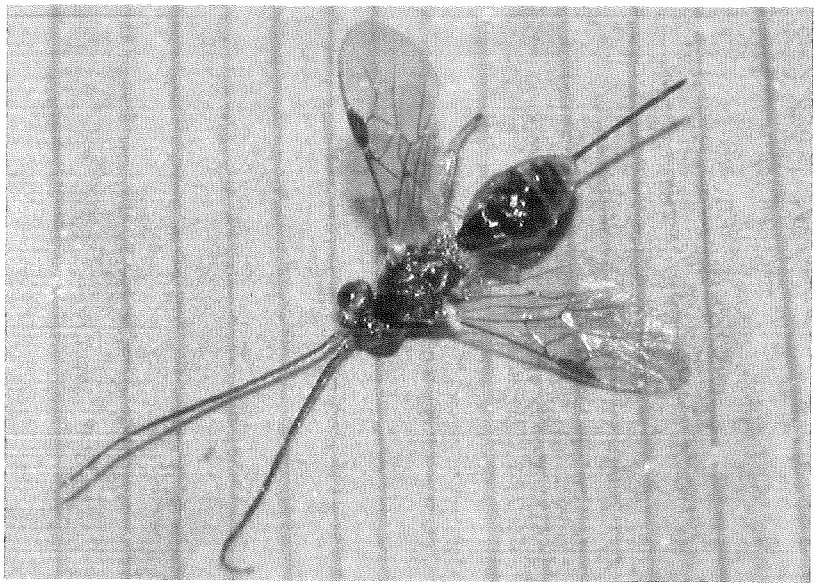

Figure 4. *Fopius arisanus* female. (photo: H. S. Yong)

were host to *B. mcgregori*. Three species of braconid wasps – *F. arisanus*, *D. longicaudata* and *P.* cf *makii* – parasitized different development stages of these fruit flies.

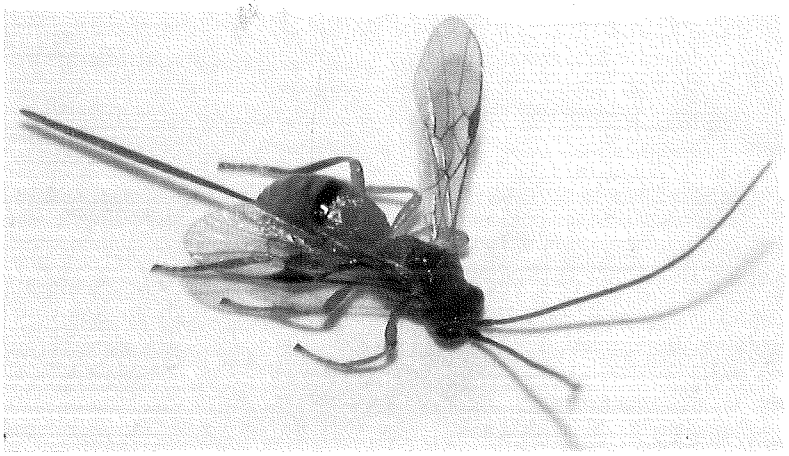

Figure 5. *Diachasmimorpha longicaudata* female. (photo: H. S. Yong)

Figure 6. *Psytallia* cf *makii* male. (photo: H. S. Yong)

Acknowledgements – We would like to thank our institutions for their support of our collaborative research. This study is funded in part by MoHE-HIR grant (H-50001-00-A000025) and University of Malaya (H-5620009).

REFERENCES

1. Drew R.A.I. and Hancock D.L. (1994) The *Bactrocera dorsalis* complex of fruit flies (Diptera: Tephritidae: Dacinae) in Asia. *Bulletin of Entomological Research* Suppl. 2, 68 pp.
2. Yong H.S. (1995) Genetic differentiation and relationships in five taxa of the *Bactrocera dorsalis* complex (Insecta: Diptera: Tephritidae). *Bulletin of Entomological Research* **85**: 431-435.
3. Carroll L.E., White I.M., Freidberg A., Norrbom A.L., Dallwitz M.J. and Thompson F.C. (2002 onwards) *Pest fruit flies of the world.* Version: 8th December 2006. Available: http://deltaintkey.com.
4. Allwood A.J., Chinajariyawong A., Kritsaneepaiboon S., Drew R.A.I., Hamacek E.L., Hancock D.L., Hengsawad C., Jipanin J.C., Jirasurat M., Kong Krong C., Leong C.T.S. and Vijaysegaran S. (1999) Host plant records for fruit flies (Diptera: Tephritidae) in Southeast Asia. *Raffles Bulletin of Zoology* Supplement n. 7: 1-92.
5. Ranganath H.R. and Veenakumari K. (1995) Notes on the dacine fruit flies (Diptera: Tephritidae) on Andaman and Nicobar Islands. *Raffles Bulletin of* Zoology **43**: 235–238.
6. Yong H.S. (1994) Host fruit preferences in two sympatric taxa of the *Bactrocera dorsalis* complex (Insecta: Diptera: Tephritidae). In Yong H.S. and Khoo S.G. (eds) *Current Research in Tropical Fruit Flies and Their Management* pp 1–8. The Working Group on Malaysian Fruit Flies, Kuala Lumpur.
7. Yong H.S. (1996) Host specificity and response to chemicals in Dacinae fruit flies (Insecta: Diptera: Tephritidae). In Turner I.M., Diong C.H., Lim S.S. and Ng P.K.L. (eds) *Biodiversity and the Dynamics of Ecosystems*. DIWPA Series Volume **1**: 191-194.
8. Hardy D.E. (1973) The fruit flies (Tephritidae – Diptera) of Thailand and bordering countries. *Pacific Insects Monograph* **31**: 1-353.
9. Yong H.S. (1994) The Gnemon fruit fly. *Nature Malaysiana* **19**: 37–40.
10. Ranganath H.R. and Veenakumari K. (1999) Notes on the Dacine fruit flies (Diptera: Tephritidae) of Andaman and Nicobar Islands – II. *Raffles Bulletin of Zoology* **47**(1): 221-224 .
11. Vueti E.T. (2000). Fruit flies in Fiji Island. *Pest Advisory Leaflet No. 28*. Secretariat of the Pacific Community, Suva.
12. van Sauers-Muller A. (2005) Host plants of the Carambola Fruit Fly, *Bactrocera carambolae* Drew & Hancock (Diptera: Tephritidae), in Suriname, South America. *Neotropical Entomology* 34(2): 203-214.

Journal of Science and Technology in the Tropics (2014) 10: 45-58

Nonlinear ion modes in a dense multi-ion plasma with strongly coupled ions and degenerate electrons

A. Paul[1], G. Mandal[1,*], A. A. Mamun[2] and M. R. Amin[1]
[1]Department of Electronics and Communications Engineering, East West University, Aftabnagar, Dhaka 1212, Bangladesh
[2]Department of Physics, Jahangirnagar University, Savar, Dhaka 1342, Bangladesh
(*E-mail: gdmandal@ewubd.edu)

Received 28-02-2014; accepted 07-05-2014

Abstract The nonlinear propagation of electrostatic ion modes in a dense relativistic degenerate strongly coupled plasma has been investigated by employing the reductive perturbation technique. It has been shown that the amplitude of the nonlinear electrostatic wave is not significantly changed when different ion viscosity is considered and that is slightly higher for strongly coupled plasmas for both weakly-relativistic and ultra-relativistic degenerate electron fluid. Also it has been observed that up to a certain limit the phase velocity of the nonlinear wave is drastically reduced for weakly coupled plasma and phase velocity is increased with heavy negative ion.

Keywords dense plasma – multi-ion plasma – coupling parameter – weakly-relativistic and ultra-relativistic degenerateelectron – shock waves

INTRODUCTION

There are many cases in the universe where matter has evolved to extreme physical conditions. Examples includewhite and brown dwarfs [1-3] and neutron stars (where the gravitational force of collapse is balanced by the quantumforces exerted by electrons and nuclear matter), black holes (where the force of gravity has won out over all other forcesand the mass density is so high that even light is gravitationally bound) and super-earth terrestrial planets aroundother stars [4]. Chandrasekhar [5-9] and Chandrasekhar and Tooper [10] have studied the matter under extremeconditions, which occurs in compact astrophysical objects and planetary systems. Recently, astrophysical aspects ofhigh density have been discussed by Fortov [11].

It is now established that degenerate electron fluids and strongly coupled non-degenerate ions are present in highdensityplasmas. Non-degenerate ions are strongly coupled because Coulomb coupling parameter Γ_i is greater thanunity, *i.e.*, $Z_i e^2/a_i k_B T_i > 1$, where Z_i is the ion charge state, e is the magnitude of electron charge, $a_i = (3/4\pi n_i)^{1/3}$ is the inter-ion spacing, n_i is the ion number density, k_B is the Boltzmann constant and T_i is the ion temperature. Itis known that when electrons are packed together, as they are in a white dwarf (white dwarf

stars have low luminosityand high surface emissivity, with masses typically less than $1M_{\odot}$ and radii typically less than $10^{-2}R_{\odot}$, where $M_{\odot}$ and $R_{\odot}$ are respectively the solar mass and radius [12]); the number of available low energy states is too small andmany electrons are forced into high energy states. When this happens, the electrons are said to be degenerate.

These high energy electrons make a significant contribution to the pressure and to deduce this electron pressure, one mustuse Fermi-Dirac statistics. Chandrasekhar [5, 7] derived a general expression for the relativistic electron degeneracy pressure, $P_e = (\pi m_e c^5/3\hbar^3)\left[\alpha(2\alpha^2-3)(\alpha^2+1)^{1/2}+3sinh^{-1}\alpha\right]$, where m_e is the electron rest mass, c is the speedof light in vacuum, $\hbar = h/2\pi$ where h is the Planck's constant, and $\alpha = p_e/m_e c$ with $p_e = (3\hbar^2 n_e/8\pi)^{1/3}$ being the momentum of an electron on the Fermi surface and n_e is the electron number density. The explicit expressions for P_e in weekly-relativistic limit are characterized by $\alpha \ll 1$ and that in ultra-relativistic limit is characterized by $\alpha \gg 1$.The expression of the degeneracy pressure can be written as

$$P_e = Kn_e^{\gamma} \tag{1}$$

where

$$\gamma = \frac{5}{3}, K = \frac{3}{5}\left(\frac{\pi}{3}\right)^{1/3}\frac{\pi\hbar^2}{m_e} \simeq \frac{3}{5}L_c\hbar c, \tag{2}$$

for the weekly-relativistic degenerate electron fluid ($L_c = \pi\hbar/m_e c = 1.2\times10^{-10}cm$) and

$$\gamma = \frac{4}{3}, K = \frac{3}{4}\left(\frac{\pi^2}{9}\right)^{1/3}\hbar c \simeq \frac{3}{4}\hbar c, \tag{3}$$

for the ultra-relativistic degenerate electron fluid [12].

To investigate linear and non-linear properties of electrostatic and electromagnetic waves, some authors [13-25] have used pressure laws (1) and (2) in their studies. They have used non-relativistic quantum hydrodynamic [13] andquantum magneto-hydrodynamic [17] models and have assumed either immobile ions or non-degenerate uncorrelatedmobile ions. It turns out that the presence of the latter and degenerate ultra-relativistic electrons with pressure law(3), admits one-dimensional (1-D) localized ion modes (IMs) supported by linear and nonlinear ion inertial forces and the pressure of degenerate electron fluid in a dense unmagnetized quantum plasma. Also, Mendonca and Serbeto [26] discussed modified Volkov solutions of the Dirac equation for electrostatic and electromagnetic waves in relativisticquantum plasmas.

Recently, Shukla *et al.* [12] have studied the properties of weakly nonlinear IMs in a dense quantum plasma composedof degenerate electron fluid and strongly coupled non degenerate ion fluid. They have considered one-dimensionalnonlinear

propagation of electrostatic IMs associated with inertialess degenerate electron fluids and strongly nondegenerate inertial ions in an unmagnetized plasma. They have shown the effects of ion correlations and electrondegeneracy on speed, width, and amplitude of both shock and solitary waves.

The negative ion plasma consists of negative ion and positive ion species in addition to electrons. It is now wellknown that considerable numbers of negative ions are present in the Earth's ionosphere [27,28] and cometarycomae[29]. More over, negative ions were found to outperform positive ions in plasma etching, therefore, the importanceof negative ion plasmas to the field of plasma physics is growing [30]. Recently, Cassini spacecraft conclusivelydemonstrated the presence of heavy negative ions in the upper region of atmosphere [31]. The nonlinear propagationof ion acoustic waves in a dense multi-ion quantum plasma is also one of the rapidly growing research areas in plasmaphysics.

Relativistically degenerated electrons occur in densities where the electron Fermi energy approaches the electronrest mass energy. Such high densities occur in astrophysical environments such as white dwarf stars, where the densityis about one million times higher than solid density.

Shukla *et al.* [12] studied the electron and ion plasma, and the existence of heavy negative ion in the same situation influence us to consider multi-ion plasma. Thus, in this paper, we study different properties of weakly nonlinear IMs in a dense quantum multi-ion plasma composed of degenerate electron fluid, strongly coupled non-degenerate ion fluid and heavy negative ion. To describe the dynamics of the IMs, here, we use the ion continuity equation and viscoelastic ion momentum equation [32-35], the inertia less electron momentum equation with the pressure laws (2) and (3), and Poisson's equation. We are particularly interested to observe the change of electrostatic potential with the change of relativistic and coupling parameters.

The paper is organized as follows. The basic governing equations describing the model are stated in the next section.By using the standard reductive perturbation technique[36-38], the Burgers' equation is derived in the section titled "derivation of Burgers' Equation". Then thesolution of Burgers' equation is analyzed in terms of different plasma parameters and the conclusion is stated after the analysis.

GOVERNING EQUATIONS

We consider a 1-D nonlinear propagation of electrostatic IMs associated with inertialess degenerate electron fluid,strongly coupled nondegenerate inertial ions, and heavy negative ion in an unmagnetized dense plasma. The nonlinear dynamics of IMs insuch a dense multi-ion plasma system is described by the following set of equations.

$$\frac{\partial n_i}{\partial t} + \frac{\partial}{\partial x}(n_i u_i) = 0, \tag{4}$$

$$en_e \frac{\partial \phi}{\partial x} - \frac{\partial P_e}{\partial x} = 0 \tag{5}$$

$$D_\tau \left[m_i n_i D_t u_i + Z_i e n_i \frac{\partial \phi}{\partial x} + k_B T_{ef} \frac{\partial n_i}{\partial x} \right] = \eta_l \frac{\partial^2 u_i}{\partial x^2}, \tag{6}$$

$$\frac{\partial^2 \phi}{\partial x^2} = 4\pi e(n_e - Z_i n_i + Z_h n_{h0}), \tag{7}$$

where u_i is the component of ion fluid velocity along the x-axis, t and x are respectively time and space variables, ϕ is the electrostatic potential, $D_\tau = 1 + \tau_m(\partial/\partial t + u_i\,\partial/\partial x)$, $D_t = \partial/\partial t + u_i\,\partial/\partial x$, where τ_m is the viscoelasticion relaxation time, m_i is the ion mass, $T_{ef}(= \mu_i T_i + T_*)$ is the effective ion temperature ($\mu_i T_i$and T_* arising fromthe ion thermal pressure and electrostatic interaction among strongly positive ions respectively), where μ_i is the ioncompressibility, η_l is the longitudinal ion viscosity coefficient, Z_h is the charge state of heavy negative ions and n_h is the number density of heavy negative ions. Here, the values of μ_i, T_* and τ_m are given by [12, 33-35, 39]:

$$\mu_i = \frac{1}{k_B T_i}\frac{\partial P_i}{\partial n_i} = 1 + \frac{1}{3}u(\Gamma_i) + \frac{\Gamma_i}{9}\frac{\partial u(\Gamma_i)}{\partial \Gamma_i}, \tag{8}$$

$$T_* = \frac{N_{nn}}{3}\frac{Z_i^2 e^2}{a_i k_B}(1+\kappa)e^{-\kappa}, \tag{9}$$

$$\tau_m = \frac{\eta_l}{n_{i0} k_B T_i}\left[1 - \mu_i + \frac{4}{15}u(\Gamma_i)\right]^{-1}. \tag{10}$$

where N_{nn} is determined by the ion structure and corresponds to the number of nearest neighbors (in thispaper, we consider $N_{nn} = 8$ for a body-centered cubic lattice in crystalline state), $\kappa = a_i/\lambda_D$, where λ_D is the Thomas-Fermi screening length, and $u(\Gamma_i)$ is a measure of the excess internal energy of the system. For weakly coupled plasmas, we have $\Gamma_i < 1$ and $u(\Gamma_i) \simeq -(\sqrt{3}/2)\Gamma_i^{3/2}$ [35]. For strongly coupled plasmas, $\Gamma_i > 1$, we have $u(\Gamma_i) \simeq -0.89\Gamma_i + 0.95\Gamma_i^{1/4} + 0.19\Gamma_i^{-1/4} - 0.81$ [40], where a small correction term due to a finite number of particles has been neglected.

Eqs. (5)-(7) are coupled with the electron number density n_e and it is determined from eqs. (1)-(3) and (4):

$$n_e = n_{e0}\left[1 + \frac{(\gamma-1)e\phi}{\gamma K n_{e0}^{\gamma-1}}\right]^{1/(\gamma-1)} \tag{11}$$

or,

$$n_e \simeq n_{e0}\left[1 + \frac{C_1}{1!}e\phi - \frac{C_2}{2!}(e\phi)^2 + \frac{C_3}{3!}(e\phi)^3 - \cdots\right] \tag{12}$$

where $C_1 = 1/\gamma K n_{s0}^{\gamma-1}$, $C_2 = (\gamma-2)/\gamma^2 K^2 n_{s0}^{2(\gamma-1)}$ and $C_3 = (\gamma-2)(\gamma-3)/\gamma^3 K^3 n_{s0}^{3(\gamma-1)}$.

DERIVATION OF BURGERS' EQUATION

To derive a dynamical equation for the nonlinear propagation of the shock wave, we use equations (4), (6)-(7) and (12),and employ reductive perturbation technique [36]. We introduce the stretched coordinates [37, 38]: $\xi = \epsilon(x - V_p t)$ and $\tau = \epsilon^2 t$ where ϵ is a smallness parameter $(0 < \epsilon < 1)$ that measures the weakness of the dispersion, and V_p is the phase speed of the electrostatic IMs. Now we expand the variables n_i, u_i and ϕ in the power series of ϵ:

$$n_i = n_{i0} + \epsilon n_i^{(1)} + \epsilon^2 n_i^{(2)} + \ldots\ldots, \quad (13)$$

$$u_i = \epsilon u_i^{(1)} + \epsilon^2 u_i^{(2)} + \ldots\ldots, \quad (14)$$

and

$$\phi = \epsilon\phi^{(1)} + \epsilon^2\phi^{(2)} + \ldots\ldots \quad (15)$$

Now substituting these expressions in equations (4) and (6)-(7), we get equations of different powers of ϵ. For thelowest power of ϵ, we get the following set of relations:

$$u_i^{(1)} = \frac{V_p s}{C_\hbar^2 \sigma_i m_i}\phi^{(1)}, \quad (16)$$

$$n_i^{(1)} = \frac{n_{s0} s}{C_\hbar^2 m_i}\phi^{(1)}, \quad (17)$$

$$V_p = C_\hbar\sqrt{\beta_T\left(1 + \frac{Z_i\sigma_i}{\beta_T}\right)}. \quad (18)$$

where $\sigma_i = n_{i0}/n_{s0}$, $\beta_T = k_B T_{sf}/Z_i\gamma K n_{s0}^{\gamma-1}$ and $C_\hbar = \left(Z_i\gamma K n_{s0}^{\gamma-1}/m_i\right)^{1/2}$. To the next higher order of ϵ, we getthe following set of relations:

$$\frac{\partial n_i^{(2)}}{\partial\xi} = A_1\frac{\partial\phi^{(2)}}{\partial\xi} - A_2\phi^{(1)}\frac{\partial\phi^{(1)}}{\partial\xi}, \quad (19)$$

$$\frac{\partial u_i^{(2)}}{\partial\xi} = -\frac{1}{n_{i0}}\frac{\partial n_i^{(1)}}{\partial\tau} + \frac{V_p}{n_{i0}}\frac{\partial n_i^{(2)}}{\partial\xi} - \frac{1}{n_{i0}}\frac{\partial}{\partial\xi}\left(n_i^{(1)}u_i^{(1)}\right), \quad (20)$$

where $A_1 = C_1 e n_{s0}/Z_i$ and $A_2 = C_2 e^2 n_{s0}/Z_i$. From (19)-(20) for $n_i^{(2)}$, $u_i^{(2)}$ and $\phi^{(2)}$ along with (16)-(17) for $n_i^{(1)}$, $u_i^{(1)}$ and $\phi^{(1)}$, we derive the following nonlinear dynamical equation for the shock wave:

$$\frac{\partial \phi^{(1)}}{\partial \tau} + A\phi^{(1)}\frac{\partial \phi^{(1)}}{\partial \xi} = C\frac{\partial^2 \phi^{(1)}}{\partial \xi^2}, \quad (21)$$

where $A = Y/X$, $C = Z/X$, $X = 2eV_p n_{s0}/C_h^2$,

$Y = V_p^2[(\gamma - 2) + 2/Z_i\sigma_i]/\mu C_h^2 + \mu - (\gamma - 2)\beta_T$,

$Z = e\eta_i V_p/C_h^2\sigma_i m_i$ and $\mu = e^2 n_{s0}^{2-\gamma}/\gamma K$.

Equation (21) is the well known Burgers' Equation describing the nonlinear propagation of Shock waves.

SOLUTION OF THE BURGERS' EQUATION

We are interested to find the solution of Burgers' equation (21) for the stationary shock wave solution, by considering $\zeta = \xi - U_0\tau'$ and $\tau' = \tau$, where, in the reference frame, U_0 is the shock wave speed. This leads us to write (21), under the steady state condition $\partial/\partial\tau' = 0$, as

$$-U_0\frac{\partial \phi^{(1)}}{\partial \zeta} + A\phi^{(1)}\frac{\partial \phi^{(1)}}{\partial \zeta} = C\frac{\partial^2 \phi^{(1)}}{\partial \zeta^2}. \quad (22)$$

From [37, 41], we can easily show that, (22) describes the shock waves, whose speed U_0 is related to the extreme values $\phi(-\infty)$ and $\phi(\infty)$ by $\phi(\infty) - \phi(-\infty) = 2U_0/A$. Therefore, ϕ is bounded at $\zeta = \pm\infty$, under this condition, the shock wave solution of (22) is [37, 41]

$$\phi = \phi_0\left[1 - tanh\left(\frac{\zeta}{\Delta}\right)\right], \quad (23)$$

where $\phi_0 = 2U_0/A$ and $\Delta = 2C/U_0$ are respectively the height and thickness of the shock waves.

NUMERICAL RESULTS AND GRAPHICAL REPRESENTATION

To have some numerical appreciation of the results of this investigation, we have numerically analyzed the waveamplitude, the width of the wave and the profile for the potential $\phi \equiv \phi^{(1)}$ of the shock wave considering the following set of parameters: $n_{i0} = 3.2 \times 10^{15}/cm^3$, $n_{s0} = 2.2 \times 10^{15}/cm^3$, $n_{h0} = 1.2 \times 10^{13}/cm^3$, $\sigma_i = 16/11$, $Z_i = 100$, $m_p = 1.6 \times 10^{-24}gm$, $U_0 = 7.2 \times 10^4 cm/s$, $m_s = 9.1 \times 10^{-28}gm$, $m_i = 39m_p$, where m_p is the proton mass, $h = 6.63 \times 10^{-27}erg - second$, $k_B = 1.38 \times 10^{-16}erg/K$, T_i varies between $1900K - 2500K$ [42, 43].The results are displayed in Figs. 1-9.

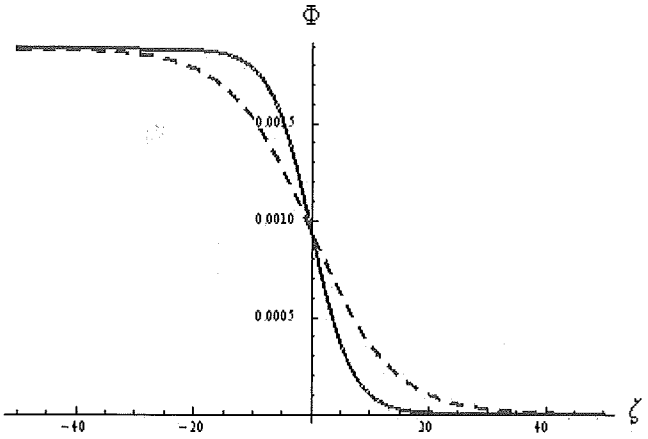

Figure 1. The variation of the solution Φ of the Burgers' equation with ζ for $\gamma = 5/3, T_i = 2319K, \Gamma_i = 3$, longitudinal ion viscosity coefficient $\eta_l = 0.1$ (solid curve) and $\eta_l = 0.2$(dotted curve).

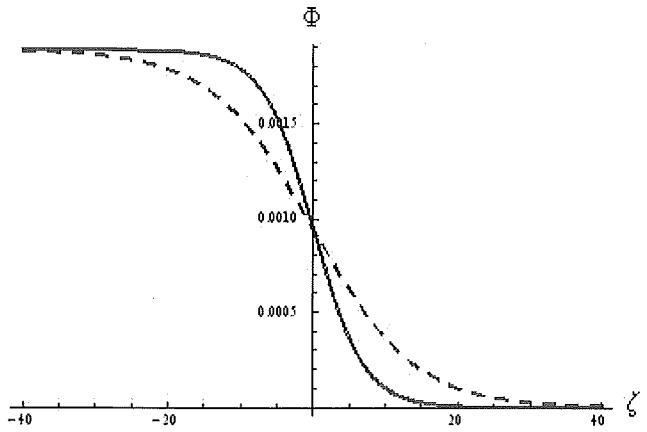

Figure 2. The variation of the solution Φ of the Burgers' equation with ζ for $\gamma = 4/3$, $T_i = 2319K$, $\Gamma_i = 3$, longitudinal ion viscosity coefficient $\eta_l = 0.1$ (solid curve) and $\eta_l = 0.2$ (dotted curve).

Figures 1 and 2 show the variation of the solution of the Burgers' equation, the wave potential $\phi = \phi^{(1)}$, as a function of the transformed position variable ζ. Solid line and dotted lines are plotted for different values of ion viscosity coefficient η_l. For these figures, a strongly coupled multi-ion quantum plasma with weakly relativistic and ultra-relativistic degenerate electrons are considered respectively. It is noticed that the ion viscosity effect is not pronounced. The shock wave behavior can be seen from the figures with positive potential.

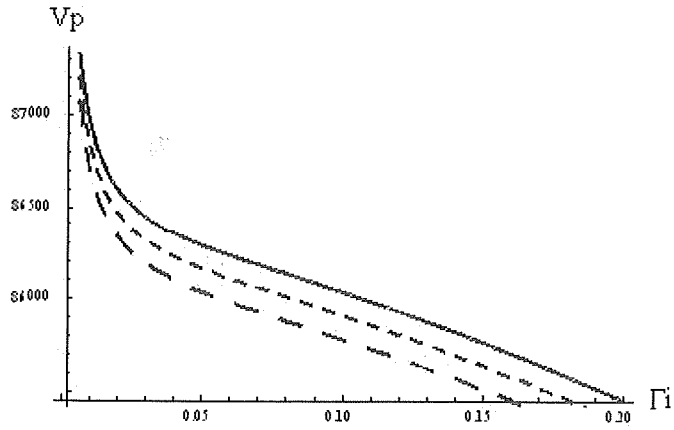

Figure 3. The variation of the wave phase velocity V_p with the coupling parameter Γ_i for weakly coupled plasma where $\eta_l = 0.1$, $\gamma = 5/3$, and Ti = 2320K (solid curve), $T_i = 2310K$ (dotted curve), $T_i = 2300K$ (dashed curve).

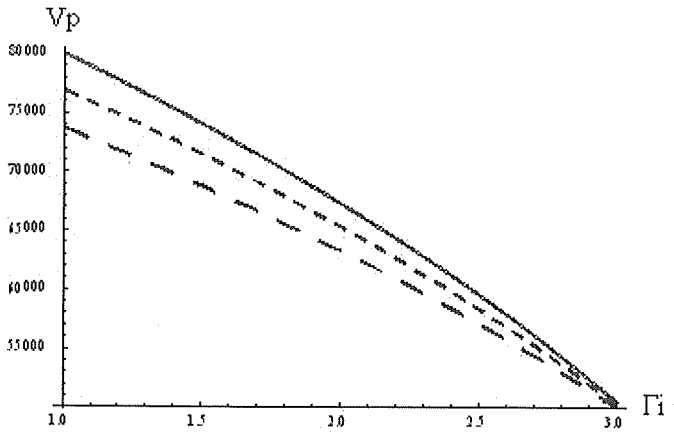

Figure 4. The variation of the wave phase velocity V_p with the coupling parameter Γ_i for strongly coupled plasma where $\eta_l = 0.1$, $\gamma = 4/3$, and Ti = 2500K (solid curve), $T_i = 2200K$ (dotted curve), $T_i = 1900K$ (dashed curve).

Figures 3 and 4 display the variation of the phase velocity of the shock wave, V_p, as a function of the coupling parameter Γ_i, for weakly relativistic and ultra-relativistic degenerate fluid respectively. In Figure 3, the solid curve is for $T_i = 2320K$, whereas the dotted curve and the dashed curve represent the phase velocities for $T_i = 2310K$ and $T_i = 2300K$ respectively. In Figures 3 and 4, it is found that the coupling effect parameter plays a significant role in the phase velocity. In Figure 4, the solid curve is for $T_i = 2500K$, whereas the dotted

curve and the dashed curve represent the phase velocities for $T_i = 2200K$ and $T_i = 1900K$ respectively. We found that up to a certain limit the phase velocity is drastically dropped for the weakly coupled plasma (Fig. 3) whereas for strongly coupled plasmas the phase velocity drops slowly (Fig. 4) everywhere. We also observed, in both figures, that as the ion temperature (T_i) increases the phase velocity also increases.

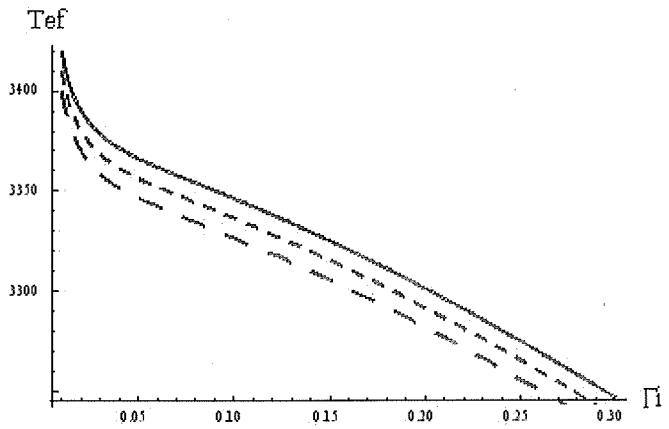

Figure 5.The variation of the effective ion temperature T_{ef} with the coupling parameter Γ_i for weakly coupled plasma where $\kappa = 9.1 \times 10^{-5}$, $N_{nn} = 8$ and $T_i = 2320K$ (solid curve), $T_i = 2310K$ (dotted curve), $T_i = 2300K$ (dashed curve).

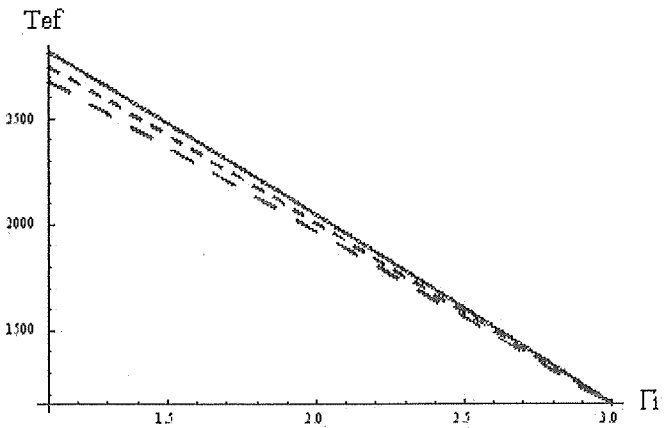

Figure 6. The variation of the effective ion temperature T_{ef} with the coupling parameter Γ_i for strongly coupled plasma where $\kappa = 9.1 \times 10^{-5}$, $N_{nn} = 8$ and $T_i = 2500K$ (solid curve), $T_i = 2400K$ (dotted curve), $T_i = 2300K$(dashed curve).

Figures 5 and 6 display the variation of the effective ion temperature, $T_{\beta f}$, as a function of the coupling parameter Γ_i, for the weakly and strongly coupled plasma respectively. In Figure 5, the solid curve is for $T_i = 2320K$, where as the dotted curve and the dashed curve represent the effective ion temperature for $T_i = 2310K$ and $T_i = 2300K$ respectively. In Figure 6, the solid curve is for $T_i = 2500K$, whereas the dotted curve and the dashed curve represent the effective ion temperature for $T_i = 2400K$ and $T_i = 2300K$ respectively. It is

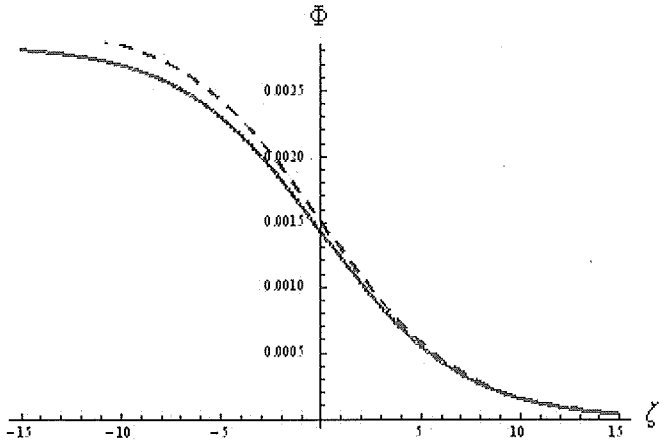

Figure 7. The variation of the solution ϕ of the Burgers' equation with ζ for $\gamma = 5/3$ (weakly relativistic), $\eta_1 = 0.1$, and coupling parameter $\Gamma_i = 0.8$ (solid curve), $\Gamma_i = 1.2$ (dotted curve).

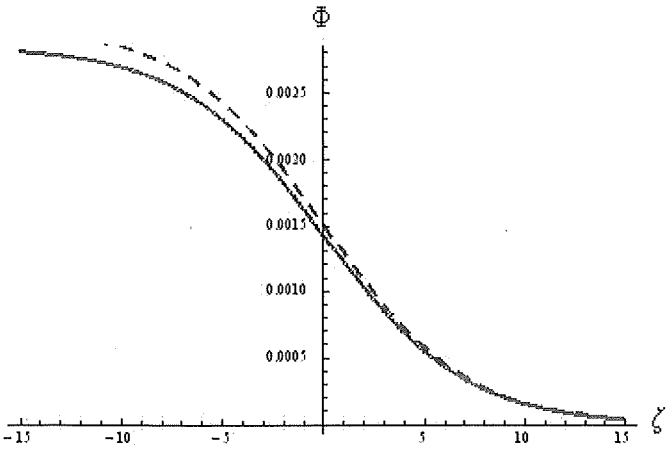

Figure 8. The variation of the solution ϕ of the Burgers' equation with ζ for $\gamma = 4/3$ (strongly relativistic), $\eta_1 = 0.1$, and coupling parameter $\Gamma_i = 0.8$ (solid curve), $\Gamma_i = 1.2$ (dotted curve).

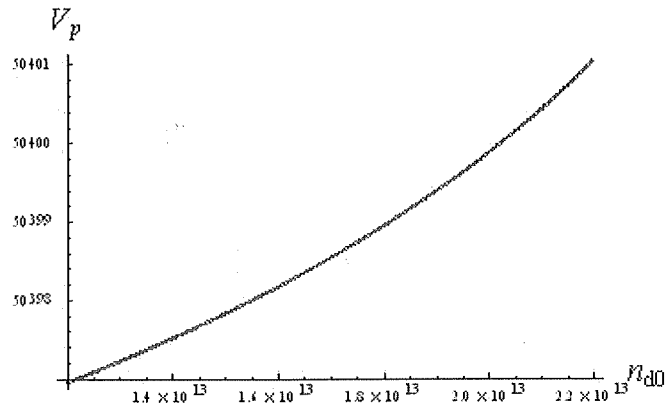

Figure 9. The variation of the wave phase velocity V_p with the heavy negative dust number density n_{h0} where $\eta_l = 0.1$, $\gamma = 5/3$, and Ti = 2320K.

observed that in both the cases by increasing the value of T_i, T_{ef} increases. In fig. 6, the slopes of the curves remain almost same.

Figures 7 and 8 show the variation of the solution of the Burgers' equation, ϕ, as a function of the transformedposition variable ζ for weakly relativistic and ultra-relativistic degenerate fluid respectively. In both figures, the solidcurve and the dotted curve represent the wave potential for $\Gamma_i = 0.8$ and $\Gamma_i = 1.2$ respectively. The shock wavebehavior can be seen from the figures with positive potential. It has been found from these figures that electrostaticpotential is slightly higher for strongly coupled plasmas for both weakly-relativistic and ultra-relativistic degenerateelectron fluid.

Figure 9 displays the variation of the phase velocity of the shock wave, V_p, as a function of the heavy negative ion n_{h0}. It is observed that when heavy negative ion number density, n_{h0} increases in this multi-ion quantum plasma then the value of phase velocity, V_p also increases.

CONCLUSION

In this paper, the nonlinear propagation of electrostatic ion modes in a dense relativistic degenerate strongly coupledplasma is studied. By utilizing the standard reductive perturbation method, the Burgers' equation is derived for thesystem. The propagation of the nonlinear shock wave is considered by analyzing the solution of the derived Burgers'equation. It is observed that the ion viscosity does not have noticeable effects on the amplitude of the shock wavebut the potential always slightly higher for strongly coupled plasmas for both weakly-relativistic and ultra-relativisticdegenerate electron fluid.

We have also studied the phase velocity of the electrostatic wave and the effective ion temperature with respectto the coupling parameter Γ_i and the ion temperature T_i. Up to a certain limit the phase velocity is drasticallyreduced for weakly coupled plasmas whereas for strongly coupled plasmas the phase velocity drops slowly with Γ_i. But the phase velocity is increased in the increment of density of heavy negative ion. Itis further observed that no effect of ion temperature is found on both the phase velocity and the effectiveion temperature.The results, which have been obtained from this investigation, would be useful in understandingthe properties of the shock waves in multi-ion plasmas.

REFERENCES

1. Harwit M. (1973)*Annu. Rev. Astron. Astrophys*, Wiley, New York.
2. Gursky H. (1976)*Frontiers of Astrophysics*. Harvard University Press, London.
3. Shapiro S.I. and Teukolsky S.A. (1983)*A Black Holes, White Dwarfs, and Neutron Stars: The Physics of Compact Objects*.Wiley, New York.
4. Fortney J.J., Glenzer S.H., Koenig M., Militzer B., Saumon D. and Valencia D. (2009)*Phys. Plasmas***16**: 041003.
5. Chandrasekhar S. (1931)TheDensity of White Dwarf Stars, Philosophical Magazine.*Phys. Plasmas***11**: 592.
6. Chandrasekhar S. (1931) The Maximum Mass of Ideal White Dwarfs? *Astrophys. J.***74**: 81.Chandrasekhar S. (1935) Stellar Configurations with Degenerate Cores (Second Paper).*Monthly Notices of the Royal Astronomical Society***95**: 676.
7. Chandrasekhar S. (1939) *An Introduction to the Study of Stellar Structure*. Dover, New York.
8. Chandrasekhar S. (1964) Dynamical Instability of Gaseous Masses Approaching the Schwarzschild Limit in General Relativity.*Phys. Rev. Lett.***12**: 114.
9. Chandrasekhar S. and Tooper R.F. (1964) The Dynamical Instability of the White-Dwarf Configurations Approaching the Limiting Mass.*Astrophys. J.***139**: 1396.
10. Fortov V.E. (2009) Extreme states of matter on Earth and in space.*Phy. Usp.***52**: 615.
11. Shukla P.K., Mamun A.A. and Mendis D.A. (2011) Nonlinear ion modes in a dense plasma with strongly coupled ions and degenerate electron fluids. *Phys. Rev. E***84**: 026405.
12. Manfredi G. (2004) How to model quantum plasmas. *Proceedings of the Workshop on Kinetic Theory: Fields Institute*, Toronto.
13. Shukla P.K. and Eliasson B. (2006) Formation and Dynamics of Dark Solitons and Vortices in Quantum Electron Plasmas. *Phys. Rev. Lett.***96**: 245001.
14. Shukla P.K. and Eliasson B. (2007) Nonlinear Interactions between Electromagnetic Waves and Electron Plasma Oscillations in Quantum Plasmas. *Phys. Rev. Lett.***99**: 096401.

15. Shaikh D. and Shukla P.K. (2007) Fluid turbulence in quantum plasmas. *Phys. Rev. Lett.***99**: 125002.
16. Brodin G. and Marklund M. (2007) Spin magnetohydrodynamics. *New J. Phys.***9**: 227.
17. Brodin G. and Marklund M. (2007) Spin solitons in magnetized pair plasmas. *Phys. Plasmas***14**: 112107.
18. Marklund M. and Brodin G. (2007) Dynamics of Spin-1/2 Quantum Plasmas. *Phys. Rev. Lett.***98**: 025001.
19. Shukla P.K. (2009) A new spin on quantum plasmas. *Nature Phys.***5:** 92.
20. Shukla P.K. and Eliasson B. (2010)Nonlinear aspects of quantum plasma physics. *Phys. Usp.***53**: 51.
21. Mamun A.A. and Shukla P.K. (2010)Arbitrary amplitude solitary waves and double layers in an ultra-relativistic degenerate dense dusty plasma. *Phys. Lett. A***324**: 4238.
22. Mamun A.A. and Shukla P.K. (2010) Solitary waves in an ultrarelativistic degenerate dense plasma. *Phys. Plasmas***17**: 104504.
23. Masood W., Eliasson B. and Shukla P.K. (2010) Electromagnetic wave equations for relativistically degenerate quantum magnetoplasmas. *Phys. Rev. E***81**: 066401.
24. Masood W. and Eliasson B. (2011) Electrostatic solitary waves in a quantum plasma with relativistically degenerate electrons. *Phys. Plasmas***18**: 034503.
25. Mendonca J.T. and Serbeto A. (2011)Volkov solutions for relativistic quantum plasmas. *Phys. Rev. E***83**: 026406.
26. Massey H. (1976) *Negative Ion*, 3rd edn..Cambrigdge University Press, Camgridge, UK.
27. Swider W. (1988) *Ionospheric modelling*. Birkhauser, Basel.
28. Chaizy P.H., Reme H., Sauuaud J.A., d'Uston C., Lin R.P., Larson D.E., Mitchell D.L., Andersen K.A., Carlson C.W., Korth A. and Mendis D.A. (1991) *Nature* **349**: 393.
29. Abdelsalam U.M. and Selim M.M. (2012) Ion-acoustic waves in a degenerate multicomponent magnetoplasma. *J. Plasma Phys.***79**: 163.
30. Coates A.J., Crary F.J., Lewis G.R., Young D.T., Waite Jr. J.H. and Sittler Jr. E.C. (2007) Discovery of heavy negative ions in Titans ionosphere. *Geophys. Res. Lett.***34**: L22103.
31. Frenkel Y. (1946) *Kinetic Theory of Liquids*. Clarendon, Oxford.
32. Ichimaru S. and Tanaka S. (1986) Generalized viscoelastic theory of the glass transition for strongly coupled, classical, one-component plasmas. *Phys. Rev. Lett.***56**: 2815.
33. Ichimaru S., Iyetomi H. and Tanaka S. (1987) Statistical physics of dense plasmas: thermodynamics, transport coefficients and dynamic correlations. *Phys. Rep.***149**: 91.
34. Shukla P.K. (2010) Properties of electrostatic waves in ultracold neutral plasmas. *Phys. Lett. A***374**: 3656.
35. Washimi H. and Taniuti T. (1966) Propagation of ion-acoustic solitary waves of some amplitude. *Phys. Rev. Lett.***17**: 996.

Journal of Science and Technology in the Tropics (2014) 10: 59-73

Nonplaner dust acoustic Gardner solitons in a dusty plasma with q-nonextensive electrons

D. K. Ghosh[1], U. N. Ghosh[1], P. Chatterjee[1], S. S. Kausik[2] and C. S. Wong[2,*]

[1]Department of Mathematics, Siksha Bhavana, Visva Bharati University, Santiniketan-731 235, West Bengal, India

[2]Plasma Technology Research Centre, Department of Physics, University of Malaya, 50603 Kuala Lumpur, Malaysia

(*Corresponding author e-mail: cswong@um.edu.my)

Received 09-05-2014; accepted 19-05-2014

Abstract The dust acoustic Gardner solitons in a dusty plasma with q-nonextensive electrons in nonplaner geometry are reported. By deriving modified Gardner (MG) equation, the properties of nonplanar (cylindrical and spherical) dust acoustic solitary waves (DASWs) in an unmagnetized, collisionless, three component dusty plasma, whose constituents are negatively charged cold dust fluid, q-nonextensive distributed electrons, and Boltzmann distributed ions are investigated. The reductive perturbation method is used to derive the MG equation. The basic features of nonplanar DA Gardner solitons (GSs) are discussed. It is found that the properties of nonplanar DAGSs (positive and negative) significantly differ as the value of the nonextensive parameter q changes.

Keywords Dust acoustic waves – Modified Gardner solitons – Nonplaner geometry – q-nonextensive electrons

INTRODUCTION

The co-existence of dust and plasmas, namely dusty plasmas have been widely investigated because of their importance in space, industry, and laboratory plasmas. Plasma and dust grains are quite common in different parts of our solar system [1-3]. The dust plays a key role in the wide range of phenomena from naturally occurring dusty plasmas to man-made dusty plasmas [4]. Dust grains in the plasma environment are charged due to variety of processes, such as interaction of dust grains with plasma particles, interaction of dust grains with energetic particles (electrons and ions), and interaction of dust grains with photons [5]. The presence of dust grains in the plasma system can modify the propagation characteristics of waves significantly.

The wave behaviour of dusty plasmas differs from that of usual electron-ion plasmas. It has been shown both theoretically and experimentally that the presence of dust particles changes the charge distribution and gives rise to a new mode called 'dust acoustic wave', where massive dust grains provide the inertia and

thermal pressure to sustain the wave coming from the plasma particles (electrons and ions) [6-10]. Rao *et al.* [6] first discussed theoretically the existence of low frequency dust acoustic waves in an unmagnetized dusty plasma. Later, this theoretical prediction was verified in laboratory experiments [9-10].

The study of dusty plasmas consisting of electrons, ions, and charged dust grains has received wide attention in recent years [11-15]. In space and laboratory plasmas, the unbounded planar geometry may not be a realistic situation. Recently, nonplaner nonlinear waves have received a good deal of attention [16-18]. It is seen from the theoretical works [16,19] that the properties of solitary waves in bounded nonplanar (cylindrical/spherical) geometry are very different from those in unbounded planar geometry. However, most of these investigations concern with the KdV equation, which produces DASWs either in planar or in nonplanar geometry in dusty plasmas. The parametric regime may create the situation for which the nonlinear term of KdV equation A~0, i.e, A is around 0 but not equal to 0. The nonlinear term around 0 gives rise to infinite large amplitude structures, which break down the validity of the reductive perturbation method [20]. To eliminate this circumstance, i.e., to study finite amplitude DASWs beyond the KdV limit, one may deduce the other type of nonlinear dynamical equation which can be valid for A~0.

Many researchers focus on Gardner (higher order KdV equation or mixed modified KdV equation) or modified Gardner solitons structures and solutions on different plasma systems [21-26]. Recently, Mannan and Mamun [27] have investigated the nonlinear propagation of Gardner solitons (GSs) in a nonplanar four-component dusty plasma and have derived the modified Gardner equation and solved it numerically. They have found that the propagation characteristics of nonplanar dust acoustic GSs are significantly different from those of planar ones.

The above discussions show that most of these plasma systems are composed of Boltzmann distributed electrons and ions, and it is well known that the Maxwell distribution is taken to be valid for the macroscopic ergodic equilibrium state. However, Maxwell distribution may be inadequate to describe the long range interactions in unmagnetized collisionless plasma, where the non-equilibrium stationary state exists. Space plasma observations clearly indicate the presence of ion and electron populations that are far away from their thermodynamic equilibrium [28-31]. A new statistical approach [32], namely non-extensive statistics or Tsallis statistics based on the derivation of Boltzmann-Gibbs-Shannon (BGS) extropic measure [33] is proposed to study the cases, where Maxwell distribution is considered inappropriate. This was first acknowledged by Renyi [32] and afterward proposed by Tsallis [33], where the entropic index q characterized the degree of non extensivity of the considered system. The parameter q that underpins the generalized entropy of Tsallis is linked to the underlying dynamics of the system and measures the amount of its nonextensivity.

36. Mamun A.A. and Shukla P.K. (2002) Cylindrical and spherical dust ion-acoustic solitary waves. *Phys. Plasma***9**: 1468.
37. Mamun A.A. (2008) Dust electron-acoustic shock waves due to dust charge fluctuation. *Phys. Lett. A***372**: 4610.
38. Berkovsky M.A. (1992) Spectrum of low frequency modes in strongly coupled plasmas. *Phys. Lett. A***166**: 365.
39. Slattery W.L., Doolen G.D. and DeWitt H.E. (1980) Improved equation of state for the classical one-component plasma. *Phys. Rev. A***21**: 2087.
40. Das G.C., Sharma J. and Roychoudhaury R.J. (2001)Some aspects of shock-like nonlinear acoustic waves in magnetized dusty plasma. *Phys. Plasmas***8**: 74.
41. Sadiq M., Ali S. and Sabry R. (2009) Propagation of the three-dimensional dust acoustic solitons in magnetized quantum plasmas with dust polarity effect. *Phys. Plasmas***16**: 013706.
42. Matta M., GalandM., Moore L., Mendillo M. and Withers P. (2014) Numerical simulations of ion and electron temperatures in the ionosphere of Mars: Multiple ions and diurnal variations. *Icarus***227**: 78.

In statistical mechanics and thermodynamics, systems characterized by the property of nonextensivity are systems for which the entropy of the whole is different from the sum of the entropies of the respective parts. In other words, the generalized entropy of the whole is greater than the sum of the entropies of the parts if $q < 1$ (superextensivity), whereas the generalized entropy of the system is smaller than the sum of the entropies of the parts if $q > 1$ (sub-extensivity). In accordance with the evidences [34-43], the q-entropy may provide a convenient frame for the analysis of many astrophysical scenarios, such as stellar poly tropes, solar neutrino problem, and peculiar velocity distribution of galaxy cluster. It may be noted that for $q < -1$, the q-distribution is unnormalizable. In the extensive limiting case ($q \rightarrow 1$), the q distribution reduces to the well known Maxwell-Boltzmann velocity distribution.

The purpose of the present paper is to investigate the dust acoustic Gardner solitons in a dusty plasma with q-nonextensive electrons in nonplaner (cylindrical and spherical) geometry. In this paper, we consider the normalized set of equations composed of negatively charged cold dust fluid, q-nonextensive distributed electrons, and Boltzmann distributed ions. By using the reductive perturbation method, we have derived the modified Gardner equaton and solved it numerically.

DERIVATION OF MG EQUATION

We consider the nonlinear propagation of nonplanar (cylindrical and spherical) dust acoustic waves in a three component collisionless, unmagnetized plasma, whose constituents are negatively charged cold dust fluid, q-nonextensive distributed electrons, and Boltzmann distributed ions. The nonlinear dynamics of dust acoustic (DA) waves in such nonplanar plasma can be described by the following set of normalized equations:

$$\frac{\partial n_d}{\partial t} + + \frac{1}{r^\nu}\frac{\partial}{\partial r}(r^\nu n_d u_d) = 0, \tag{1}$$

$$\frac{\partial u_d}{\partial t} + u_d \frac{\partial u_d}{\partial r} = \frac{\partial \phi}{\partial r}, \tag{2}$$

$$\frac{1}{r^\nu}\frac{\partial}{\partial r}(r^\nu \frac{\partial \phi}{\partial r}) = \rho, \tag{3}$$

$$\rho = n_d + n_e - n_i, \tag{4}$$

where $\nu = 0$ in case of 1D planar geometry and $\nu = 1(2)$ in case of nonplanar cylindrical (spherical) geometries, respectively, n_d is the dust particle number density normalized by its equilibrium value n_{d0}, u_d is the dust fluid velocity

normalized by dust acoustic speed $C_d = \left(\frac{z_{d0} k_B T_i}{m_d}\right)^{\frac{1}{2}}$, and ϕ is the electrostatic wave potential normalized by $\frac{k_B T_i}{e}$, where m_d is the dust mass, k_B being the Boltzmann constant, Z_{d0} is the number of electrons at equilibrium residing on the dust grain surface, and ρ is the net normalized surface charge density. The time and space variables are in units of the dust plasma period $\omega_{pd}^{-1} = \left(\frac{m_d}{4\pi n_{d0} z_{d0}^2 e^2}\right)^{\frac{1}{2}}$ and the Debye length $\lambda_{Dm} = \left(\frac{k_B T_i}{4\pi n_{d0} z_{d0} e^2}\right)^{\frac{1}{2}}$, respectively.

We use q-nonextensive distribution for electrons [34] and Boltzmann distribution for ions. Therefore, the normalized number densities of electrons [14, 43] and ions are accordingly expressed as $n_e = \frac{p}{1-p}\left[1+(q-1)\sigma\phi\right]^{\frac{(q+1)}{2(q-1)}}$ and $n_i = \frac{1}{(1-p)} e^{-\phi}$, respectively, where q is the parameter quantifying the degree of nonextensivity and is larger than -1 ($q > -1$), $p = \frac{n_{e0}}{n_{i0}}$, $\sigma = \frac{T_i}{T_e}$, n_{e0}, n_{i0} are the electron and ion number densities at equilibrium, respectively, and T_e, T_i are the electron and ion temperatures, respectively.

To study the dust acoustic Gardner solitons (DAGSs) in this plasma model using Eqs.(1)-(4) by the reductive perturbation technique, we first introduce the stretched coordinates [20] as

$$\zeta = \varepsilon(r - v_p t), \quad \tau = \varepsilon^3 t \qquad (5)$$

where ε is a small parameter ($0 < \varepsilon < 1$) measuring the weakness of the dispersion and v_p (normalized by C_d) is the phase speed of the perturbation mode, and expand all the dependent variables (viz. n_d, u_d, ϕ, and ρ) in power series of ε :

$$n_d = 1 + \varepsilon n_d^{(1)} + \varepsilon^2 n_d^{(2)} + \varepsilon^3 n_d^{(3)} + \ldots\ldots, \qquad (6)$$

$$u_d = 0 + \varepsilon u_d^{(1)} + \varepsilon^2 u_d^{(2)} + \varepsilon^3 u_d^{(3)} + \ldots\ldots, \qquad (7)$$

$$\phi = 0 + \varepsilon\phi^{(1)} + \varepsilon^2\phi^{(2)} + \varepsilon^3\phi^{(3)} + \ldots\ldots, \qquad (8)$$

$$\rho = 0 + \varepsilon\rho^{(1)} + \varepsilon^2\rho^{(2)} + \varepsilon^3\rho^{(3)} + \ldots\ldots, \qquad (9)$$

Now, expressing Eqs.(1)-(4) in terms of ζ and τ and substituting Eqs.(6)-(9) into the resulting equations [Eqs.(1)-(4) expressed in terms of ζ and τ], one can easily develop different set of equations in various powers of ε. To the lowest order in ε, we obtain

$$u_d^{(1)} = -\frac{\phi}{v_p}, \quad n_d^{(1)} = -\frac{\phi}{v_p^2}, \quad \rho^{(1)} = 0, \tag{10}$$

$$v_p = \sqrt{\frac{2(1-p)}{2+p\sigma(q+1)}} \tag{11}$$

where $\phi = \phi^{(1)}$. The expression (11) represents the linear dispersion relation for the DA waves propagating in the plasma model under consideration. To the next order in ε, one obtains another set of equations, which after using Eqs.(10)-(11) can be simplified as

$$u_d^{(2)} = \frac{\phi^2}{2v_p^3} - \frac{\phi^{(2)}}{v_p}, \quad n_d^{(2)} = \frac{3\phi^2}{2v_p^4} - \frac{\phi^{(2)}}{v_p^2}, \tag{12}$$

$$\rho^{(2)} = \frac{1}{2}A\phi^2 = 0, \quad A = \frac{3}{v_p^4} + \frac{p\sigma^2(q+1)(3-q)}{4(1-p)} - \frac{1}{1-p} \tag{13}$$

It is obvious from Eq.(13) that $A = 0$ since $\phi \neq 0$. The solution of $A = 0$ yields $q = q_c$, where q_c is found from the equation,

$$3\{2+p\sigma(q+1)\}^2 + p(1-p)\sigma^2(q+1)(3-q) - 4(1-p) = 0 \tag{14}$$

It is obvious that Eq.(13) is satisfied for $q = q_c$. So for q around its critical value q_c, i.e., for $|q - q_c| = \varepsilon$ corresponding to $A = A_0$, one can expressed A_0 as

$$A_0 \cong s\left(\frac{\partial A}{\partial q}\right)_{q=q_c} |q - q_c| = sA_q\varepsilon, \tag{15}$$

where $A_q = \frac{3p\sigma\{2+p\sigma(q+1)\}}{2(1+p)^2} + \frac{p\sigma^2(1-q)}{2(1-p)}$, $s = 1$ for $q > q_c$, and $s = -1$ for $q < q_c$.

So, for $q \neq q_c$, one can express $\rho^{(2)}$ as

$$\rho^{(2)} \cong \frac{1}{2}s\varepsilon A_q\phi^2 \tag{16}$$

This means that for $q \neq q_c$, $\rho^{(2)}$ must be included in the third order Poisson's equation. To the next higher order in ε, one obtains the third set of equations:

$$\frac{\partial n_d^{(1)}}{\partial \tau} - v_p\frac{\partial n_d^{(3)}}{\partial \xi} + \frac{\partial u_d^{(3)}}{\partial \xi} + \frac{\partial F_n}{\partial \xi} + \frac{v}{v_p\tau}u_d^{(1)} = 0, \tag{17}$$

$$\frac{\partial u_d^{(1)}}{\partial \tau} - v_p\frac{\partial u_d^{(3)}}{\partial \xi} + \frac{\partial F_u}{\partial \xi} - \frac{\partial \phi^{(3)}}{\partial \xi} = 0, \tag{18}$$

$$\frac{\partial^2\phi}{\partial\xi^2}+\frac{1}{2}sA_q\phi^2-n_d^{(3)}-\frac{p}{(1-p)}$$
$$\left[\frac{(q+1)}{2}\sigma\phi^{(3)}+\sigma^2\frac{(q+1)(3-q)}{4}\phi\phi^{(2)}+\sigma^3\frac{(q+1)(3-q)(5-3q)}{48}\right] \quad (19)$$
$$+\frac{1}{(1-p)}\left[-\phi^{(3)}+\phi\phi^{(2)}-\frac{\phi^3}{6}\right]=0,$$

where $F_n = n_d^{(1)}u_d^{(2)} + n_d^{(2)}u_d^{(1)}$ and $F_u = u_d^{(1)}u_d^{(2)}$. Now, using Eqs.(10)-(13) and (17)-(19), one finally obtains a nonlinear dynamical equation of the form:

$$\frac{\partial\phi}{\partial\tau}+\frac{\nu}{2\tau}\phi+\alpha_1\phi\frac{\partial\phi}{\partial\xi}+\alpha_2\phi^2\frac{\partial^2\phi}{\partial\xi^2}+\alpha_3\frac{\partial^3\phi}{\partial\xi^3}=0, \quad (20)$$

where

$$\alpha_1=\frac{sA_qv_p^3}{2} \quad (21)$$

$$\alpha_2=\frac{v_p^3}{2}\left[\frac{15}{2v_p^6}-\frac{p\sigma^3(q+1)(3-q)(5-3q)}{16(1-p)}-\frac{1}{2(1-p)}\right], \quad (22)$$

$$\alpha_3=\frac{v_p^3}{2}, \quad (23)$$

Equation (20) is the MG equation. The modification is due to the extra term $(\nu/2\tau)$ ϕ, which arises due to the effects of the nonplanar geometry. We have already mentioned that $\nu = 0$ corresponds to a 1D planar geometry, which reduces (20) to a standard Gardner (SG) equation. Eq.(20) is not a modified KdV indeed. In fact, it contains both $\phi\frac{\partial\phi}{\partial\xi}$ (nonlinear term of KdV) and $\phi^2\frac{\partial\phi}{\partial\xi}$ (nonlinear term of modified KdV) in the framework of nonplanar geometry, which is known as modified Gardner equation. The second term gives us the effect of nonplanar geometry. Taking separately the nonlinear third term or 4th term along with the rest terms, we get the KdV or modified KdV, respectively in the framework of nonplanar geometry. The nonplanar KdV equation can be obtained by neglecting the 4th term, i.e, when $\phi^2\frac{\partial\phi}{\partial\xi}$ tends to 0. Thus, nonplanar KdV equation is a particular case of our derived MG equation and this nonplanar KdV equation can be derived by using the lower-order stretched variables, viz., $\zeta = \varepsilon^{1/2}(r - v_p\tau)$, $\tau = \varepsilon^{3/2}t$ rather than the stretching, which we have used.

NUMERICAL RESULTS AND DISCUSSIONS

Now, we solve the MG equation [Eq. (20)] numerically. For this, we first analyze the stationary GSs solution of Gardner equation (i.e., with $v = 0$). To do this, we first introduce a transformation $\xi = \zeta - U_0\tau$, which allows us to write Eq. (20) under the steady state condition as

$$\frac{1}{2}\left(\frac{\partial\phi}{\partial\xi}\right)^2 + V(\phi) = 0, \tag{24}$$

where $V(\phi)$ is the pseudo-potential given by

$$V(\phi) = -\frac{U_0}{2\alpha_3}\phi^2 + \frac{\alpha_1}{6\alpha_3}\phi^3 + \frac{\alpha_2}{12\alpha_3}\phi^4. \tag{25}$$

It is obvious from Eq. (25) that

$$V(\phi)\big|_{\phi=0} = \left.\frac{dV(\phi)}{d\phi}\right|_{\phi=0} = 0 \tag{26}$$

$$\left.\frac{d^2V(\phi)}{d\phi^2}\right|_{\phi=0} < 0 \tag{27}$$

The conditions of Eqs. (26) and (27) imply that SW solution of Eq. (24) exists if

$$V(\phi)\big|_{\phi=\phi_m} = 0. \tag{28}$$

The latter can be solved as

$$U_0 = \frac{\alpha_1}{3}\phi_{m1,2} + \frac{\alpha_2}{6}\phi_{m1,2}^2, \tag{29}$$

$$\phi_{m1,2} = \phi_m\left[1 \mp \sqrt{1 + \frac{U_0}{V_0}}\right], \tag{30}$$

where $\varphi_m = -\frac{\alpha_1}{\alpha_2}$ and $V_0 = \frac{\alpha_1^2}{6\alpha_2}$. Now, using Eqs. (25) and (30) in Eq. (24), we have

$$\left(\frac{d\phi}{d\xi}\right)^2 + \gamma\phi^2(\phi - \phi_{m1})(\phi - \phi_{m2}) = 0, \tag{31}$$

where $\gamma = \frac{\alpha_2}{6\alpha_3}$. The SW solution of Eqs. (24) and (31) is therefore given by,

$$\phi = \left[\frac{1}{\phi_{m2}} - \left(\frac{1}{\phi_{m2}} - \frac{1}{\phi_{m1}}\right)\cosh^2\left(\frac{\xi}{\delta}\right)\right]^{-1}, \tag{32}$$

where $\phi_{m1,2}$ are given in Eq. (30) and SWs width δ is

$$\delta = \frac{2}{\sqrt{-\gamma\phi_{m1}\phi_{m2}}}. \tag{33}$$

We now turn to the Eq. (20) with the term $(\nu/2\tau)\phi$, which is due to the effects of the nonplanar (cylindrical/spherical) geometry. An exact analytical solution of Eq. (20) is not possible. Hence, we have numerically solved Eq. (20) and have discussed the effects of cylindrical and spherical geometries on time-dependent dust acoustic Gardner solitons (DAGSs). The numerical results are plotted in Figs. 1-8. The initial condition, which we have used in our numerical analysis, is in the form of the stationary solution of Eq. (20) without the term $(\nu/2\tau)\phi$.

The numerical solutions of Eq. (20) show that for a large value of τ, the cylindrical and spherical solitary waves are similar to planar ones. This is because for a large value of τ (e.g., $\tau = 30$), the term $(\nu/2\tau)\phi$, which is due to the effects of the cylindrical or spherical geometry, is no longer dominant. However, as the value of τ decreases, the term $(\nu/2\tau)\phi$ becomes dominant and both cylindrical and spherical solitary wave structures differ from planar geometry. It is found that as the value of τ decreases, the amplitude of these localized pulses increases. It is also found that the amplitude of the cylindrical or spherical DASWs (for both positive and negative GSs) decreases as the value of nonextensive parameter q increases. We have also found that the amplitude of the DA positive GSs decreases as the value of σ (ratio of ion temperature to electron temperature) increases in both cylindrical and spherical geometries.

Figures 1 and 2 show the effects of cylindrical geometry on positive DAGSs for $q = -0.1$, $U_0 = 0.1$, $p = 0.2$, and $\sigma = 0.3$ and for $q = 1.1$, $U_0 = 0.1$, $p = 0.2$, and $\sigma = 0.3$, respectively. It is clear from Figs. 1 and 2 that the amplitude of the cylindrical DAGSs (positive) decreases as the value of nonextensive parameter q increases (here, q takes the value - 0.1 and 1.1). Figures 3 and 4 show the effects of spherical geometry on positive DAGSs for $q = -0.1$, $U_0 = 0.1$, $p = 0.2$, and $\sigma = 0.3$and for $q = 1.1$, $U_0 = 0.1$, $p = 0.2$, and $\sigma = 0.3$, respectively. It is also clear from Figs. 3 and 4 that the amplitude of the spherical DAGSs (positive) decreases as the value of nonextensive parameter q increases (here, also q takes the value -0.1 and 1.1). From the above figures, it is seen that the potential profiles of the spherical DAGSs (positive) significantly change than that of the cylindrical DAGSs (positive) when time τ becomes lower in values(i.e., from $\tau = 20$ to $\tau = 10$).

Figures 5 and 6 show the the potential profiles of the cylindrical DAGSs (negative) and spherical DAGSs (negative), respectively. It is seen from the above figures that the potential profiles of the spherical DAGSs (negative) significantly change than that of the cylindrical DAGSs (negative), when time τ becomes lower in values (i.e., from $\tau = 20$ to $\tau = 10$).

From Figures 1 and 7, it is clear that the amplitude of the cylindrical DAGSs (positive) decreases as the value of σ (ratio of ion temperature to electron temperature) increases. It is also clear from Figures 3 and 8 that the amplitude of the spherical DAGSs (positive) decreases as the value of σ increases.

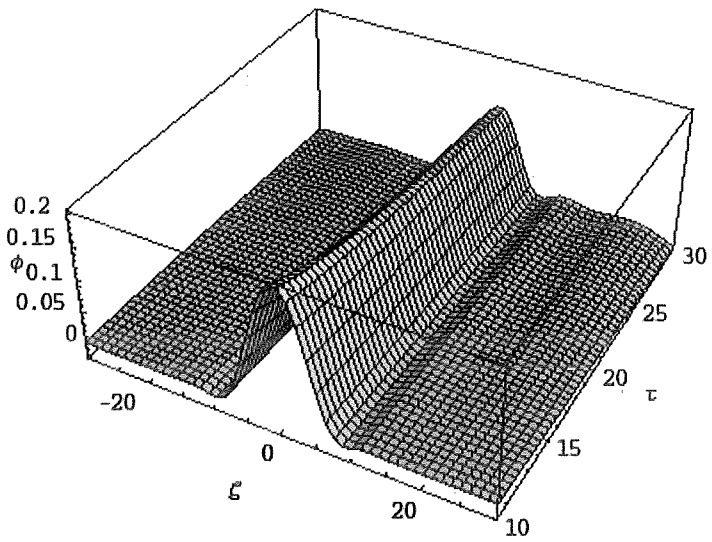

Figure 1. The effects of cylindrical geometry on positive DAGSs for $q = -0.1$, $U_0 = 0.1$, p = 0.2, and $\sigma = 0.3$.

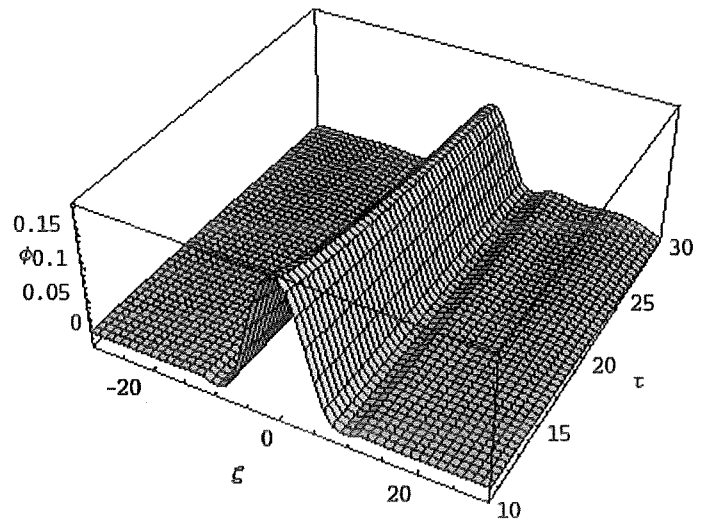

Figure 2. The effects of cylindrical geometry on positive DAGSs for $q = 1.1$, $U_0 = 0.1$, p = 0.2, and $\sigma = 0.3$.

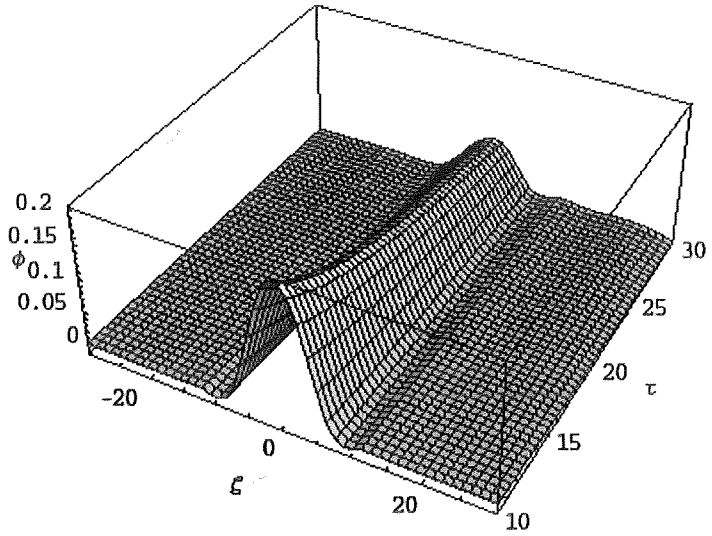

Figure 3. The effects of spherical geometry on positive DAGSs for $q = -0.1$, $U_0 = 0.1$, p = 0.2, and $\sigma = 0.3$.

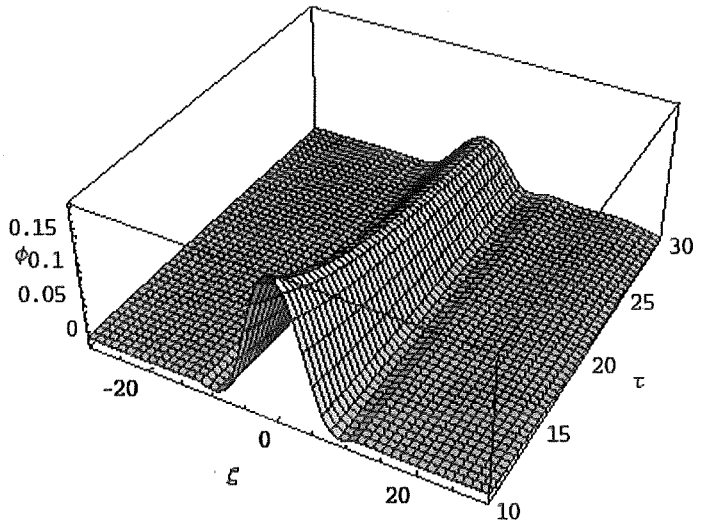

Figure 4. The effects of spherical geometry on positive DAGSs for $q = 1.1$, $U_0 = 0.1$, p = 0.2, and $\sigma = 0.3$.

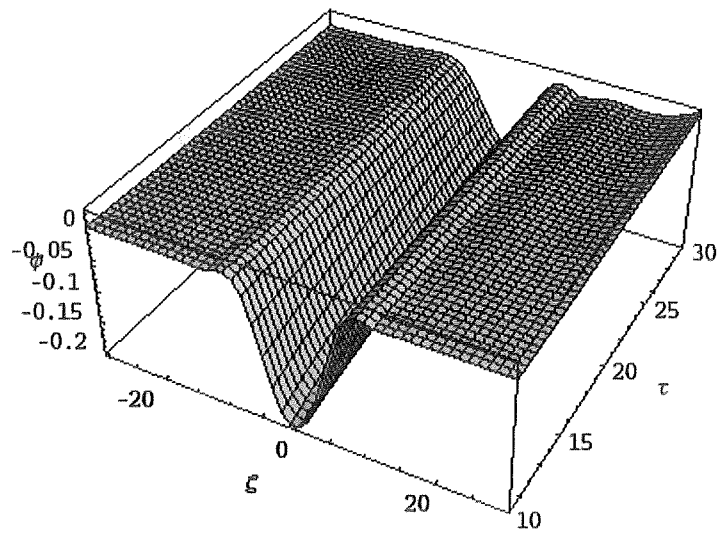

Figure 5. The effects of cylindrical geometry on negative DAGSs for $q = -0.1$, $U_0 = 0.1$, p = 0.2, and $\sigma = 0.3$.

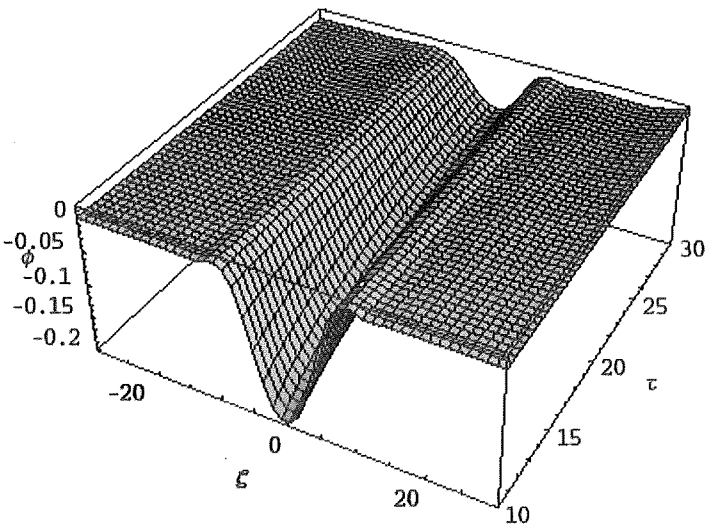

Figure 6. Showing the effects of spherical geometry on negative DAGSs for $q = -0.1$, $U_0 = 0.1$, p = 0.2, and $\sigma = 0.3$.

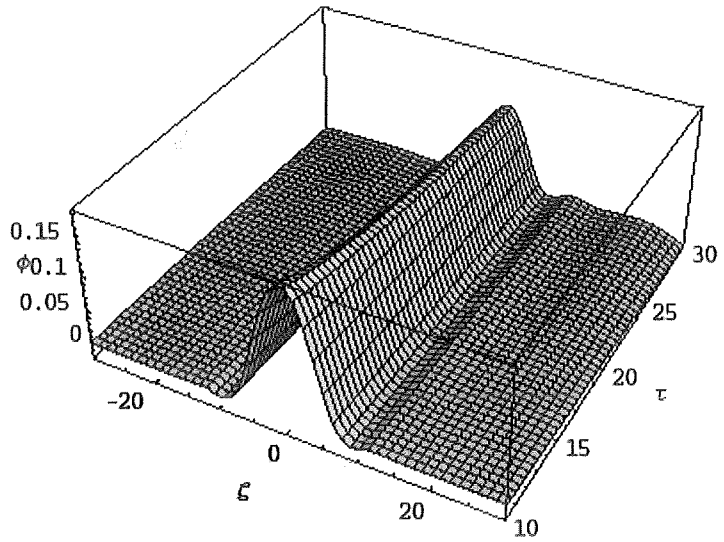

Figure 7. The effects of cylindrical geometry on positive DAGSs for $q = -0.1$, $U_0 = 0.1$, p = 0.2, and $\sigma = 0.5$.

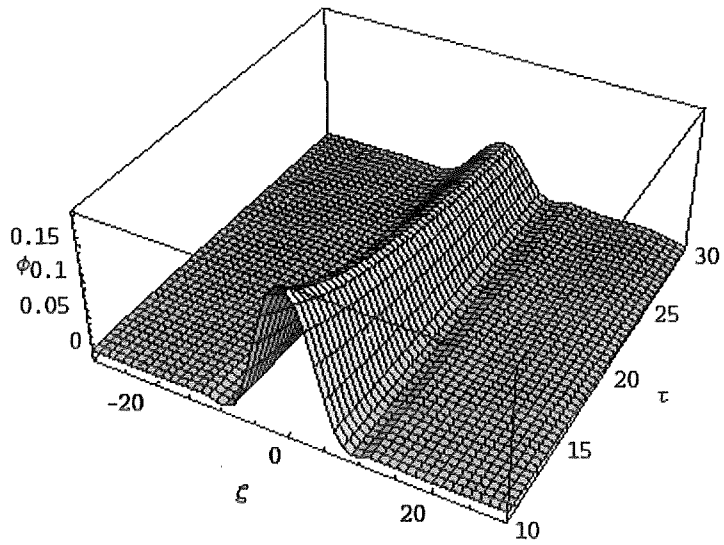

Figure 8. Showing the effects of spherical geometry on positive DAGSs for $q = -0.1$, $U_0 = 0.1$, p = 0.2, and $\sigma = 0.5$.

CONCLUSION

To conclude, we have studied the DAGSs in three component dusty plasma, which is composed of negatively charged cold dust fluid, q-nonextensive distributed electrons, and Boltzmann distributed ions in nonplanar (cylindrical and spherical) geometry. The MG equation has been derived based on the reductive perturbation method. The basic features of nonplanar DAGSs are discussed. It is found that the properties of nonplanar DAGSs (positive and negative) are significantly different as the value of nonextensive parameter q changes. It is seen that as the value of q increases, the amplitude of the DAGSs (positive and negative) decreases significantly in both cylindrical and spherical geometries. Furthermore, it is seen that as ratio of ion temperature to electron temperature (σ) increases, the amplitude of the DAGSs (positive) significantly varies in both cylindrical and spherical geometries. The present results could be useful for understanding of DAGSs and the effects of nonplanar geometry on these waves in both space and laboratory plasma systems.

Acknowledements: S.S. Kausik and C.S. Wong are being supported by University of Malaya Research Grant RP008-13AFR to participate in this work.

REFERENCES

1. Goertz C.K. (1989) Dusty plasmas in the Solar system. Rev. Geophys. 27: 271-292.
2. Angelis U. de (1992) The physics of dusty plasmas. Physica Scripta 45: 465-474.
3. Havnes O. (1984) Charges on dust particles. Adv. Space Res. 4: 75-83.
4. Merlino R.L. (2006) Dusty plasmas and applications in space and industry. Grabbe C. (Ed.) Plasma Physics Applied pp. 73-110. Transworld Research Network, India.
5. Shukla P.K. and Mamun A.A. (2002) Introduction to Dusty Plasma Physics. Institute of Physics, Bristol.
6. Rao N.N., Shukla P.K. and Yu M.Y. (1990) Dust-acoustic waves in dusty plasmas. Planet. Space Sci. 38: 543-546.
7. El-Labany S.K., El-Shamy E.F., El-Taibany W.F. and Moslem W.M. (2007) Dust-acoustic solitary waves in a two-temperature electrons with charge fluctuations and nonisothermal ions. Chaos, Solitons & Fractals 34: 1393-1400.
8. Pakzad H.R. and Javidan K. (2009) Solitary waves in dusty plasmas with variable dust charge and two temperature ions. Chaos, Solitons & Fractals 42: 2904-2913.
9. Barkan A., Merlino R.L. and D'Angelo N. (1995) Laboratory observation of the dust acoustic wave mode. Phys. Plasmas 2: 3563-3565.
10. D'Angelo N. (1995) Coulomb solids and low-frequency fluctuations in RF dusty plasmas. J. Phys. D: Appl. Phys. 28: 1009-1010.
11. Maitra S. and Roychoudhury R. (2003) Speed and shape of dust acoustic solitary waves. Phys. Plasmas 10: 2230-2235.
12. Dubinov A.E., Kolotkov D.Yu. and Sazonkin M.A. (2011) Nonlinear ion acoustic

waves in a quantum degenerate warm plasma with dust grains. Plasma Phys. Rep. 37: 64-74.
13. Dzlieva E.S., Ermolenko M.A. and Karasev V.Yu. (2012) Properties of dust-plasma structures formed in a glow discharge above the lower wall of the discharge chamber. Plasma Phys. Rep. 38: 540-544.
14. Prudskikh V.V. (2012) Ion flux associated with an ion-acoustic cnoidal wave in magnetized dusty plasma. Plasma Phys. Rep. 38: 545-550.
15. Asaduzzaman M. and Mamun A.A. (2012) Dust-acoustic waves in a nonuniform adiabatic dusty plasma in the presence of polarization force. Plasma Phys. Rep. 38: 743-750.
16. Mamun A.A. and Shukla P.K. (2002) Cylindrical and spherical dust ion–acoustic solitary waves. Phys. Plasmas 9: 1468-1470.
17. Sahu B. (2010) Positron acoustic shock waves in planar and nonplanar geometry. Phys. Scr.82: 065504-065508.
18. Eslami P., Mottaghizadeh M. and Pakzad H.R. (2011) Nonplanar ion-acoustic solitary waves in electron–positron–ion plasmas with electrons following a q-nonextensive distribution. Phys. Scr. 83: 065502-065507.
19. Xue J.K. (2003) Cylindrical dust acoustic waves with transverse perturbation. Phys. Plasmas 10: 3430-3431.
20. Washimi H. and Taniuti T. (1966) Propagation of ion-acoustic solitary waves of small amplitude. Phys. Rev. Lett. 17: 996-998.
21. Wazwaz A.M. (2007) New solitons and kink solutions for the Gardner equation. Commun. Nonlin. Sci. Numer. Simul. 12: 1395-1404.
22. Wazwaz A.M. (2009) Partial differential equations and solitary waves theory. Higher Education Press, Springer.
23. Lee N.C. (2009) Small amplitude electron-acoustic double layers and solitons in fully relativistic plasmas of two-temperature electrons. Phys. Plasmas 16: 042316-042316-10.
24. Vassilev V.M., Djondjorov P.A., Hadzhilazova M.Ts. and Mladenov I.M. (2011) Traveling wave solutions of the Gardner equation and motion of plane curves governed by the mKdV flow. AIP Conf. Proc. 1404: 86-93.
25. Ghosh U.N., Ghosh D.K., Chatterjee P. and Sahu B. (2012) Superthermal effect of electrons on nonplanar dust-ion-acoustic solitary waves and double layers in a dusty plasma. Astrophys. Space Sci. 342: 449-456.
26. Ghosh, D.K., Ghosh, U.N. and Chatterjee, P. (2013). Non-planar ion acoustic Gardner solitons in electron-positron-ion plasma with superthermal electrons and positrons. J. Plasma Phys. 79: 37-44.
27. Mannan A. and Mamun A.A. (2011) Nonplanar dust-acoustic Gardner solitons in a four-component dusty plasma. Phys. Rev. E 84: 026408-026413.

28. Shukla P.K., Rao N.N., Yu M.Y. and Tsintsadze N.L. (1986) Relativistic nonlinear effects in plasmas. Phys. Rep. 138: 1-149.
29. Ghosh S. and Bharuthram R. (2008) Ion acoustic solitons and double layers in electron–positron–ion plasmas with dust particulates. Astrophys. Space Sci. 314: 121-127.
30. Pakzad H.R. (2009) Ion acoustic solitary waves in plasma with nonthermal electron and positron. Phys. Lett. A 373: 847-850.
31. Pakzad H.R. (2010) Ion acoustic solitary waves in plasma with nonisothermal electron, positron, and ion components. Astrophys. Space Sci. 326: 77-81.
32. Renyi A. (1955) On a new axiomatic theory of probability. Acta Math. Hung. 6:285-335.
33. Tsallis C. (1988) Possible generalization of Boltzmann-Gibbs statistics. J. Stat. Phys. 52:479-487.
34. Lima J.A.S., Silva Jr. R. and Santos J. (2000) Plasma oscillations and nonextensive statistics. Phys. Rev. E 61: 3260-3263.
35. Abe S., Martinez S., Pennini F. and Plastino A. (2001) Nonextensive thermodynamic relations. Phys. Lett. A 281: 126-130.
36. Kaniadakis G. (2001) H-theorem and generalized entropies within the framework of nonlinear kinetics. Phys. Lett. A 288: 283-291.
37. Tribeche M. and Merriche A. (2011) Nonextensive dust-acoustic solitary waves. Phys. Plasmas 18, 034502-034502-4.
38. Wada T. (2002) On the thermodynamic stability conditions of Tsallis' entropy. Phys. Lett. A 297, 334-337.
39. Silva R., Plastino A. and Lima J. (1998) A Maxwellian path to the q-nonextensive velocity distribution function. Phys. Lett. A 249: 401-408.
40. El-Awady E.I. and Moslem W.M. (2011) On a plasma having nonextensive electrons and positrons: Rogue and solitary wave propagation. Phys. Plasmas 18: 082306-082306-8.
41. Eslami P., Mottaghizadeh M. and Pakzad H.R. (2011) Nonplanar dust acoustic solitary waves in dusty plasmas with ions and electrons following a q-nonextensive distribution. Phys. Plasmas 18: 102303-102303-6.
42. Pakzad H.R. (2011) Cylindrical and spherical electron acoustic solitary waves with nonextensive hot electrons. Phys. Plasmas 18: 082105-082105-5.
43. Sahu B. (2011) Ion acoustic solitary waves and double layers with nonextensive electrons and thermal positrons. Phys. Plasmas 18: 082302- 082302-6.

Journal of Science and Technology in the Tropics (2014) 10: 75-80

Kuala Lumpur Engineering and Science Fair (KLESF): A Students' Interest in Science and Technology Enhancement Programme

Sze-Wei Lee[1], Lee-Pee Hong[2] and Mohd Yusoff Sulaiman[3]
[1]Faculty of Engineering and Science, Universiti Tunku Abdul Rahman, Malaysia
(Email:leeszewei@utar.edu.my)
[2]ASEAN Academy of Engineering and Technology (Email: hlp@edasu.com)
[3]Malaysian Industry-Government Group for High Technology, Malaysia
(Email: yusoff@might.org.my)

Abstract This paper presents Kuala Lumpur Engineering and Science Fair (KLESF) programme implemented in Malaysia to enhance the interest of school-age children and teenagers in science, technology, engineering and mathematics (STEM). Vision and concepts of the programme will be presented followed by the corresponding programme structure and implementation plan. Report on how some of the components of the programme have been implemented and the results of the initial study on their impacts will also be presented.

Keywords STEM – hands-on learning – STI

INTRODUCTION

Interest in science, technology, engineering and mathematics (STEM) has been declining globally. Fewer than 40% of students in United States (US) who enter college intending to major in a STEM field complete a STEM degree [1]. It was reported in 2010 that only about 15.6 percent of bachelor's degrees awarded in US were in STEM [2]. The President's Council of Advisors on Science and Technology of US recommended steps to increase the number of college and university graduates in STEM fields by 1 million in the next decade for healthy economic growth [1]. Less than 40% of graduates of public universities in Malaysia pursued courses in STEM fields [3] compared to the targeted STEM:non-STEM student ratio of 60:40 set by the Malaysian Government for long term socio-economic growth of the country.

KUALA LUMPUR ENGINEERING SCIENCE FAIR (KLESF)

KLESF is a programme that is aimed to promote interest in science, technology, engineering and mathematics (STEM) among primary and secondary school students in Malaysia. It was initiated by the ASEAN Academy of Engineering and Technology (AAET), Malaysian Industry-Government Group for High Technology (MIGHT), Universiti Tunku Abdul Rahman (UTAR), The Institution

of Engineers Malaysia (IEM) and the National Science Centre. It is also one of the key programmes under the "Science to Action (S2A)" initiative launched by the Prime Minister of Malaysia on 1st November 2013.

Concepts

KLESF programme comprises a series of activities that promote the importance of science, technology and innovation (STI), interaction of students with engineering and science professions, complement the existing school STEM curriculum with more hands-on learning components, outreaching of sciences to suburban and rural communities and the enhancement of science literacy among the general public.

The sub-programmes and objectives

Based on the above concept, KLESF encompasses the following sub-programmes thus far:

1. KLESF: The Fair
2. School Engineering and Science Design Mentorship (SESDM) Scheme,
3. Mobile KLESF, and
4. KLESF Workshop and Gallery.

The SESDM scheme and KLESF Fair have been implemented since January 2014 while Mobile KLESF and KLESF Workshop and Gallery will be initiated in 2015. More new sub-programmes may also be developed and incorporated into KLESF in future.

KLESF: The Fair

KLESF Fair was mooted end of 2013 and happened on 25 to 27 April 2014 at the National Science Centre of Malaysia. Targeted audience were mainly school children (primary and secondary), parents, teachers and educators. The event attracted more than 200 visiting schools and 50,000 visitors over the 3 days.

The objectives of the KLESF Fair were:

1. To enhance school students' interest in science, technology, engineering and mathematics (STEM),
2. To enhance the awareness of public on the roles and importance of STEM in socio-economic well-being and sustainable development,
3. To enhance the awareness and participation of business and industry in promoting learning and career development in areas related to STEM among school students and community, and
4. To provide networking for schools, educators, industries, public and private sector to share information and experiences on projects, extra-curriculum and good practices in science and mathematics education in schools.

The fair consisted of the following components:

1. Science hands-on demos and experiments,
2. Mathematics and mental literacy activities,
3. School STEM project exhibition and demo,
4. Industry science, technology and engineering exhibition,
5. STEM poster and video exhibition, and
6. Fun in science: the science of magic.

The science hands-on demos and experiments were mainly hands-on experiments and activities in Physics, Chemistry, Biology and Mathematics that were aimed at illustrating interesting phenomena and daily life experience which could be explained and understood through scientific principles (Figs. 1–2). A total of about 20 experiments and activities were designed and carried out under this component.

The mathematics and mental literacy component of the fair attempted to address one of the most challenging aspects in school education, i.e. getting children to be interested in numeracy and mathematics. The fun aspect of mathematics was focused on in order to raise students' interest in it.

Although not fully completed in April most of the SESDM school projects were exhibited in KLESF Fair. Besides that, some other schools were invited and participated in the fair by showing some of their design projects (Figs. 3-4).

One important but often overlooked player in encouraging and educating future generations in STEM is the major end beneficiary of the education process, i.e. the industry and businesses. Analysis shows that the choice of education by students and parents is strongly related to the future career choice and preference envisioned by and for the young. Public perception on some STEM based careers such as engineering, agriculture, etc. appears to be not as positive as the non-STEM based careers and thus affecting the interest and number of students choosing STEM subjects in schools and courses in universities. Industry being the ultimate career destination for the younger generations can play a vital role to rectify the problem. Thus, their participation in KLESF Fair was important.

For the industry science, technology and engineering exhibition component of KLESF Fair 20 companies and organisations participated as exhibitors (Figs. 5 and 6). Their participation could be generally categorized as follows:

1. Exhibition of product technologies with presentation tailored towards educational purposes, and
2. Design workshops designed and conducted by company technical staff.

To make science more interesting to young children a KLESF component on the science of magic (Fig. 7) was organised. It was hoped that children would be more interested in science after watching magic trick performance and explanation of how these tricks were designed and carried out based on some scientific principles. The response from the children was very positive.

Figure 1. Demonstrators explaining to children on an experiment in Chemistry.

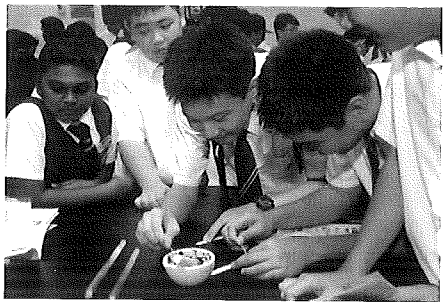

Figure 2. Students performing an experiment in Biology.

Figure 3. A school project team member explaining their system to visitors.

Figure 4. A school team setting up their project for exhibition.

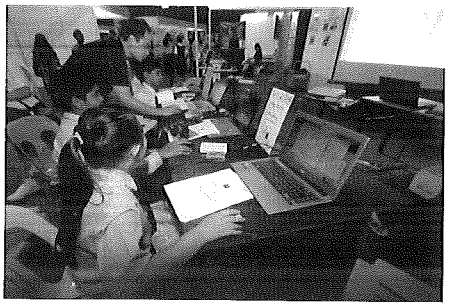

Figure 5. A workshop session conducted by a company.

Figure 6. A company exhibitor explaining a system on demo to students.

KLESF Fair: Impact Study

A survey was conducted during the fair and below are some important findings. About 68% and 64% of the primary and secondary school students respectively stated that their interest in STEM increased after visiting the KLESF 2014.

School Engineering and Science Design Mentorship (SESDM) Scheme

Experiential learning has been well studied and proven to be highly effective

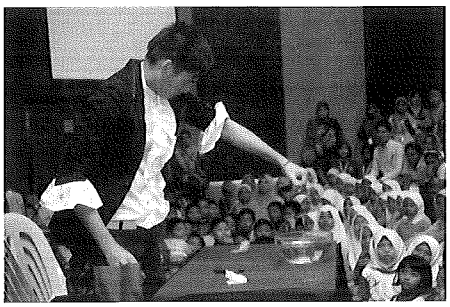

Figure 7. A magician performing a trick before explaining the science behind it.

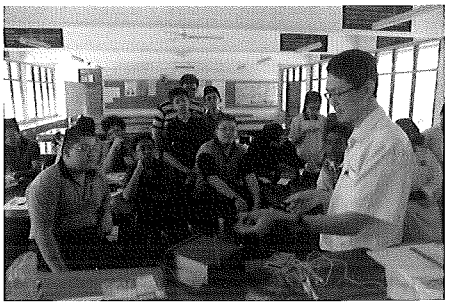

Figure 8. A mentor explaining electronic fundamentals to students under the SESDM Electronic Track.

Figure 9. A mentor working with students on a project of extracting natural dyes from plants under the SESDM Chemistry Track.

Figure 10. Mentors explaining a showcase system to students at the initial stage of the SESDM Electronic Track.

in the learning of subjects especially those in STEM which involve more high-order thinking. Based on the principle, the organizer set off with the aim of complementing the existing school STEM curriculum which may lack hands-on components.

The SESDM scheme is based on the concept of guiding and mentoring students on STEM investigative and design activities and projects (Figs. 8 - 10). The scheme typically involves 2 mentors guiding a group of 20 students who are sub-divided into teams of 2 to 3 persons per team. Each group of students undergoes 3 to 6 periods of mentorship track with weekly face-to-face sessions of 2 to 3 hours with the mentors. A pilot run of the scheme was started with 7 secondary schools in Perak and Klang Valley regions of Peninsular Malaysia.

To date, tracks based on the following themes and topics have been designed and implemented in the pilot run of the scheme:

1. Electronic design track (7 schools),
2. Chemistry track (2 schools), and
3. Biology track (1 school).

Development of tracks based on other themes and topics have been planned and will be carried out in future. Thus far, mentors in the pilot run of the scheme have been academics and students of Universiti Tunku Abdul Rahman (UTAR). The mentor team of KLESF will be expanded through the recruitment of more university academics and students, professionals (engineers, scientists, computer and IT experts, technologists, etc.), school teachers and educators, etc.

The SESDM scheme has thus far involved and achieved the following:

1. No of schools: 7,
2. No of school students: 250, and
3. No of mentors: 25.

The first pilot run of the scheme is expected to be concluded in July 2014. Feedbacks from the schools teachers and students have been positive. A proper impact study will be carried out on the scheme after its completion.

CONCLUSION

KLESF, a programme that involves all the key stakeholders in promoting interest in STEM among school students has been started and carried out. Although the programme is a work-in-progress some significant results have been achieved. It has benefited more than 200 schools and 50,000 students, teachers and parents thus far. About 68% and 64% of primary and secondary students respectively have their interest in STEM increased after visiting the KLESF Fair. More than 500 volunteer university academics, students, industrial technologists and professionals have participated in the KLESF programme thus far. The aim of engaging all stakeholders in promoting STEM will continue to be pursued. More volunteers and sub-programmes will be engaged and developed in future.

REFERENCES

1. The President's Council of Advisors on Science and Technology, Executive Office of the President (2012) *Engage to Excel: Producing One Million Additional College Graduates With Degrees in Science, Technology, Engineering, and Mathematics*, Report To The President, p. 1. Available: http://www.whitehouse.gov/sites/default/files/microsites/ostp/pcast-executive-report-final_2-13-12.pdf.
2. Business-Higher Education Forum's (BHEF) (2010) *Increasing the Number of STEM Graduates: Insights from the U.S. STEM Education & Modeling Project*, p. 4. Available: http://www.ncci-cu.org/downloads/BHEF_STEM.pdf.
3. Ministry of Higher Education Malaysia (2012) *National Education Statistic: Higher Education Sector 2012*, pp. 61–63. Available: http://www.mohe.gov.my/web_statistik/Perangkaan_SPT_2012.pdf.